

AN ABSTRACT OF THE THESIS OF

Joseph Bryce Lotrario for the degree of Doctor of Philosophy in Civil Engineering presented on October 31, 2000. Title: The Activity and Growth of a Chlorophenol Reductively Dechlorinating Soil Culture in the Presence of Exogenous Hydrogen.

Abstract approved: **Redacted for privacy**

Sandra L. Woods

The addition of exogenously supplied hydrogen stimulates PCP reductive dechlorination and increases bacterial growth. While research focuses mainly on pure cultures, few exist capable of aryl reductive dechlorination, and few markers exist to identify reductively dechlorinating bacteria within mixed cultures. Furthermore, most active bioremediation projects stimulate mixed cultures of native biota. This work describes a method to estimate reductively dechlorinating bacterial growth within a mixed soil culture under controlled environmental conditions.

The experiments discussed in this paper were performed in a fed-batch reactor. The reactor was operated in a way to maintain environmental conditions such as pH, E_H , headspace concentration, and temperature constant while substrate is allowed to degrade without the corruption of additional changes. Substrate utilization and cell growth were examined under an array of environmental conditions.

This dissertation examined the correlation between hydrogen concentration and the growth rate of reductively dechlorinating bacteria. Under low hydrogen partial pressures, between 9.4×10^{-5} and 2.9×10^{-4} atm, the growth rate of reductively dechlorinating bacteria increased as predicted by dual Monod kinetics with respect to hydrogen and chlorophenol concentration; however, studies showed

that the relationship was more complex. At higher concentrations of hydrogen, the observed growth rate of reductively dechlorinating bacteria declined. A dual Monod kinetics model with hydrogen substrate inhibition approximates experimental data.

Reductive dechlorination of 2,3,4,5-tetrachlorophenol and 3,4,5-trichlorophenol were also studied. Pentachlorophenol reductive dechlorination primarily produces 3,4,5-trichlorophenol via 2,3,4,5-tetrachlorophenol. The reductive dechlorination of 2,3,4,5-tetrachlorophenol parallels that of pentachlorophenol, and the estimated growth rates based on pentachlorophenol and 2,3,4,5-tetrachlorophenol are very similar. Reductive dechlorination of 3,4,5-trichlorophenol was catalyzed by the PCP reductively dechlorinating bacterial culture after a lag period. 3,4,5-Trichlorophenol was not maintained for extended periods, and multiple additions of 3,4,5-trichlorophenol did not result in measurable growth.

©Copyright by Joseph Bryce Lotrario
October 31, 2000
All Rights Reserved

The Activity and Growth of a Chlorophenol Reductively Dechlorinating Soil Culture
in the Presence of Exogenous Hydrogen

by

Joseph Bryce Lotrario

A THESIS

submitted to

Oregon State University

in partial fulfillment of
the requirements for the
degree of

Doctor of Philosophy

Completed October 31, 2000
Commencement June 2001

Doctor of Philosophy thesis of Joseph Bryce Lotrario presented on October 31, 2000

APPROVED:

Redacted for privacy

Major Professor, representing Civil Engineering

Redacted for privacy

Head of Department of Civil, Construction, and Environmental Engineering

Redacted for privacy

Dean of Graduate School

I understand that my thesis will become part of the permanent collection of Oregon State University libraries. My signature below authorizes release of my thesis to any reader upon request.

Redacted for privacy

Joseph Bryce Lotrario, Author

Acknowledgments

Upon completion of an endeavor such as this, the task of mentioning every person deserving of gratitude and thanks is daunting. I have neither the wisdom nor the skill to finish that job now in this small space, and so I will begin here and then try to show my appreciation and gratitude each and every day.

My love and thanks go out to my parents, Joseph and Pamela, who gave me the independence and perseverance I needed so much during these past years. They also taught me to have faith in my abilities and to believe that I really can do anything that I try.

Angela, you have my heart, and after encouraging me through the toughest times you have my gratitude too. You have supported my outlandish schemes as well as my genuinely good ideas. Completion of this paper is more your doing than most can realize.

Jason Cole and Darin Trobaugh, thank you both for extending my graduate school education with climbing lessons, kayaking adventures, skiing trips, and camping excursions that have become a huge part of who I am. Graduate school can be fun.

Dr. Craig, you brought me to Corvallis, Oregon, then to Barrow, Alaska, and then you sent me back to New Brunswick, New Jersey. When did I have time to start a dissertation? Thank you for everything. I thank my committee members Drs. Ken Williamson, Lew Semprini, and Bob Burton for their time and effort.

If there is one person who deserves my gratitude, it is Dr. Sandra Woods. Sandy, I truly do not know what I would have done without you. I consider you my friend as well as my major professor. You guided me when I was lost and you inspired me when I was down. Your incredible work ethic is inspiring if not frightening and made me want to work harder. Thank you.

Table of Contents

	<u>Page</u>
Chapter One: Introduction and Background	1
Chapter Two: Materials and Methods.....	7
Reactor System.....	7
Microbial Culture.....	10
Culture Source	10
Media Preparation	11
Chemicals.....	12
Analytical techniques.....	12
Chapter Three: The Effects of Hydrogen Partial Pressure on the Rate of PCP Reductive Dechlorination.....	14
Introduction.....	14
Materials and Methods.....	19
Reactor System	19
Data Analysis	20
Results.....	25
PCP Reductive Dechlorination.....	25
Pseudo-first-order Removal.....	28
Apparent E_H	29
Lag Period.....	30
Acceleration of Reductive Dechlorination.....	30
Hydrogen and the Growth of Reductively Dechlorinating Bacteria.....	47
Cell Growth.....	51
Cell Decay.....	53
Discussion.....	54
PCP Reductive Dechlorination.....	54
Pseudo-first-order Removal.....	55
Acceleration of Reductive Dechlorination.....	56
Activity Doubling Times.....	58
Cell Decay.....	59

Table of Contents (continued)

	<u>Page</u>
Conclusions.....	59
Chapter Four: The Reductive Dechlorination of 2,3,4,5-TeCP and 3,4,5-Trichlorophenol by a Mixed Soil Culture.....	61
Introduction	61
Materials and Methods.....	62
Results.....	63
Pathway	63
2,3,4,5-Tetrachlorophenol	70
3,4,5-Trichlorophenol.....	79
Discussion.....	86
2,3,4,5-Tetrachlorophenol	86
3,4,5-Trichlorophenol.....	87
Conclusions.....	89
Chapter Five: Conclusions and Engineering Significance	91
Stuart's growth estimation model can be applied to low cell density soil bacterial cultures.	91
Hydrogen partial pressure affects the apparent growth rate of PCP and 2,3,4,5-TeCP reductively dechlorinating bacteria.....	92
The reductive dechlorination of PCP and 2,3,4,5-TeCP is different from that of 3,4,5-TCP.	93
Bibliography	95
Appendices	105
Appendix A: Activity of a PCP Reductively Dechlorinating Mixed Soil Culture.....	106
Appendix B: Experimental Protocol	137
Appendix C: E_H and pH Time Course Studies.....	139

Table of Contents (continued)

	<u>Page</u>
Appendix D: Chlorophenol, Headspace, and Acetate Concentration Data	142
Appendix E: Rates of Reductive Dechlorination	161
Appendix F: Computer Simulation	162
Appendix G: Apparent Growth Rate Data	168
Appendix H: Monod Kinetic Model Studies	169
Appendix I: S_{\min} calculations	172

List of Figures

<u>Figure</u>	<u>Page</u>
2.1 Schematic of fed-batch reactor: 1 - Reference electrode, 2 - Platinum electrode, 3 - pH electrode, 4 - Gas outlet line, 5 - Syringe sample port, and 6 - Large bore liquid sample port.	9
3.1 Measured (◆) and modeled (—) reductive dechlorination of a single addition of PCP compared with 2,3,4,5-TeCP (●); 2,3,4,6-TeCP (▲); and 3,4,5-TCP (×) reductive dechlorination, sum (O) ± one standard deviation and averaged sum (- -) of total measurable chlorophenol congeners	27
3.2 Time course study of PCP (◆) reductive dechlorination, sum of measurable chlorophenol congeners (O), and cumulative PCP addition (—) under 2.2×10^{-4} atm of hydrogen	31
3.3 Time course study of PCP (*) first-order reductive dechlorination and derived exponential growth curve (—) at 2.2×10^{-4} atm of hydrogen	33
3.4 Time course study of PCP (◆) reductive dechlorination, sum of measurable chlorophenol congeners (O), and cumulative PCP addition (—) under 9.4×10^{-5} atm of hydrogen	35
3.5 Cell growth estimation based on the acceleration of PCP reductive dechlorination rate (+) at 9.4×10^{-5} atm of hydrogen	36
3.6 Time course study of PCP (◆) reductive dechlorination, sum of measurable chlorophenol congeners (O), and cumulative PCP addition (—) under 2.9×10^{-4} atm of hydrogen.....	37
3.7 Cell growth estimation based on the acceleration of PCP reductive dechlorination rate (+) at 2.9×10^{-4} atm of hydrogen	38
3.8 Time course study of PCP (◆) reductive dechlorination, sum of measurable chlorophenol congeners (O), and cumulative PCP addition (—) under 5.7×10^{-4} atm of hydrogen.....	39
3.9 Cell growth estimation based on the acceleration of PCP reductive dechlorination rate (+) at 5.7×10^{-4} atm of hydrogen	40

List of Figures (continued)

<u>Figure</u>	<u>Page</u>
3.10 Time course study of PCP (◆) reductive dechlorination, sum of measurable chlorophenol congeners (O), and cumulative PCP addition (—) under 7.8×10^{-3} atm of hydrogen.....	41
3.11 Cell growth estimation based on the acceleration of PCP reductive dechlorination rate (+) at 7.8×10^{-3} atm of hydrogen	42
3.12 Time course study of PCP (◆) reductive dechlorination, sum of measurable chlorophenol congeners (O), and cumulative PCP addition (—) under 3.9×10^{-2} atm of hydrogen.....	43
3.13 Cell growth estimation based on the acceleration of PCP reductive dechlorination rate (+) at 3.9×10^{-2} atm of hydrogen	44
3.14 Computer simulation of growth rate as a function of hydrogen partial pressure based on dual Monod kinetics.....	48
3.15 Computer simulation of growth rate as a function of hydrogen partial pressure based on dual Monod kinetics with substrate inhibition term of 0.0020 (---), 0.0010 (—), and 0.0005 (— —) atm	49
3.16 Apparent growth rates of reductive dechlorination \pm one standard error estimated compared with a substrate inhibition model when $K_i = 0.0020$ atm and $K_H = 0.0005$ atm (---)	50
3.17 Activity doubling times calculated from apparent growth rates.....	52
4.1 A time course study of PCP (◇); 3,4,5-TCP (O); and 3,5-DCP (◆); incubated at 5.7×10^{-4} atm of hydrogen.....	65
4.2 A time course study of 3,4,5-TCP (O); 3,5-DCP (◆); and 3,4-DCP (×) incubated at 9.8×10^{-4} atm of hydrogen	66
4.3 A time course study of PCP (◇); 3,4,5-TCP (O); and 3,5-DCP (◆); incubated at 9.4×10^{-5} atm of hydrogen.....	67
4.4 A time course study of 3,4,5-TCP (●); 3,5-DCP (◆); and 3,4-DCP (×) incubated at 7.8×10^{-4} atm of hydrogen	68

List of Figures (continued)

<u>Figure</u>	<u>Page</u>
4.5 A time course study of PCP (---); 2,3,4,5-TeCP (▪); and 3,4,5-TCP (●) incubated at 2.9×10^{-4} atm of hydrogen.....	69
4.6 Time course study of 2,3,4,5-TeCP (+) first-order reductive dechlorination and derived exponential growth curve (—) at 2.2×10^{-4} atm of hydrogen.....	72
4.7 Time course study of 2,3,4,5-TeCP (+) first-order reductive dechlorination and derived exponential growth curve (—) at 9.4×10^{-5} atm of hydrogen.....	73
4.8 Time course study of 2,3,4,5-TeCP (+) first-order reductive dechlorination and derived exponential growth curve (—) at 2.9×10^{-4} atm of hydrogen.....	74
4.9 Time course study of 2,3,4,5-TeCP (+) first-order reductive dechlorination and derived exponential growth curve (—) at 5.7×10^{-4} atm of hydrogen.....	75
4.10 Time course study of 2,3,4,5-TeCP (+) first-order reductive dechlorination and derived exponential growth curve (—) at 7.8×10^{-3} atm of hydrogen.....	76
4.11 Time course study of 2,3,4,5-TeCP (+) first-order reductive dechlorination and derived exponential growth curve (—) at 3.9×10^{-2} atm of hydrogen.....	77
4.12 Comparison of the acceleration calculated from PCP (■) and 2,3,4,5-TeCP (◆) reductive dechlorination with hydrogen partial pressure (the hydrogen substrate inhibition model (---) from Chapter 4 is included)	80
4.13 Correlation between lag time before reductive dechlorination of PCP (—◆—), 3,4,5-TCP (---■---), the ratio of PCP/TCP lag (—×—) and hydrogen partial pressure.....	82
4.14 Long term reductive dechlorination of 3,4,5-TCP (○) and PCP (—◆—).....	85

List of Tables

<u>Table</u>	<u>Page</u>
3.1 Measured hydrogen concentrations associated with redox active reactions.....	16
3.2 Partial pressures of hydrogen and E_H values established during reactor experiments	29
3.3 A comparison of doubling time and hydrogen concentration	45
3.4 Doubling times of reductively dechlorinating organisms	52
3.5 Decay rate analysis	53
4.1 Reductive dechlorination of 3,4,5-TCP	64
4.2 A comparison of apparent acceleration rates as measured by PCP and 2,3,4,5-TeCP reductive dechlorination.....	78
4.3 Reductive dechlorination rate of 3,4,5-TCP at varying hydrogen partial pressures measured during one reactor experiment	83

List of Appendix Figures

<u>Figure</u>	<u>Page</u>
A.1 Progress curves of simulated PCP reductive dechlorination when the initial cell concentration is 0.01 mg/L (▲), 0.005 mg/L (□), 0.001 mg/L (×), 0.0005 mg/L (▪), 0.0001 mg/L (+), 0.00005 mg/L (○), and 0.00001 mg/L (◇).....	117
A.2 Progress curves of simulated PCP reductive dechlorination when the hydrogen partial pressure is 0.00005 atm (□), 0.0001 atm (◇), 0.0005 atm (■), 0.001 atm (+), and 0.005 atm (●).....	120
A.3 Multiple addition simulation of PCP concentration (▲) between 0.04 to 0.4 μM and cell concentration (×) in mg/L.....	126
A.4 Lotrario's (—) and Stuart's (▪) estimations of cell growth for computer simulated data when PCP is between 0.04 to 0.4 μM based on $\Delta\text{PCP}/\Delta t$ (×) and first-order rates (■) respectively	126
A.5 Multiple addition simulation of PCP concentration (▲) between 0.11 to 0.26 μM and cell concentration (×) in mg/L.....	130
A.6 Lotrario's (—) and Stuart's (▪) estimations of cell growth for computer simulated data when PCP is between 0.11 to 0.26 μM based on $\Delta\text{PCP}/\Delta t$ (×) and first-order rates (■) respectively.....	130
A.7 Multiple addition simulation of PCP concentration (▲) μM and cell concentration (×) in mg/L with zero-order reductive dechlorination.....	132
A.8 Lotrario's (—) and Stuart's (▪) estimations of cell growth for computer simulated data when PCP is between 0.30 to 0.75 μM based on $\Delta\text{PCP}/\Delta t$ (×) and zero-order rates (■) respectively	132
C.1 Time course of pH and E_H data measured during PCP reductive dechlorination at 9.4×10^{-5} atm of hydrogen.....	139
C.2 Time course of pH and E_H data measured during PCP reductive dechlorination at 2.2×10^{-4} atm of hydrogen.....	139
C.3 Time course of pH and E_H data measured during PCP reductive dechlorination at 2.9×10^{-4} atm of hydrogen.....	140

List of Appendix Figures (continued)

<u>Figure</u>	<u>Page</u>
C.4 Time course of pH and E_H data measured during PCP reductive dechlorination at 5.7×10^{-4} and 3.9×10^{-2} atm of hydrogen.....	140
C.5 Time course of pH and E_H data measured during PCP reductive dechlorination at 7.8×10^{-3} atm of hydrogen.....	141
F.1 Sample input of multiple addition reactor simulation	162
H.1 Monod kinetics based curve fit of growth rate as a function of hydrogen partial pressure (—) based on Stuart's (◆) and Lotrario's (■) apparent growth rate data	170
H.2 Apparent growth rates of reductive dechlorination \pm one standard error estimated using Stuart's model (—x—), and Lotrario's model (—◆—) compared with a substrate inhibition model (- - -)	171

List of Appendix Tables

<u>Table</u>	<u>Page</u>
A.1 Summary of Lotrario's and Stuart's models	111
A.2 Monod kinetic coefficients and estimated values	113
A.3 Parameters used during computer simulations to test the effect of initial cell concentration	115
A.4 Cell Concentration after one addition of PCP	118
A.5 Parameters used during computer simulations of multiple PCP addition reactions	123
A.6 Acceleration rates based on determination method	127
A.7 Actual and estimated growth rates as PCP concentration approaches a constant value	129
D.1 Chlorophenol concentrations (μM) measured during the reactor experiment incubated at a hydrogen partial pressure of 2.2×10^{-4}	142
D.2 Headspace (atm) and acetate (μM) concentrations measured during the reactor experiment incubated at a hydrogen partial pressure of 2.2×10^{-4}	144
D.3 Chlorophenol concentrations (μM) measured during the reactor experiment incubated at a hydrogen partial pressure of 9.8×10^{-4}	144
D.4 Measured headspace (atm) concentrations measured during the reactor experiment incubated at a hydrogen partial pressure of $9.8 \times$ 10^{-4}	146
D.5 Chlorophenol concentrations (μM) measured during the reactor experiment incubated at a hydrogen partial pressure of 5.7×10^{-4}	146
D.6 Headspace (atm) and acetate (μM) concentrations measured during the reactor experiment incubated at a hydrogen partial pressure of 5.7×10^{-4}	148
D.7 Chlorophenol concentrations (μM) measured during the reactor experiment incubated at a hydrogen partial pressure of 9.4×10^{-5}	148

List of Appendix Tables (continued)

<u>Table</u>	<u>Page</u>
D.8 Headspace (atm) and acetate (μM) concentrations measured during the reactor experiment incubated at a hydrogen partial pressure of 9.4×10^{-5}	151
D.9 Chlorophenol concentrations (μM) measured during the reactor experiment incubated at a hydrogen partial pressure of 7.8×10^{-3}	152
D.10 Headspace (atm) and acetate (μM) concentrations measured during the reactor experiment incubated at a hydrogen partial pressure of 7.8×10^{-3}	155
D.11 Chlorophenol concentrations (μM) measured during the reactor experiment incubated at a hydrogen partial pressure of 2.9×10^{-4}	157
D.12 Chlorophenol concentrations (μM) measured during the reactor experiment incubated at a hydrogen partial pressure of 2.9×10^{-4}	159
D.13 Headspace (atm) and acetate (μM) concentrations measured during the reactor experiment incubated at a hydrogen partial pressure of 2.9×10^{-4}	160
E Calculated Reductive Dechlorination Rates	161
G.1 Activity growth rates of PCP reductively dechlorinating bacteria.....	168
G.2 Activity growth rates of 2,3,4,5-TeCP reductively dechlorinating bacteria.....	168
H.1 Monod constants	169
H.2 Constants used in substrate inhibition model	171
I.1 Monod Coefficients used in S_{\min} Calculations.....	172
I.2 S_{\min} values for Varying Hydrogen Partial Pressures	173

Abbreviations

Abbreviation	Definition
PCP	Pentachlorophenol
2,3,4,5-TeCP	2,3,4,5-Tetrachlorophenol
2,3,5,6-TeCP	2,3,5,6-Tetrachlorophenol
2,4,5,6-TeCP	2,4,5,6-Tetrachlorophenol
3,4,5-TCP	3,4,5-Trichlorophenol
2,3,5-TCP	2,3,5-Trichlorophenol
2,4,5-TCP	2,4,5-Trichlorophenol
3,5-DCP	3,5-Dichlorophenol
3,4-DCP	3,4-Dichlorophenol
2,5-DCP	2,5-Dichlorophenol
2,4-DCP	2,4-Dichlorophenol
3-CP	3-Chlorophenol

Symbols

Symbol	Definition	Units
X	Cell mass of bacteria	mg/L
k_m	Maximum substrate utilization rate	$\mu\text{M}_{\text{substrate}} \text{ mg}_{\text{cells present}}^{-1} \text{ hour}^{-1}$
Y	Cell yield	$\text{mg}_{\text{cells produced}} \mu\text{M}_{\text{substrate}}^{-1}$
K_s	Half velocity coefficient	μM
K_H	Hydrogen half velocity coefficient	atm
K_i	Hydrogen inhibition coefficient	atm
S	PCP or other modeled chlorophenol	μM
b	Cell decay coefficient	hour^{-1}
α	Stuart's acceleration coefficient	
E	Electrode potential	
T	Absolute temperature	Volts
z	Number of equivalents for the chemical equation as written	Kelvin
(ox)	Activity of species on the oxygenated side of the chemical equation	
(red)	Activity of species on the reduced side of the chemical equation	
°	Standard state	

The Activity and Growth of a Chlorophenol Reductively Dechlorinating Soil Culture in the Presence of Exogenous Hydrogen

Chapter One: Introduction and Background

This dissertation contains two manuscripts that describe research performed to examine the effects of hydrogen partial pressure on the reductive dechlorination of chlorinated phenolic congeners by soil derived mixed cultures. Hydrogen concentration is one of several environmental factors including E_H , sulfate concentration, and temperature that affect reductive dechlorination (4, 15, 17, 22, 24, 32, 38, 45, 74, 76). The first manuscript, Chapter 3, examines the correlation between the apparent growth rates of reductively dechlorinating bacteria and hydrogen partial pressure. For publication, Chapter 4 will be combined with additional research performed by a colleague and examines a reductively dechlorinating population incubated with hydrogen and either 2,3,4,5-tetrachlorophenol (2,3,4,5-TeCP) or 3,4,5-trichlorophenol (3,4,5-TCP).

Many of the world's most toxic soil and groundwater contaminants, including chlorinated solvents and chlorinated aromatic compounds, can be degraded by reductive dechlorination. Reductive dechlorination can transform either alkyl or aryl halides, by hydrogenolysis, during which a chloride substituent is replaced by a hydrogen atom (54, 84). Halogenated aliphatic congeners are reduced by a number of transition metals and transition metal complexes (TMCs) (84). Because these TMCs are used for electron transfer in living organisms, reactions between halogenated aliphatic congeners and TMCs provide models for living organisms (84). Reductive dehalogenation can be catalyzed by biological molecules such as cytochrome P-450 and coenzyme F430 (34, 57, 80). Biological studies show that freshwater lake sediment can reductively dehalogenate halobenzoate congeners (29), and under methanogenic conditions, tetrachloroethylene can be transformed to

vinyl chloride with some mineralization to CO_2 (85). A number of pure cultures are capable of aryl reductive dehalogenation (2, 10, 14-16, 46, 83, 87), and alkyl reductive dehalogenation by pure cultures are compiled in a number of review articles (21, 26, 54, 84). Under the correct conditions, chlorinated aromatic compounds like pentachlorophenol (PCP) can be reductively dechlorinated and completely mineralized (39, 52, 58). To understand their environmental fate or to design an efficient treatment system, factors affecting the reductive dechlorination of chlorinated aromatic congeners must be well understood. Information about dechlorination pathways, reaction rates, and bacterial competition for substrates can all be used to better design bioremediation treatment systems.

The reductive dechlorination of PCP can begin at each of the ring positions resulting in a number of different dechlorination pathways. Mixed cultures without prior acclimation to chlorophenol congeners usually initiate reductive dechlorination at an *ortho* positioned chlorine to produce 2,3,4,5-tetrachlorophenol (45, 48, 58). A second *ortho* positioned dechlorination follows to produce 3,4,5-TCP and then the *para* positioned chlorine is removed to form 3,5-dichlorophenol (3,5-DCP). Some environmentally isolated cultures exhibit reductive dechlorination in the order of *ortho, ortho, para*; or *para, ortho, ortho* (35). Researchers have selected specific reductive dechlorinating pathways by acclimating cultures to specific mono- and dichlorophenol congeners (8, 14, 52). Recent work suggests that different enzyme systems are responsible for *ortho* and *meta* reductive dechlorination (48), and results from this research supports that conclusion.

Reductive dechlorination is a common biotransformation reaction in which chlorine atoms are replaced by hydrogen atoms producing HCl. Hydrogen is the preferred electron donor of bacteria that reductively dechlorinate. For example, tetrachloroethane reductively dechlorinating bacteria can use hydrogen as an electron donor (17, 50), and research has recently shown that hydrogen can stimulate the reductive dechlorination of aromatic hydrocarbons (4, 6, 75). When

catalyzed by bacteria, reductive dechlorination can be an energy producing metabolic process.

Usually, the rate of a metabolic reaction is calculated as a function of cell, protein, or enzyme mass. This normalization enables the comparison between replicate samples and experiments. In a complex, mixed culture, however, normalization to cell or enzyme mass is not feasible because there is no definitive way to separate the active cells responsible for the desired activity from the bulk population. Because of this, common kinetic coefficients cannot be easily attained from traditional mixed culture studies. Difficulty in measuring the cells responsible for reductive dechlorination makes comparison of dechlorination rates and growth of dechlorinating organisms a complex problem.

Within a mixed culture, the growth of a specific sub-population of organisms can be estimated by monitoring reactions exclusively catalyzed by that population. In a defined methanogenic coculture, reductive dechlorination is linked to a growth yield increase (20). In vitro studies of vinyl chloride reductive dechlorination showed an exponential rate increase during growth experiments (64). Mineralization curves depend on the interactions of substrate concentration and population density (68), and models exist that estimate the growth of bacteria by examining substrate progress curves (66, 75). The acceleration of reductive dechlorination reflects the growth of a small sub-population of reductively dechlorinating bacteria within a mixed soil culture. By modeling this phenomenon, the effects of environmental conditions on reductively dechlorinating bacteria can be examined within mixed soil cultures (75).

A feedback controlled pseudo-batch reactor was used to control and monitor environmental conditions such as temperature, pH, E_H , acetate concentration, and hydrogen partial pressure. The concentration of hydrogen in solution from headspace measurements was calculated. PCP was added to the reactor in distinct concentrated spikes, and its concentration was monitored with time. From chlorophenol depletion data, reductive dechlorination rates of PCP and 2,3,4,5-

TeCP were calculated. These dechlorination rates were then used to estimate the growth of reductively dechlorinating bacteria within the mixed soil culture.

A computer simulation of the reactor experiments was designed and is described in Appendix A. This simulation mimicked the operation parameters of the reactor experiments, thus allowing easy and efficient estimations of the two models and the experimental parameters. Like other dechlorination models, this simulation is based on the Monod kinetics model (48, 69).

Experimental evidence shows that some bacterial reactions are limited by hydrogen partial pressures. Hydrogen levels can select for bacterial populations that produce and/or compete for hydrogen as shown by one modeling experiment (23). A bacterial isolate, *Methanosarcina thermophili* TM-1, that produces and consumes hydrogen shows metabolic responses to hydrogen partial pressure (1). Reductive dechlorination of chloroethenes has a half-velocity coefficient for hydrogen one tenth that reported for methanogens; therefore, as hydrogen concentrations decrease reductive dechlorination should continue after methanogenesis ceases (4, 70). Minimum hydrogen concentrations – termed hydrogen thresholds – can be used to select specific terminal electron-accepting processes (TEAPs) including chlororespiration (40).

Continuing in one of the more promising areas of Stuart's research, the effects of hydrogen concentration on a reductively dechlorinating sub-population within a mixed soil culture are examined. Early work by Stuart et al. showed that there may be a correlation between hydrogen partial pressure and growth rates of PCP reductively dechlorinating bacteria (74). This work attempts to demonstrate a correlation between growth rates and hydrogen partial pressure. The study examines the effect of hydrogen partial pressure on reductive dechlorination rates and the growth of reductively dechlorinating bacteria.

The objectives of this research are to:

1. Show a correlation between the apparent growth rate of a PCP reductively dechlorinating sub-population and hydrogen partial pressure
2. And examine the similarities and differences between the reductive dechlorination of PCP, 2,3,4,5-TeCP, and 3,4,5-TCP.

Expanding on the hypothesis that the hydrogen partial pressure affects the growth rate of PCP reductively dechlorinating bacteria, Chapter 3 uses the theoretical model developed at Oregon State University by Sheryl L. Stuart to examine the effect of hydrogen partial pressure on the apparent growth rate of PCP reductively dechlorinating bacteria within a mixed soil culture (74). This work further demonstrates the link between bacterial growth and hydrogen partial pressure. The apparent growth rates of a PCP reductively dechlorinating sub-population within a mixed soil culture are examined under hydrogen partial pressures between 9.1×10^{-5} and 3.1×10^{-2} atm. Those growth rates are shown to follow a substrate inhibition model with changing hydrogen partial pressure. This chapter also examines the potential of Stuart's model to determine cell decay.

Stuart et al. also began to examine the potential to reductively dechlorinate 3,4,5-TCP and other metabolites of PCP reductive dechlorination (74). The work presented in Chapter 4 represents my contribution to a paper examining the reductive dechlorination of PCP metabolites by a PCP stimulated culture. Some early studies suggested that TeCPs and TCPs are less subject to reductive dechlorination than PCP (52, 54, 84). Researchers show difficulty in reductively dechlorinating 3,4,5-TCP (46, 58). Furthermore, some suggest avoiding this congener is necessary to facilitate the mineralization of PCP (86). Despite similar reaction energies between PCP and 3,4,5-TCP reductive dechlorination, research has shown that 3,4,5-TCP may not support bacterial growth due to its toxicity (44) and because it acts as a proton dissipater (72). The effect of hydrogen partial pressure on the growth of PCP reductively dechlorinating bacteria when incubated on either 2,3,4,5-TeCP or 3,4,5-TCP is examined. PCP incubation experiments

suggest that these same bacteria were utilizing PCP and 2,3,4,5-TeCP, but a different consortia was responsible for the reductive dechlorination of 3,4,5-TCP. Like earlier research this work further supports the hypothesis that 3,4,5-TCP does not support measurable growth of reductively dechlorinating bacteria.

The work discussed in this dissertation advances research of reductive dechlorination in at least two different areas. A new correlation between hydrogen partial pressure and growth rates of PCP reductively dechlorinating bacteria is presented that strongly suggests hydrogen substrate inhibition. The work presented in Chapter 4 supports other studies that suggest the need for separate enzymes for *ortho* and *para* positioned reductive dechlorination, and the inability of 3,4,5-TCP reductive dechlorination to support microbial growth.

Chapter Two: Materials and Methods

Many of the materials and methods used for the research in Chapters 3 and 4 were the same. Those procedures are outlined below. Any changes or additional methods are explained in the specific chapter to which they apply.

Reactor System

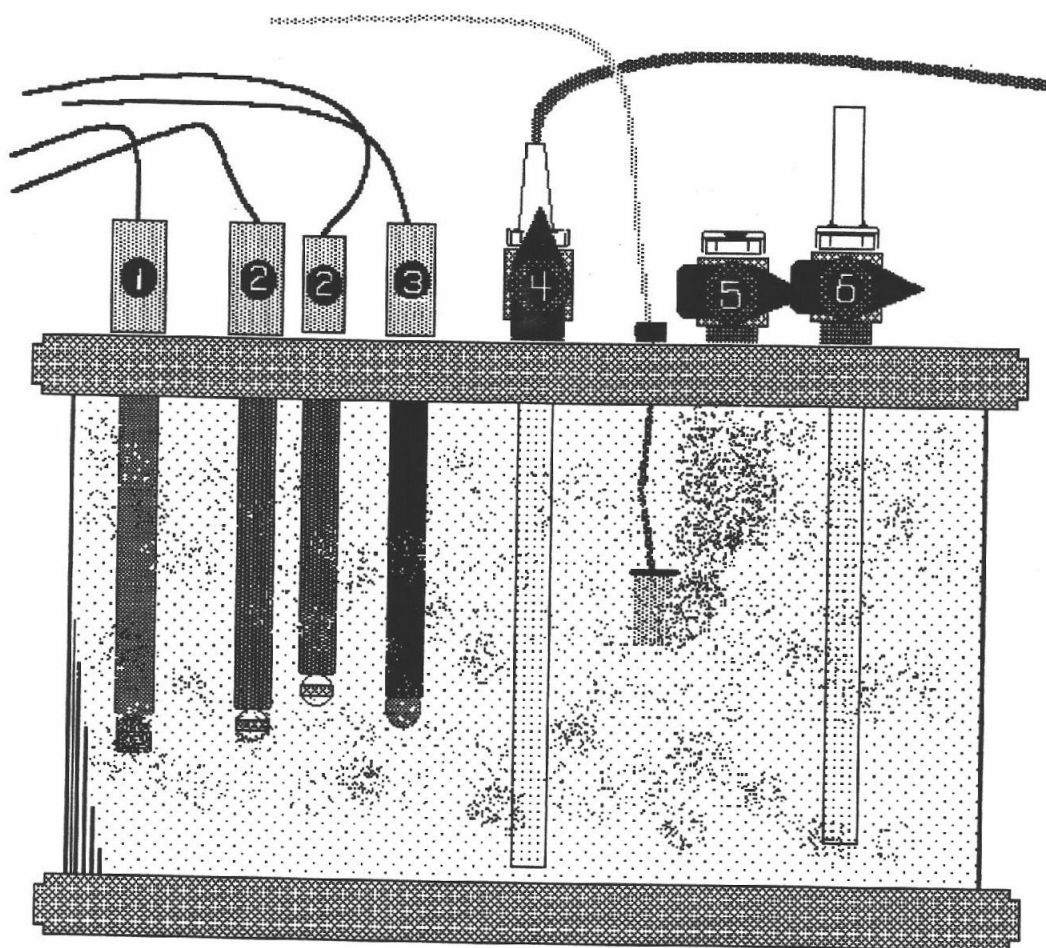
Time course studies were performed in a computer-monitored/feedback controlled bioreactor designed to monitor and hold constant temperature, pH, acetate concentration, redox potential, and hydrogen concentration while PCP transformation occurred. This reactor is described as a modified batch reactor because it degraded PCP, the primary substrate, like a batch reactor, while other conditions were held constant. Multiple spikes of PCP were added to the system, and the disappearance of PCP was observed and measured. Five incubations were performed at different hydrogen headspace partial pressures, which spanned two and one half orders of magnitude, to observe the effects of hydrogen partial pressure on the rate of reductive dechlorination and growth of a reductively dechlorinating sub-population within a mixed microbial culture. In addition, several attempts to estimate the culture's rate of decay were made following an estimation of the observable growth rate.

The 2.5-L batch reactor was constructed of Kimax beaded-process glass pipe with stainless steel and Teflon-lined flange fittings (Ace Glass company; Vineland, N.J.). The top plate was fitted with ports to accommodate a relief valve, three pump fittings, five electrodes, a liquid sample valve, and a headspace sample valve. A schematic of the reactor is shown in Figure 2.1. The electrodes and pumps were attached to a computer that recorded data with time and controlled acetate injections. Acetate was added to the reactor via a computer-controlled pump (FMI micro π -petter; Syosset, N.Y.) in order to maintain a constant acetate concentration. Once measured, acetate concentrations were input into the computer and the program calculated and added the necessary volume of acetate stock to maintain a one molar concentration within the reactor. The use of this reactor has been explained previously by Stuart (75).

Incubations were conducted at 31°C and a pH of 6.81 (± 0.27). The E_H was allowed to reach a steady state with the established hydrogen head space concentration while the first PCP spike was degraded.

The hydrogen and nitrogen gases used in the reactor were scrubbed of oxygen using OMI indicating purifiers (Supelco 2-3906; St. Louis, MO). The gas mixture, bubbled into the reactor, was maintained at a constant concentration using a mass flow controller (Tylan RO-28 and Tylan FC-280; Sable Systems International; Henderson, NV) to mix and regulate gas flow from three separate gas tanks. In the mixture, nitrogen measured about 90%, carbon dioxide measured about 10%, and the concentration of hydrogen – different for each incubation – ranged between 9.1×10^{-5} and 3.9×10^{-2} atm (Equal to 70-30,000 nM).

Figure 2.1: Schematic of feed-batch reactor: 1 - Reference electrode, 2 - Platinum electrode, 3 - pH electrode, 4 - Gas outlet line, 5 - Syringe sample port, and 6 - Large bore liquid sample port.



Beginning with the inoculation preparation, each of the reactor experiments was performed according to the same protocol. The reactor was purged of oxygen using a gas mixture of $\text{N}_2:\text{CO}_2:\text{H}_2$ (90:10:set hydrogen) until no O_2 was measurable in reactor gas samples. Two liters of reactor media was added to the reactor through a funnel. When O_2 was no longer measurable, Teflon rods were exchanged for electrodes, and the reactor was purged for an additional 30-60 minutes. When the reactor was again free of O_2 , the supernatant was siphoned from an inoculum culture flask into the reactor through a feed tube suspended mid-depth in the reactor, the electrodes were connected, and the monitoring program was begun.

Liquid samples were taken regularly with a glass syringe for chlorophenol and acetate concentration analysis. Subsequently, a concentrated stock solution of PCP in water was added to the reactor to produce a spiked concentration of $0.4 \mu\text{M}$ when the concentration of PCP measured $0.04 \mu\text{M}$ or less. Headspace samples were taken with a $500 \mu\text{L}$ -gas tight syringe to measure hydrogen concentration.

Microbial Culture

Culture Source

Experiments were performed with a mixed microbial soil culture derived from commercially available river bottom sand (The Bark Place; Philomath, OR). This was chosen as the inoculum because it was widely available, provided a broad source of bacteria, and was not initially enriched for dechlorinating organisms. The soil properties were measured at the Oregon State University Soils Laboratory to be: $\text{pH} = 6.3$, phosphorous = 20 ppm, sulfur as sulfate = 16.5 ppm, cation exchange coefficient = 12.0 meq/100g, soluble salts = 0.2 mmhos/cm, 0.27% carbon, and 0.02% nitrogen. Each culture used for these experiments was grown and incubated

under identical conditions prior to each reactor experiment. The culture was derived by mixing river bottom sand with the reactor media (150 g: 400 ml) in a 500-ml flask. The mixture was sparged for 15 minutes with nitrogen, capped with a butyl rubber stopper, vented into water with a relief tube, and incubated for four weeks at 31°C. After four weeks, the supernatant from the flask was siphoned into the prepared reactor, and data collection began. Measurements from the flask showed a four-day lag period before PCP and acetate degradation began. Degradation continued into the third week of incubation when the substrate concentrations were lowered below detection limits.

Media Preparation

The salt concentrations of the reactor media were based on an anaerobic media described in the literature (60). The reactor media was made by mixing 100 mg of acetate, 100 µg of PCP (as a solution), 7.25 mg of $(\text{NH}_4)_2\text{HPO}_4$, 100 mg $\text{NaC}_2\text{H}_3\text{O}_2$, 16.25 mg NaHCO_3 , 22.5 mg $\text{CaCl}_2 \cdot 2\text{H}_2\text{O}$, 35.9 mg NH_4Cl , 162 mg $\text{MgCl}_2 \cdot 6\text{H}_2\text{O}$, 117 mg KCl , 1.80 mg $\text{MnCl}_2 \cdot 4\text{H}_2\text{O}$, 2.7 mg $\text{CoCl}_2 \cdot \text{H}_2\text{O}$, 0.513 mg H_3BO_3 , 0.243 mg $\text{CuCl}_2 \cdot 2\text{H}_2\text{O}$, 0.23 mg $\text{Na}_2\text{MoO}_4 \cdot 2\text{H}_2\text{O}$, 0.189 mg ZnCl_2 , 0.0018 mg biotin, 0.0018 mg folic acid, 0.009 mg pyridoxine hydrochloride, 0.0045 mg riboflavin, 0.0045 mg thiamin, 0.0045 mg nicotinic acid, 0.0045 mg pantothenic acid, 0.0009 mg B_{12} , 0.0045 mg p-amino benzoic acid, 0.0045 mg thioctic acid, 0.112 mg PCP, 33.3 mg $\text{FeCl}_2 \cdot 4\text{H}_2\text{O}$, and 45 mg $\text{Na}_2\text{S} \cdot 9\text{H}_2\text{O}$ to a total volume of 1 L of DI H_2O .

Chemicals

Pentachlorophenol (99+%) was obtained from Aldrich Chemical Co. (St. Louis, MO); 2,3,4,5-tetrachlorophenol, 3,4,5-trichlorophenol (95+%), and chlorinated phenol analytic standards were obtained from Ultra Scientific (North Kingstown, RI). Others salts used to prepare the reactor media were obtained from Aldrich Chemical Co.

Analytical techniques

Headspace and liquid samples were withdrawn from the reactor at regular time intervals, and hydrogen, acetate, and chlorophenol concentrations were analyzed by three different gas chromatographic (GC) methods.

A GC equipped with a thermal conductivity detector (TCD) measured gas concentrations of the headspace samples. Headspace samples of 500 μL , taken with a 1-mL gas tight syringe, were immediately injected onto a Supelco 60/80 Carboxen 1000 column. The inlet and detector temperatures were 275°C. The oven temperature profile began at 50°C for four minutes, increased 0.5°C/min for 2 minutes, increased 32°C/min for 2 min, increased 20°C/min for 5.5 minutes, and held constant at 225°C for 2.5 minutes.

Chlorophenol and salt concentrations within the reactor were determined by measuring liquid samples by gas and ionic chromatography. Liquid samples of 0.4 ml were withdrawn; by a glass, gas tight syringe; from the reactor one to two inches below the liquid surface. Each sample was injected into a glass target vial insert (Fisher Scientific; Pittsburgh, PA) and placed within a microfuge tube. The sample was centrifuged for 5 minutes at 8,000 rpm in a microfuge tube.

Acetate concentrations in the media were measured using a flame ionization detector (FID). A 100- μL aliquot of the centrifuged liquid sample was mixed with 2

μL of 10-M phosphoric acid 10 seconds in a microfuge tube. A 1 μL aliquot of the acidified liquid sample was injected (splitless) using a 1 μL syringe with a Chaney adapter onto a Hewlett Packard Innowax capillary column ($30\text{ m} \times 0.25\text{ mm} \times 0.25\text{ }\mu\text{m}$). The inlet and detector temperatures were set at 250°C . The oven was set to 120°C for 1 minute, increased $16.6^{\circ}\text{C}/\text{min}$ for 6.02 minutes, and held at 220°C for 1 minute.

Centrifuged, liquid samples for chlorophenol analysis were acetylated and extracted into hexane prior to analysis by a method described by Stuart et al. (1998). In a 10-ml glass test tube, 500 μL of an internal standard solution containing 30.4 g/L of K_2CO_3 and 500 $\mu\text{g}/\text{L}$ of 2,4,6-tribromophenol, 100 μL of acetic acid anhydride, and 100 μL of the sample were mixed. The tube was capped with a Teflon lined screw cap and mixed for 10 minutes using a wrist action shaker. In this, one ml of hexane was added and shaken for 10 minutes; that hexane portion was removed placed into an amber glass GC vial capped with a Viton septum.

The chlorophenol analysis was performed using GC with an electron capture detector (ECD). A 1 μL liquid sample was injected using an autosampler on to DB-5 ($30\text{ m} \times 0.32\text{ mm} \times 0.25\text{ }\mu\text{m}$) capillary column. The inlet temperature and pressure were 250°C and 9.8 psi respectively. The detector temperature was 350°C with and anode gas flow of 6 ml/min and a make-up gas flow of 60 ml/min. The injection was splitless with 55 ml/min of flow. The oven was set to 40°C for one minute, increased $25^{\circ}\text{C}/\text{min}$ for 4 min, and increased $10^{\circ}\text{C}/\text{min}$ for 13 min to a temperature of 250°C .

Chapter Three: The Effects of Hydrogen Partial Pressure on the Rate of PCP Reductive Dechlorination

Introduction

While the development and production of chlorinated hydrocarbons has left, as its legacy, contaminated soil and groundwater, microbial reductive dechlorination is one promising method of remediating those sites (54, 78). Among the chlorinated hydrocarbon congeners, pentachlorophenol (PCP) is a common pollutant in the Pacific Northwest as a result of wood preservation processes. Under certain anaerobic conditions, aromatic compounds such as PCP can be reductively dechlorinated and completely mineralized (39, 52, 58). Molecular hydrogen serves as the primary electron donor and the chlorinated organic compound serves as the electron acceptor (51, 54, 84). Hydrogen has recently been shown to stimulate the reductive dechlorination of aromatic hydrocarbons (4, 6, 74). Still, the correlation between hydrogen partial pressure and the rate of reductive dechlorination is not well defined. To understand the environmental fate or design an efficient treatment system, factors affecting the reductive dechlorination process, like hydrogen partial pressure, must be well understood.

This study describes the effects of hydrogen partial pressure on a PCP reductively dechlorinating population. Experiments performed with environmental samples are more predictive of bioremediation applications than those performed with pure cultures (3). Because mixed cultures can change with time, it is important to understand how bacterial populations interact within a mixed culture rather than as isolated populations. The experiments evaluate the activity of a reductively dechlorinating sub-population within a mixed soil culture as it metabolizes PCP and hydrogen. The results show a correlation between hydrogen partial pressure and the apparent growth rate of the PCP dechlorinating population.

There is strong evidence to suggest that reductive dechlorination depends on the availability of hydrogen. Extensive research on the reductive dechlorination of chlorinated aryl and alkyl compounds shows elemental hydrogen to be the preferred electron donor of dechlorinating bacteria (4, 15, 20, 29, 82). Resting cell cultures of *Desulfomonile tiedjei* consume hydrogen as the electron donor while dehalogenating various halogenated aromatic congeners (15). Laboratory studies of anaerobic enrichment cultures indicate that hydrogen serves as the electron donor in the reductive dechlorination of trichloroethylene (TCE) to vinyl chloride and ethene over periods of 14- 40 days (17). In the field, the presence of elemental iron oxidized to form hydrogen enhances bacterial reductive dechlorination of carbon tetrachloride (6).

The partial pressure of hydrogen may affect the activity of reductively dechlorinating bacteria. Hydrogen partial pressure correlates to the microbially catalyzed redox sensitive reactions in both groundwater and sediment environments. The minimum hydrogen concentration that can be consumed, the hydrogen threshold, is controlled by the energetics of the terminal electron-accepting process (TEAP) as shown in Table 3.1 (40). Laboratory studies conducted in constantly stirred tank reactors with a mixed methanogenic culture demonstrate that hydrogenic and hydrogenotrophic reactions depend directly on the partial pressure of hydrogen (71). In mixed cultures, trace hydrogen is transferred to the bacteria able to utilize the preferred terminal electron acceptor so that hydrogen concentration measured in environmental samples can indicate the predominant terminal electron acceptor in that environment (13, 43). In the field, measured hydrogen concentrations of 7-10 nM are indicative of methanogenesis compared to sediments in which nitrate reduction is the dominant reaction and hydrogen only measures 0.05 nM (42). In laboratory studies, hydrogen measures around 2 nM when reductive dechlorination of carbon tetrachloride is the dominant reaction (89). Hydrogen thresholds of 0.125 - 0.235 nM are exhibited by cultures in the presence of chlorinated aliphatic compounds like tetrachloroethene (PCE) and its metabolites

(40). The thermodynamics of the terminal electron-accepting reaction establish a characteristic steady state hydrogen threshold (40).

Table 3.1: Measured hydrogen concentrations associated with redox active reactions

Reaction	Hydrogen Threshold Concentration (nM)	ΔG° (kJ/mole of H_2)	Reference
Acetogenesis	336-3,640	-26.1	(7, 13)
Methanogenesis	7-10	-33.9	(12, 13, 41, 43)
Sulfate reduction	1-15	-38.0	(12, 13, 43)
Fumarate reduction	0.015	-86.2	(13)
Chlororespiration	0.3-2	-130 to -187	(40, 89)
Ammonification	0.015-0.025	-149.9	(12, 13)
Fe (III) reduction	0.1-0.8	-228.3	(12, 42, 43)
Nitrate reduction	0.05	-240	(42, 43)

Within a mixed microbial culture, populations of bacteria are growing and decaying at varying rates. This creates a microbial system dependent upon population dynamics. In the model being analyzed, the acceleration of reductive dechlorination is linked to both growth and decay of the population responsible for those reactions. In a mixed culture, the most competitive bacteria will grow and express their metabolic functions; therefore, reductive dechlorination is best expressed when reductively dechlorinating bacteria out-compete other organisms for hydrogen. At low hydrogen concentrations, reductively dechlorinating bacteria have a competitive advantage over methanogenic bacteria based on their respective rate constants. Reductively dechlorinating bacteria have a hydrogen half velocity coefficient, $K_s(H_2)$, one tenth that of methanogenic bacteria; therefore, they can utilize hydrogen at much lower concentrations than methanogens (4, 70). When the hydrogen concentration is low, reductively dechlorinating bacteria can continue to gain energy when methanogenic reactions are no longer energy producing.

Even at high hydrogen partial pressures, when the kinetics and thermodynamics of methanogenesis are most favorable, sustained reductive dechlorination in recycle reactors persists (9). Calculated Gibb's free energies of reductive dechlorination compared to fermentation reactions suggest a thermodynamic advantage of reductive dechlorination over methanogenesis (19). With each turn of their metabolism, reductively dechlorinating bacteria produce more energy than their fermentative counterparts. It is expected that dechlorinating bacteria will outgrow methanogenic bacteria, and reductive dechlorination will occur at high as well as low hydrogen partial pressures. At low hydrogen levels, reductively dechlorinating bacteria will still be able to utilize hydrogen when methanogens can no longer gain energy from the reaction. At high hydrogen levels, the more active reductively dechlorinating bacteria should out grow other organisms.

Reductively dechlorinating bacteria can represent a small fraction of a mixed population so that bulk properties like most probable number (MPN), protein mass, and volatile suspended solids (VSS) are seldom relevant to characterizing reductive dechlorination rates. Results from enumerating techniques rarely distinguish between ecologically relevant strains and opportunistic species that prosper under the culture conditions (25). Difficult to isolate, the measured population of reductive dechlorinating bacteria may be much smaller than the actual population (11).

The rate of reductive dechlorination increases with the number of the reductively dechlorinating sub-population. Reductively dechlorinating bacteria use PCP and hydrogen in a stoichiometric ratio suggesting that the reaction is metabolic rather than cometabolic (74). Because PCP reductive dechlorination is metabolic, the catalyzing bacteria grow cells from the energy derived from this reaction. When substrate consumption is linked to growth, the number of catalytic units, or activity, increases with time (63). The biomass or density of microorganisms can be estimated by substrate mineralization curves of a specific metabolic function (66). The growth of reductively dechlorinating bacteria can be evaluated by the

acceleration of the reductive dechlorination rate. By using the acceleration of a metabolic function as an indicator of growth, the effects of hydrogen partial pressure on a reductively dechlorinating bacterial culture can be examined in a mixed microbial environment. This study uses substrate depletion data to estimate the growth rate of reductively dechlorinating bacteria within a mixed culture consortium by measuring the rate of change of reductive dechlorination (75). This observable growth rate is the rate of growth demonstrated by a culture's activity and is a function of both the maximum growth rate coefficient and the cell decay coefficient.

An estimate of cell decay can also be made based on a change in substrate utilization rate after the substrate has been withheld for a period of time. The cell decay rate of relevant microbial species is necessary to correctly assess the growth rate of these organisms as a function of microbial activity. When the substrate is withheld, growth is suspended and only cell decay remains. This should more accurately predict a decay rate than other types of experiments performed outside the mixed culture environment.

New studies show that the hydrogen partial pressure affects the rate of reductive dechlorination and growth of reductively dechlorinating bacteria (75). One effective mathematical model of chloroethane dechlorination by a mixed consortium estimates the rate of reductive dechlorination as a dual Monod function of chloroethane and hydrogen concentration (23, 40, 49). Based on a dual Monod model, the rate of reductive dechlorination correlates with hydrogen partial pressure. Reactor experiments with a soil bacterial culture, PCP, and constant hydrogen concentrations measure the effect of hydrogen partial pressure on the growth rate of reductively dechlorinating bacteria. The results presented here show a correlation between hydrogen partial pressure and the growth of reductively dechlorinating bacteria.

The objectives of this research are:

1. To determine the pathway of PCP reductive dechlorination by a mixed soil culture grown on PCP,

2. To maintain a reductively dechlorinating soil population for extended periods with the addition of PCP and exogenous hydrogen,
3. To estimate the apparent growth rate of reductively dechlorinating bacteria within a mixed microbial culture at different hydrogen partial pressures,
4. To show a correlation between hydrogen partial pressure and the growth of reductively dechlorinating bacteria,
5. And to estimate cell decay of reductively dechlorinating bacteria within the mixed microbial culture.

Materials and Methods

Reactor System

Time course studies were performed in a computer-monitored/feedback-controlled bioreactor as explained in Chapter 2. Incubations were examined using Stuart's theoretical model (74). Five incubations were performed at different hydrogen headspace partial pressures, which spanned two and one half orders of magnitude, to observe the effects of hydrogen partial pressure on the rate of reductive dechlorination and growth of a reductively dechlorinating sub-population within a mixed microbial culture.

The decay rate of the reductively dechlorinating bacteria within the mixed culture was measured. Once the activity growth rate was determined, substrate addition ceased. Without chlorophenol congeners in the reactor, growth of the reductively dechlorinating organisms was assumed negligible and cell decay was measured. After a period to allow decay, PCP was added to the reactor and the rate of reductive dechlorination was measured. The apparent growth rate determined earlier in the experiment was used to estimate the reductive dechlorination rate for the next PCP addition. This expected rate was compared with the measured rate to

determine a decay rate. This method is further explained in the Data Analysis section.

Data Analysis

The data analysis of PCP reductive dechlorination data was performed using Stuart's model (74). The first-order model was a good approximation provided changes in active biomass or intracellular enzyme were small over the period in which the rate is measured (79). For each injection of PCP, the production and disappearance of PCP, 2,3,4,5-TeCP, and 3,4,5-TCP were measured. The respective reductive dechlorination rates of PCP and 2,3,4,5-TeCP were calculated by least squares approximation of the data to the first-order equations of Stuart's model. By design, PCP spikes, added to the reactor, were held to concentrations below the half velocity coefficient, estimated at 0.4 μM or greater (47, 74), so that the reductive dechlorination of PCP would fit a first-order reaction model.

Model Derivation

Equation 3.1 and Equation 3.2 are the integrated forms of the Monod degradation of PCP and 2,3,4,5-TeCP respectively.

$$\text{Equation 3.1} \quad P = P_0(e^{-k_P t})$$

$$\text{Equation 3.2} \quad T = \frac{k_P P_0}{k_T - k_P} [e^{-k_P t} - e^{-k_T t}] + T_0(e^{-k_T t})$$

Where

P, T = PCP and 2,3,4,5-TeCP concentrations, respectively, μM

P_0, T_0 = initial PCP and 2,3,4,5-TeCP concentrations, respectively, μM

k_P, k_T = pseudo-first-order rate constant for PCP and 2,3,4,5-TeCP, hour^{-1}

t = time in the individual progress curve scale, hour

The values P_0, T_0, k_P , and k_T were approximated using the optimization program (Microsoft Excel 7.0; Solver) based on the reduced gradient algorithm as described by Lasdon et al. (36). The four parameters: P_0, T_0, k_P , and k_T , were adjusted to best fit two curves to PCP and 2,3,4,5-TeCP progress curves. Confidence intervals (95%) for the individual rate parameters (k_P and k_T) were obtained iteratively. A parameter above or below the best fit value was arbitrarily selected, and the remaining parameters were optimized by minimizing χ^2 , as above. The parameter of interest was again adjusted and the χ^2 minimization was repeated until a change in the optimum χ^2 , represented a 95% confidence interval with one degree of freedom (61, 74).

Discrete amounts of the substrate, PCP, were added to the reactor according to an exponential pattern with time. When the concentration of PCP was at a very

low level, less than 0.04 μM , a PCP spike was injected. In this way, the actively dechlorinating bacteria determined the PCP addition by their rate of reductive dechlorination. Variables related to substrate addition including reductive dechlorination rates were represented by the first-order model in Equation 3.3 (75).

Equation 3.3
$$C = C_0(e^{\alpha t})$$

Where

C = reductive dechlorination rate or any parameter related substrate addition

C_0 = the parameter value at time zero

α = the exponential rate of change

t = the time measured across the overall experimental time scale

Experiments were performed so that substrate, PCP, was added exponentially. Any parameter linked to substrate addition should also increase exponentially (75). In Equation 3.3, the alpha term represented the exponential increase in any parameter as it was related to the PCP utilization. For a pseudo-first-order rate coefficient k that increased exponentially, Equation 3.3 became Equation 3.4.

Equation 3.4
$$k_t = k_{t=0}(e^{\alpha t})$$

The observed acceleration of reductive dechlorination, α , by a mixed dechlorinating population estimates the increase in the culture's activity. Equation 3.4 estimated the observed acceleration of reductive dechlorination, α , by a mixed dechlorinating population when PCP was added at discrete increments. While

increases in the per cell concentration of enzymes could attribute to the observed acceleration, this method assumes that per cell enzyme concentrations are constant.

By assuming that the PCP reductive dechlorination rate changes with cell number, X and X_0 were substituted for rate constants, k and k_0 , and Equation 3.4 became Equation 3.5.

$$\text{Equation 3.5} \quad X_t = X_{t=0}(e^{\alpha t})$$

Doubling Time

For first-order growth the equation is $X/X_0 = e^{\alpha t}$. For the situation when X doubles, $X/X_0 = 2$, the doubling time is equal to the natural log of 2 divided by the growth rate, α . Activity doubling time decreases as the growth rate increases. An activity doubling time, τ_{double} , may be determined by Equation 3.6, where α is the exponential rate constant from Equation 3.5.

$$\text{Equation 3.6} \quad \frac{\ln 2}{\alpha} = \tau_{\text{double}}$$

Because the pseudo-first-order rate coefficient indicated the culture's dechlorinating activity, Stuart termed it an "activity" doubling time (75). If rate increases were due to growth as assumed, then the "activity" doubling time was equal to the population doubling time, and a change in rate could be used to estimate the population's growth.

Cell Decay

The observable growth rate of a bacterial culture is the sum of cell growth and cell decay. If a decay term, b , is included in Stuart's model, Equation 3.4 becomes Equation 3.7 and acceleration is dependent on a first-order growth rate coefficient, a , and a decay coefficient, b .

Equation 3.7
$$k_t = k_{t=0}(e^{(a-b)t})$$

When substrate is withheld from the reactor the first-order growth term, a , becomes zero and the change in rate relies solely on decay. The coefficient $k_{t=0}$ was estimated using the calculated, apparent growth rate to determine the PCP reductive dechlorination rate in the reactor at the precise time that substrate was withheld. This was greater than the most recently measured dechlorination rate due to cell growth. After some time, t , PCP was added and PCP reductive dechlorination was calculated. This measured rate, the value k , in Equation 3.7 was used to solve for b , the decay rate of reductively dechlorinating bacteria in the reactor.

Dual Monod Model

A dual Monod model that related cell growth to the concentration of both PCP and hydrogen as substrates was initially used. This fit well provided that the acceleration rate did not decline with an increase in one of the substrate concentrations. By changing from the standard dual Monod kinetics model to a substrate inhibition model, based on Equation 3.8, hydrogen inhibition on the reductively dechlorinating culture can be modeled. This equation is based on a

system in which a portion of the enzyme is misdirected by excess hydrogen and slows down the desired reaction. As hydrogen increases the rate initially rises and then declines. This equation becomes the standard dual Monod equation by removing the term $[H_2]^2/K_i$. Both versions of this dual Monod model are compared with the experimental data. Also, the concentration of PCP in the reactor was maintained above theoretical S_{min} values calculated for both the dual Monod and substrate inhibition situations. The model is further explained in Appendix H and S_{min} calculations are shown in Appendix I.

$$\text{Equation 3.8} \quad \frac{dPCP}{dt} = - \frac{Xk_m[PCP]}{K_P + [PCP]} \frac{[H_2]}{K_H + H_2 + \frac{[H_2]^2}{K_i}}$$

Results

In this section, the PCP reductive dechlorination pathway, first-order reductive dechlorination, activity increases in reductively dechlorinating cultures, and activity decay are presented. Six experiments are described that examine a reductively dechlorinating culture under different hydrogen partial pressures. Stuart's model is used because it has previously been accepted by peer review, and the experimental procedure conformed to the assumptions of Stuart's model.

PCP Reductive Dechlorination

The PCP reductive dechlorination pathway proceeded through 2,3,4,5-TeCP to 3,4,5-TCP via two sequential *ortho* positioned reactions. This reductive dechlorination pattern was observed for subsequent incubations at various hydrogen

concentrations, and production and reductive dechlorination of 2,3,4,5-TeCP consistently produced accumulating concentrations of the metabolite 3,4,5-TCP. Trace amounts of other chlorophenol congeners: 2,3,4,6-TeCP; 2,3,5,6-TeCP; 2,3,4-TCP; 2,3,5-TCP; 3,4-DCP; 3,5-DCP; 3-CP were observed but did not accumulate to measurable concentrations (data not shown). Liquid concentration measurements of a single, representative PCP injection made during the incubation (hydrogen partial pressure = 2.2×10^{-4} atm) are plotted according to time in Figure 3.1. The experiment during which hydrogen was maintained at 2.2×10^{-4} atm was representative of the other experiments and was centered within the range of hydrogen partial pressures tested. This PCP spike was added after 210 hours of incubation during the reactor experiment. During the 200 hours prior to this PCP addition, PCP was added and reductively dechlorinated as explained in the methods (Chapter 2). This one addition is shown as representative of the PCP addition and reductive dechlorination in the reactor.

At the time of this addition, the molar sum of the cumulative PCP addition equaled 1.95 μ M compared to the measured sum of chlorophenol congeners of 2.03 ± 0.087 μ M. The 2.50% error associated with the sum of measured chlorophenol congeners compares well with the sampling error of 2.04% (Figure 3.1).

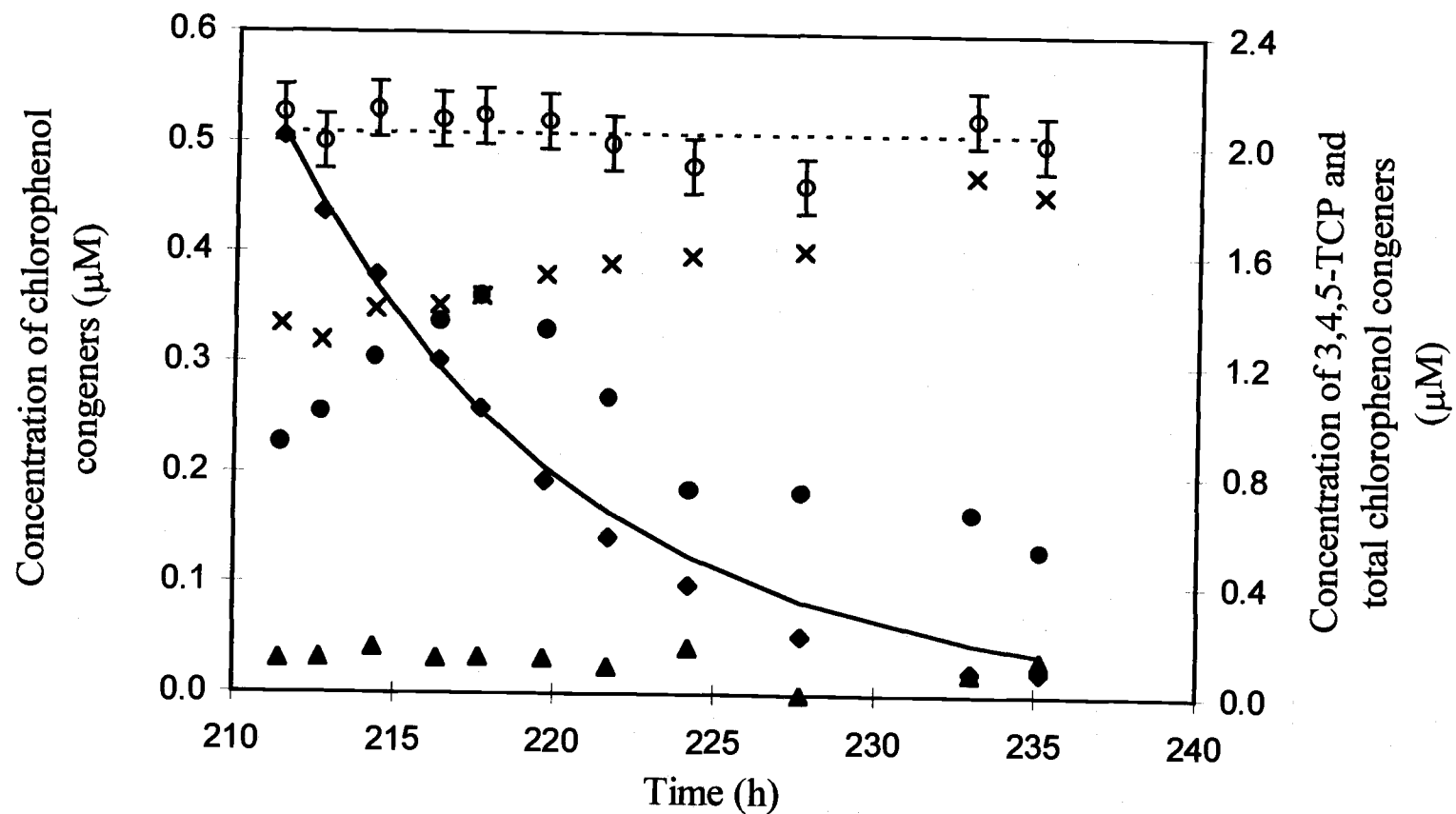


Figure 3.1: Measured (\blacklozenge) and modeled (—) reductive dechlorination of a single addition of PCP compared with 2,3,4,5-TeCP (\bullet); 2,3,4,6-TeCP (\blacktriangle); and 3,4,5-TCP (\times) reductive dechlorination, sum (\circ) \pm one standard deviation and averaged sum (---) of total measurable chlorophenol congeners

Pseudo-first-order Removal

The removal of PCP shown in Figure 3.1 follows pseudo-first-order kinetics. Constant hydrogen headspace concentration was provided and negligible cell growth during the degradation of one spike was assumed so that the reduction can be estimated as first-order with respect to PCP concentration. Simultaneously curve fitting the PCP and 2,3,4,5-TeCP dechlorination data to an exponential model with a least squares estimation method determined both initial substrate concentrations and dechlorination rates (74). The dechlorination rate for the curve shown in Figure 3.1 was calculated to be -0.11 hour^{-1} . An exponential rather than linear fit was chosen because the theoretical model describes a first-order relationship between substrate and dechlorination rate, and visual examination of the data suggests that the degradation is not linear. During one experiment, each PCP spike was modeled according to pseudo-first-order kinetics and a separate rate was calculated for the degradation of each PCP spike.

Five experiments were performed in the computer controlled fed-batch reactor to examine the effects of hydrogen concentration on the rate of reductive dechlorination and on the activity change of a reductively dechlorinating population of bacteria. In each of the reactor experiments, a hydrogen flow rate was set to establish a constant partial pressure of hydrogen in the headspace. This differed for one reactor experiment that was first operated at $5.7 \times 10^{-4} \text{ atm}$ and then at $3.9 \times 10^{-2} \text{ atm}$. With five experiments, a total of six distinct hydrogen partial pressures were examined as shown in Table 3.2. The aqueous concentration in nM was calculated using the Henry's law constant for hydrogen gas in equilibrium with a solution (77). During several reactor study experiments, the increase in hydrogen partial pressure caused a dramatic rise in the rate of reductive dechlorination (data not shown). While qualitative in nature, this data suggested that the concentration of hydrogen, the preferred electron donor, affected the rate of reductive dechlorination.

Table 3.2: Partial pressures of hydrogen and E_H values established during reactor experiments

H ₂ partial pressure (atm)	Calculated equilibrium H ₂ aqueous concentration (nM)	Measured E_H (mV) ¹	Calculated E_H (mV) ²
9.4×10^{-5}	75	-250±10	-300
2.2×10^{-4}	175	-260±10	-311
2.9×10^{-4}	230	-270±30	-315
5.7×10^{-4}	453	-180±40	-323
7.8×10^{-3}	6200	-340±20	-356
3.9×10^{-2}	31,000	-320±40	-379

¹ Measured with duplicate hydrogen electrodes

² Calculated using the Nernst equation ($E = E^\circ - (RT/zF)\ln[(\text{red})/(\text{ox})]$) for $T = 303.15$ K and $\text{pH} = 7$

Apparent E_H

At the beginning of each experiment, the apparent redox potential slowly dropped during the dechlorination of the first PCP spike (first 25 to 100 hours) and then stabilized. A comparison between the hydrogen level and the E_H at which reductive dechlorination began did not show a correlation (data not shown). The apparent E_H in the reactor, as measured by replicate platinum electrodes, was allowed to reach equilibrium with the hydrogen headspace concentration during the course of the experiment. It was difficult to measure the apparent E_H in the reactor over the course of an experiment, and Stuart et al. observed that the redox potential measured by a platinum electrode did not correlate well with H₂ in the media (76). There was no attempt made to establish a correlation between the apparent E_H and hydrogen partial pressure during this study. Still, there was an observable decrease in the measured E_H with the increase in hydrogen partial pressure. The experiment at 5.7×10^{-4} atm of hydrogen did not follow this trend possibly because the reactor

had not yet reached equilibrium. The apparent E_H values measured in the reactor were considerably higher than the calculated reduction electrode potentials as shown in Table 3.2. Higher potentials were indicative of other redox sensitive species that raised the apparent E_H values measurable in the reactor.

Lag Period

The lag period ranged between 25 and 200 hours, and did not appear to correspond with the growth rate of the cells (Table 3.2). Most likely the lag was due to a low initial cell number that would not show measurable substrate utilization until a larger population was grown (Chapter 2). The experimental plan for the reactor experiments in Chapter 3 was based on the initial slow growth of a dilute microbial culture. Different growth rates with varying hydrogen concentrations combined with a different initial cell mass would explain the difference in lag time lengths.

Acceleration of Reductive Dechlorination

A time course study of PCP and 2.2×10^{-4} atm of hydrogen, shown in Figure 3.2, is representative of the observed PCP reductive dechlorination data from the fed-batch reactor studies. This experiment was conducted for over 300 hours during which six spikes of PCP were added to the reactor to yield a concentration of $0.5 \mu\text{M}$ PCP. PCP was added as discrete spikes so that the cumulative addition of PCP was non-continuous. The reactor showed very little reductive dechlorination during the first 100 hours, and that data was not used for Stuart's model. The sum of measured chlorophenol congeners (open circles) equaled the calculated molar addition of PCP stock solution (dotted line).

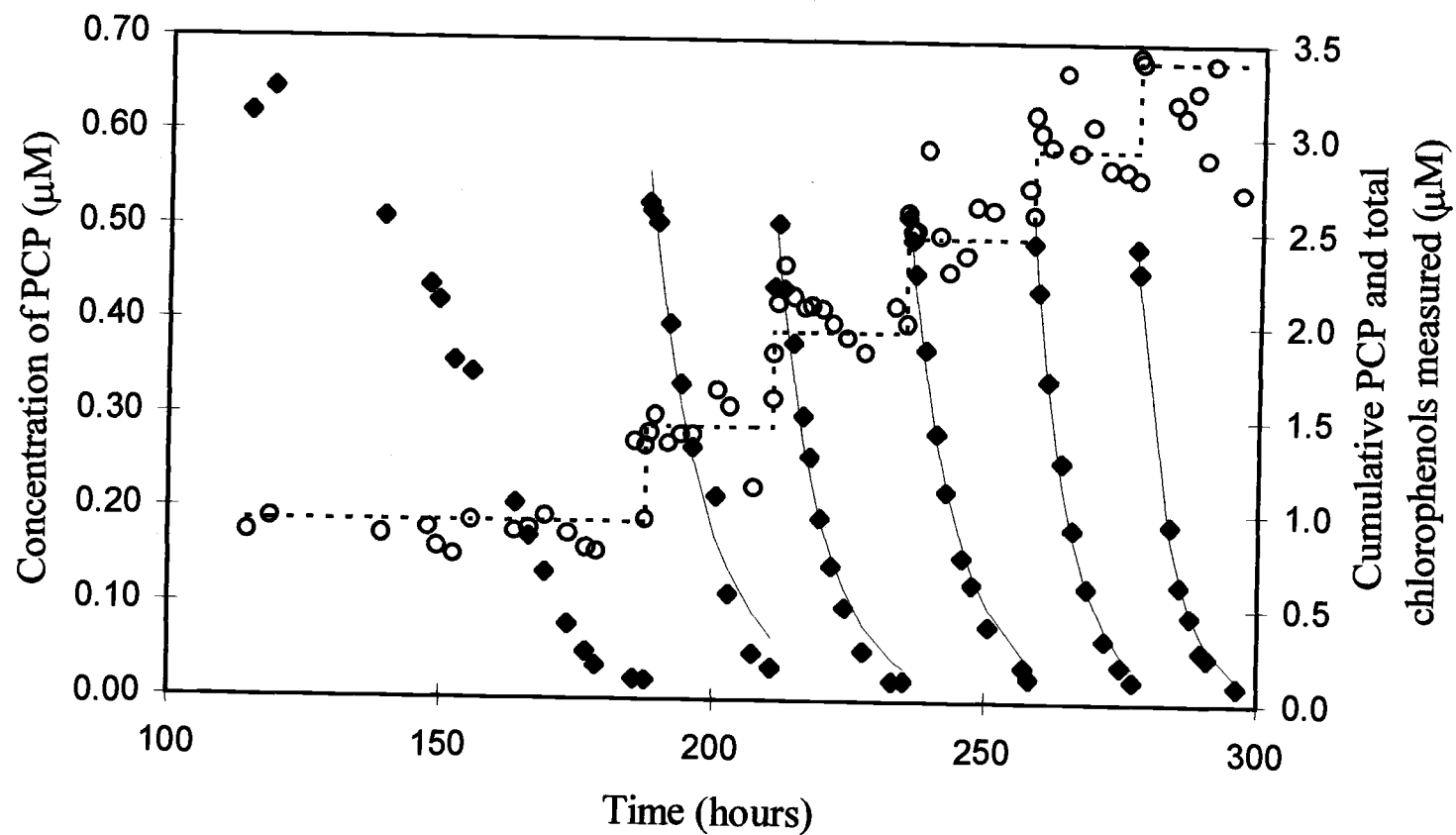


Figure 3.2: Time course study of PCP (◆) reductive dechlorination, sum of measurable chlorophenol congeners (○), and cumulative PCP addition (---) under 2.2×10^{-4} atm of hydrogen

Thus, measured chlorophenol congener concentrations equaled PCP_{in} (Figure 3.2). There was an increase in the measured E_H that corresponded with each addition of PCP stock solution due to oxygen dissolved in the solution. With those exceptions, the E_H remained constant at -260 mV during the incubation. Once begun, PCP reductive dechlorination followed pseudo-first-order kinetics; the rate of degradation decreased with the PCP concentration.

PCP removal curves shown in Figure 3.2 were modeled using Equation 3.1 to calculate first-order rates of reductive dechlorination. Individually measured rates of reductive dechlorination were calculated for removal curves of each PCP spike. Each point in Figure 3.3 represents a reductive dechlorination rate coefficient calculated by a first-order regression of the corresponding PCP dechlorination curve shown in Figure 3.2. Because the first addition of PCP was not used for Stuart's model estimation, there is no rate coefficient that correlates to the first PCP addition shown in Figure 3.2. The first-order PCP reductive dechlorination rates increase exponentially with time as shown in Figure 3.3. According to Stuart's model that exponential increase is indicative of an activity increase in reductively dechlorinating bacteria.

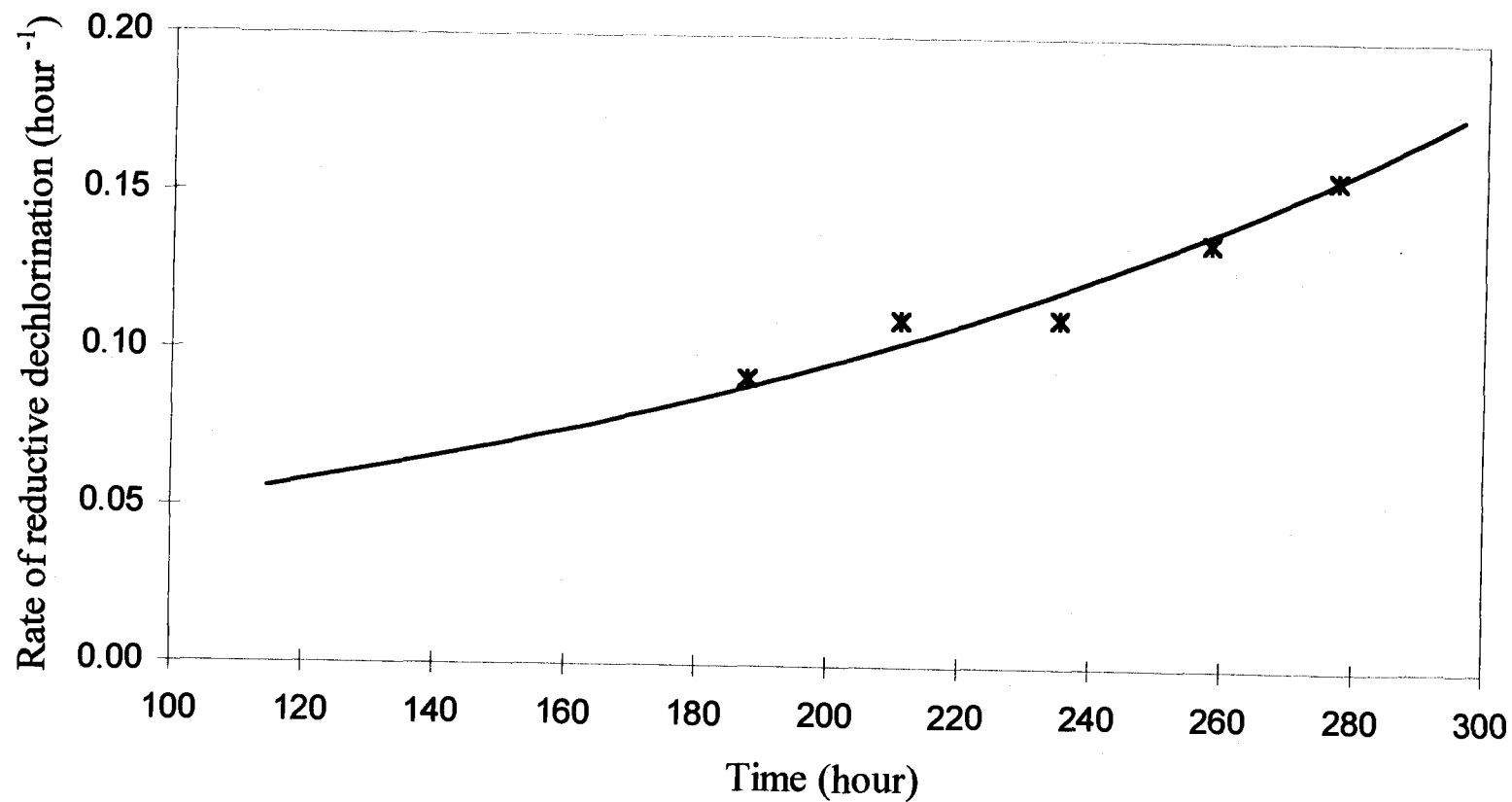


Figure 3.3: Time course study of PCP (*) first-order reductive dechlorination and derived exponential growth curve (—) at 2.2×10^{-4} atm of hydrogen

The acceleration rate was estimated by nonlinear regression using S-Plus (MathSoft, Inc.; 1997-98) statistical software and was used to estimate the cell doubling time. This relationship is supported by the theoretical model and observed results. The acceleration of reductive dechlorination rate was linked to the hydrogen concentration in the reactor. By fitting this data to an exponential curve, the increase in culture activity with time was estimated according to Stuart's model. An acceleration term for PCP reductive dechlorination from Equation 3.3, α , was equal to $0.0056 \pm 0.0010 \mu\text{M PCP h}^{-2}$ at a hydrogen partial pressure of 2.2×10^{-4} atm. The effect of hydrogen headspace concentration on the rate of reductive dechlorination and growth rate of reductively dechlorinating bacteria was evaluated using this method.

The four additional reactor experiments were performed and tested five additional hydrogen concentrations (Figure 3.4 to Figure 3.13). In each of these experiments, the first PCP addition shown in each figure was not used for the analyses. Data taken prior to the beginning of reductive dechlorination in the reactor was not shown in any of the figures for improved clarity. The experiment performed at 2.9×10^{-4} atm showed PCP concentrations held between a smaller range of 0.35 and 0.07 μM as shown in Figure 3.6. The discrepancy between the sum of measurable congener concentrations and the cumulative PCP addition in Figure 3.12 was due to the degradation of PCP metabolites while the hydrogen partial pressure was being established for this experiment after the experiment at 5.7×10^{-4} atm of hydrogen (Figure 3.8).

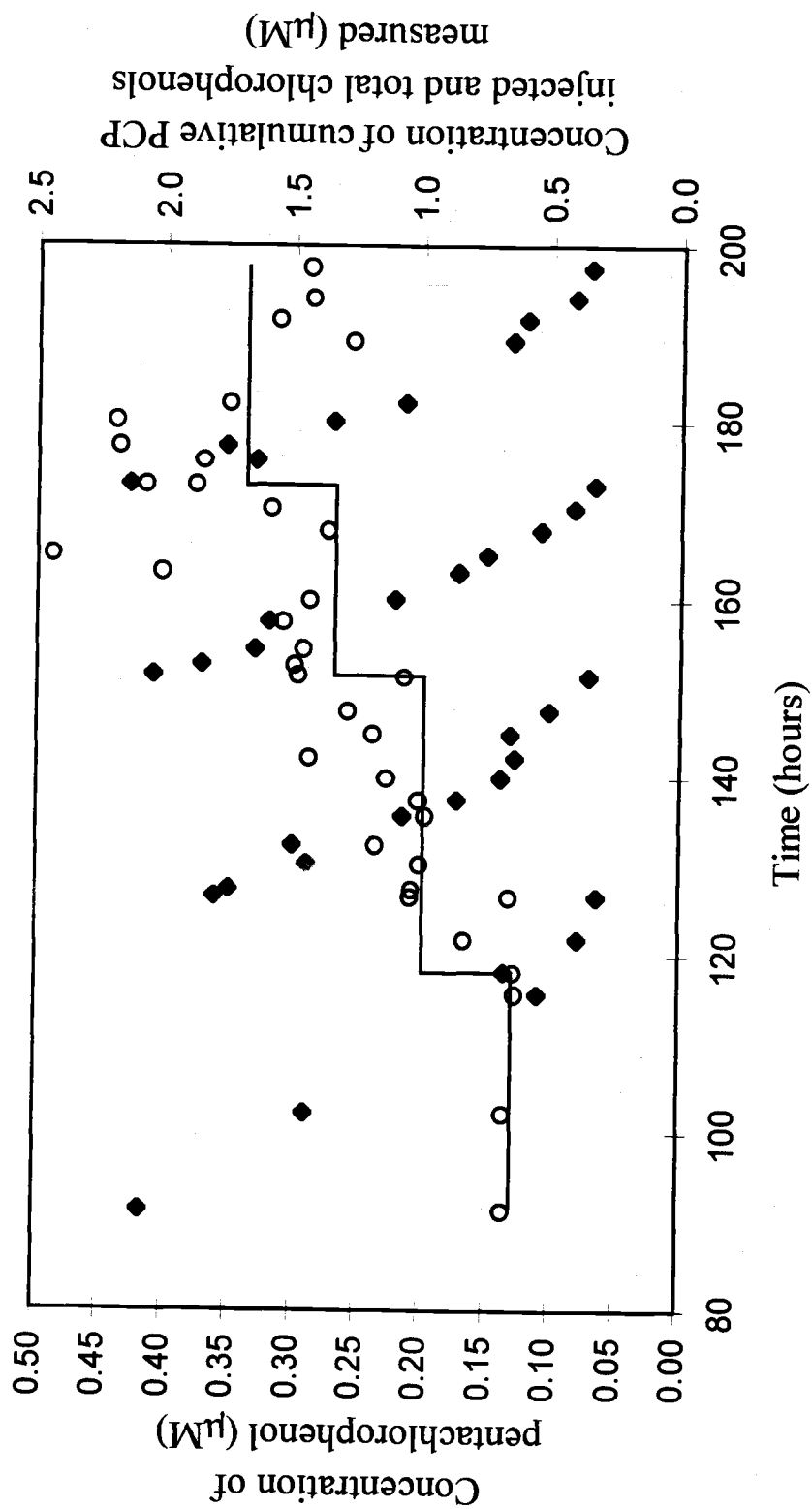


Figure 3.4: Time course study of PCP (◆) reductive dechlorination, sum of measurable chlorophenol congeners (○), and cumulative PCP addition (—) under 9.4×10^{-5} atm of hydrogen

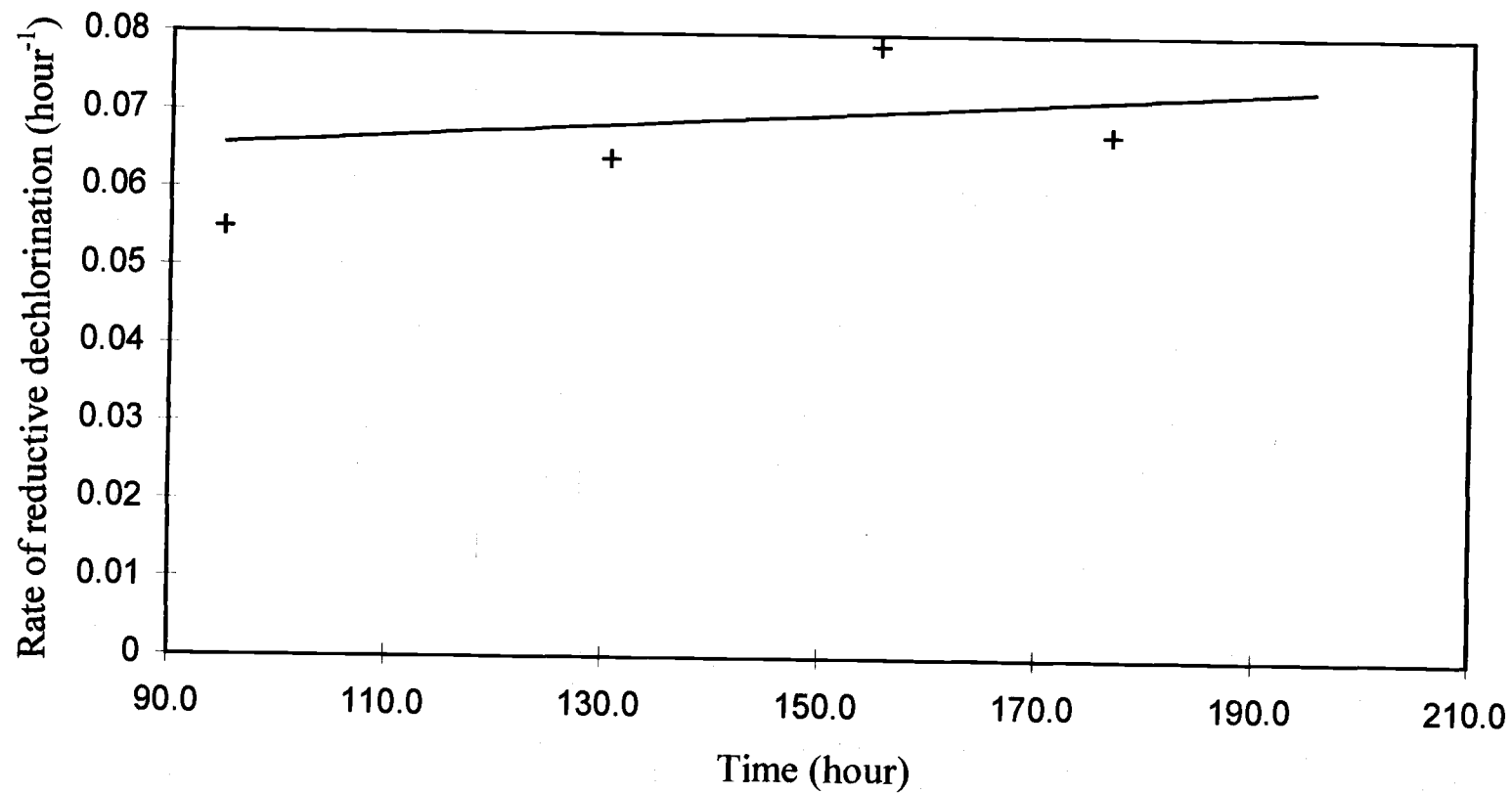


Figure 3.5: Cell growth estimation based on the acceleration of PCP reductive dechlorination rate (+) at 9.4×10^{-5} at of hydrogen

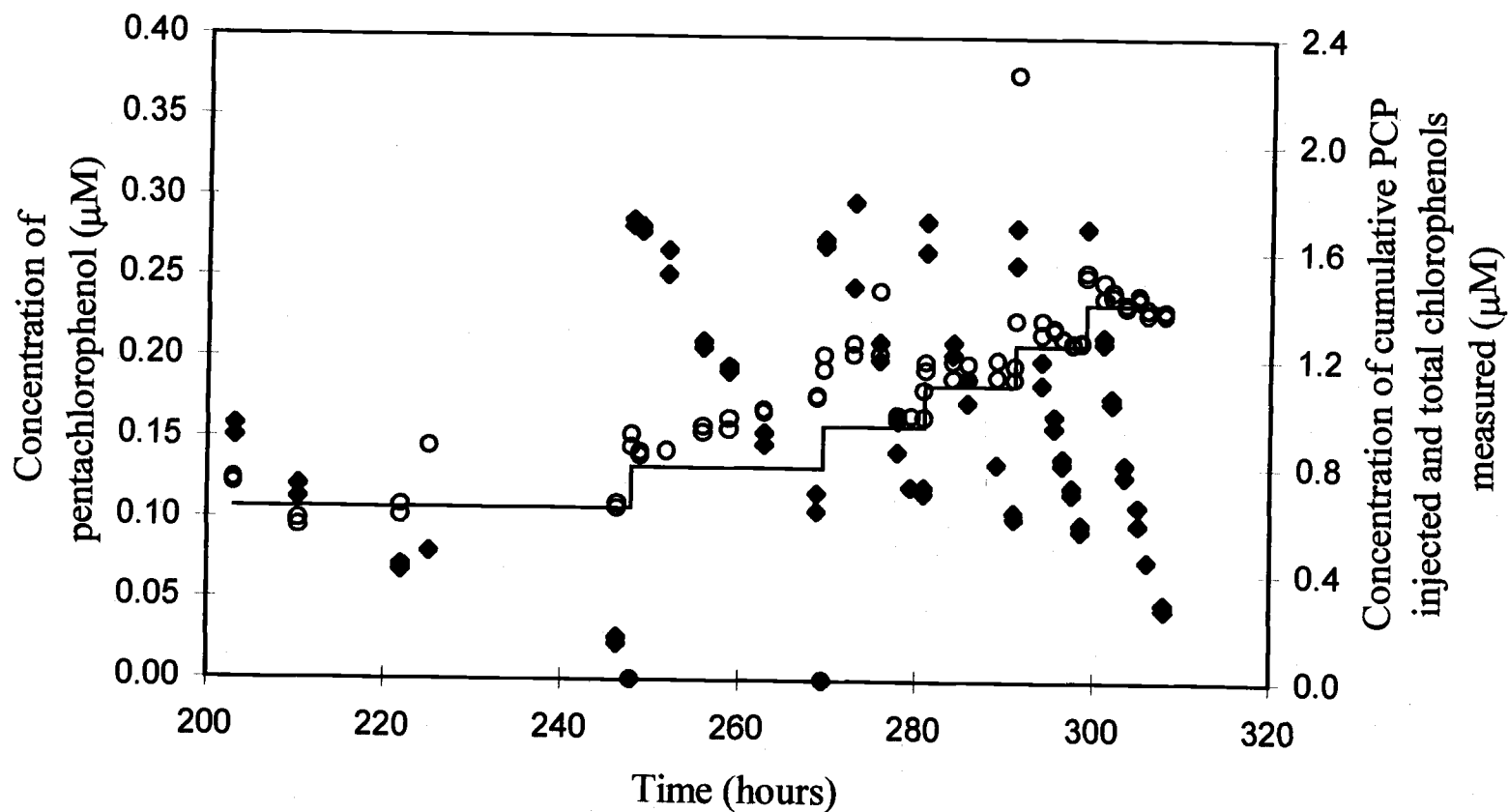


Figure 3.6: Time course study of PCP (◆) reductive dechlorination, sum of measurable chlorophenol congeners (○), and cumulative PCP addition (—) under 2.9×10^{-4} atm of hydrogen

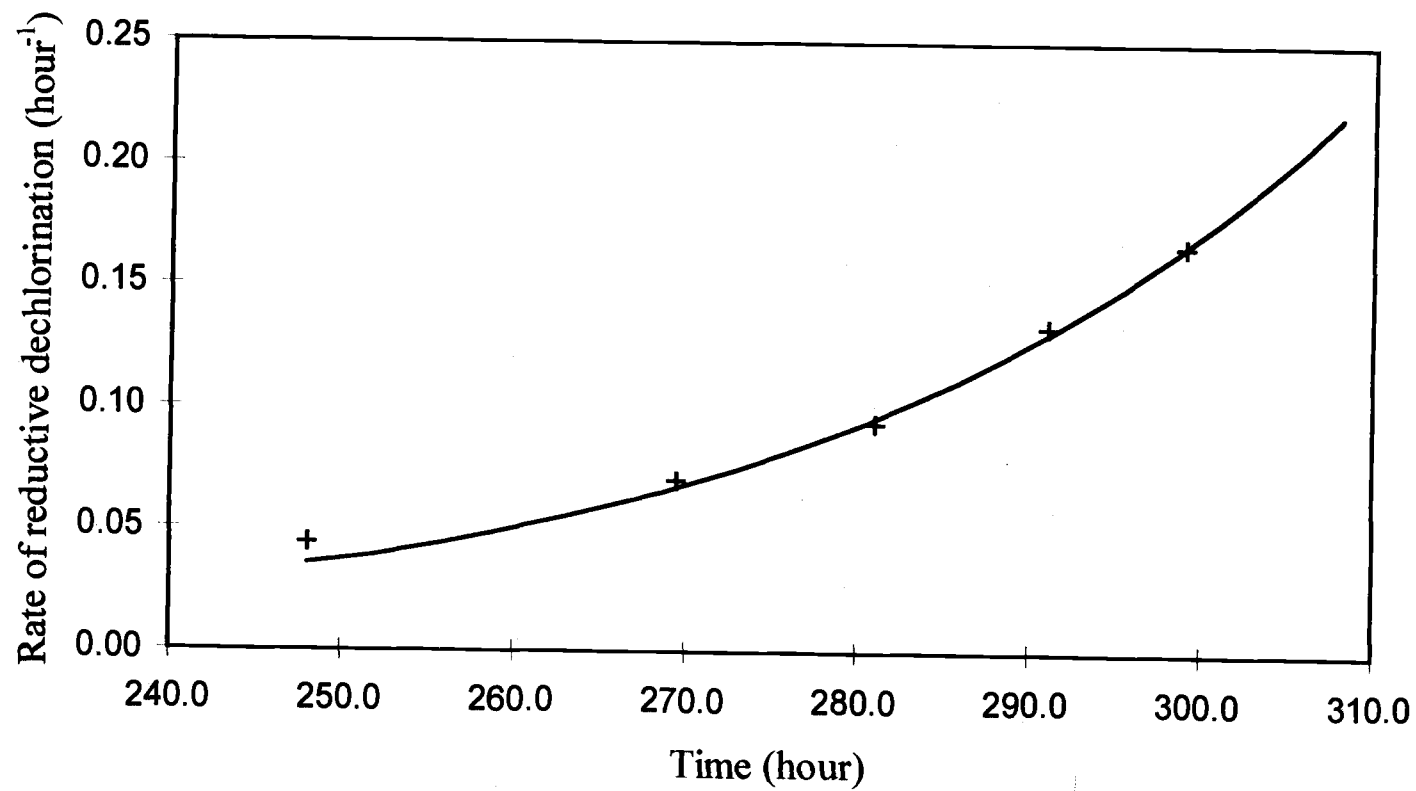


Figure 3.7: Cell growth estimation based on the acceleration of PCP reductive dechlorination rate (+) at 2.9×10^{-4} atm of hydrogen

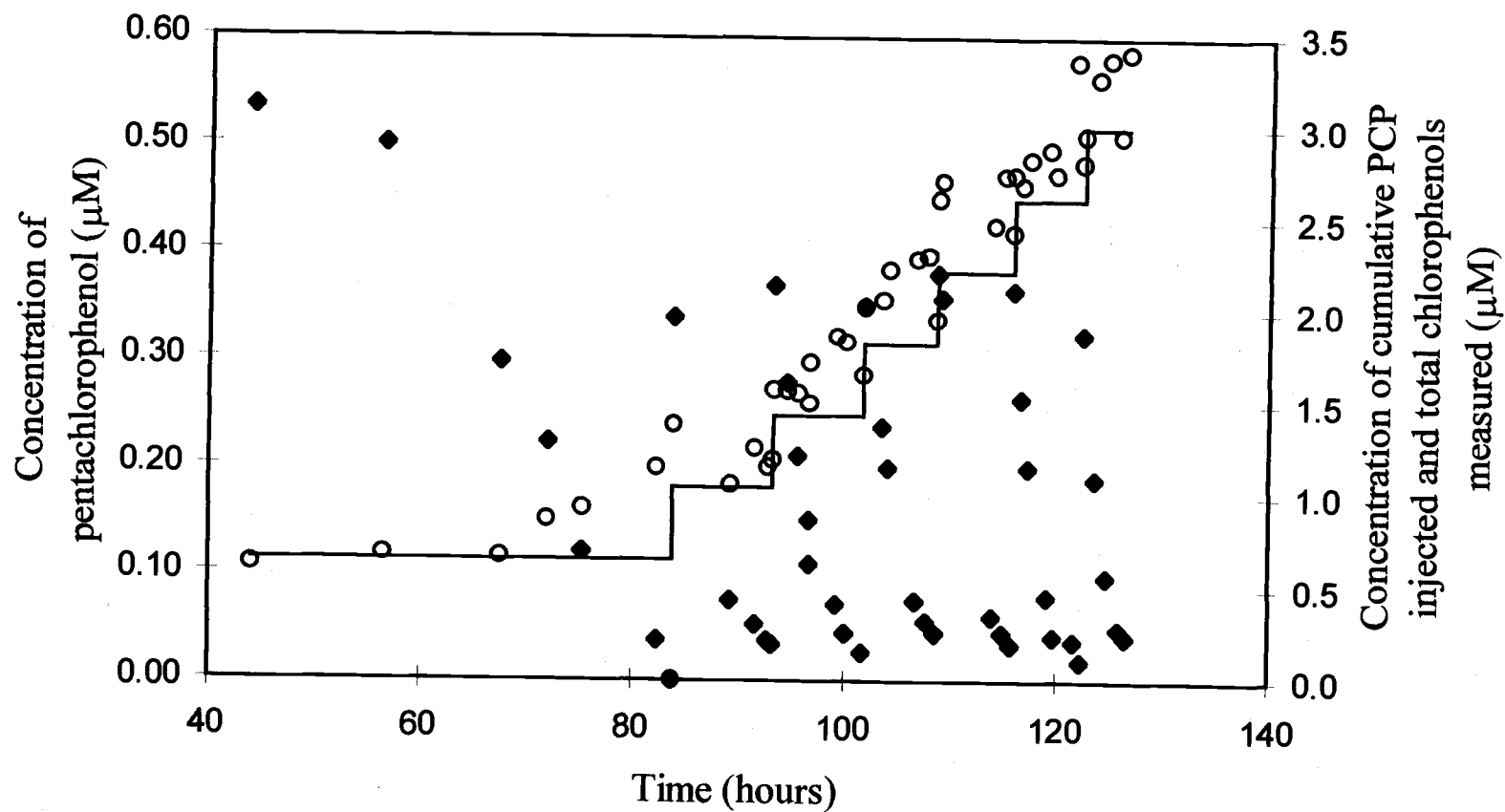


Figure 3.8: Time course study of PCP (◆) reductive dechlorination, sum of measurable chlorophenol congeners (○), and cumulative PCP addition (—) under 5.7×10^{-4} atm of hydrogen

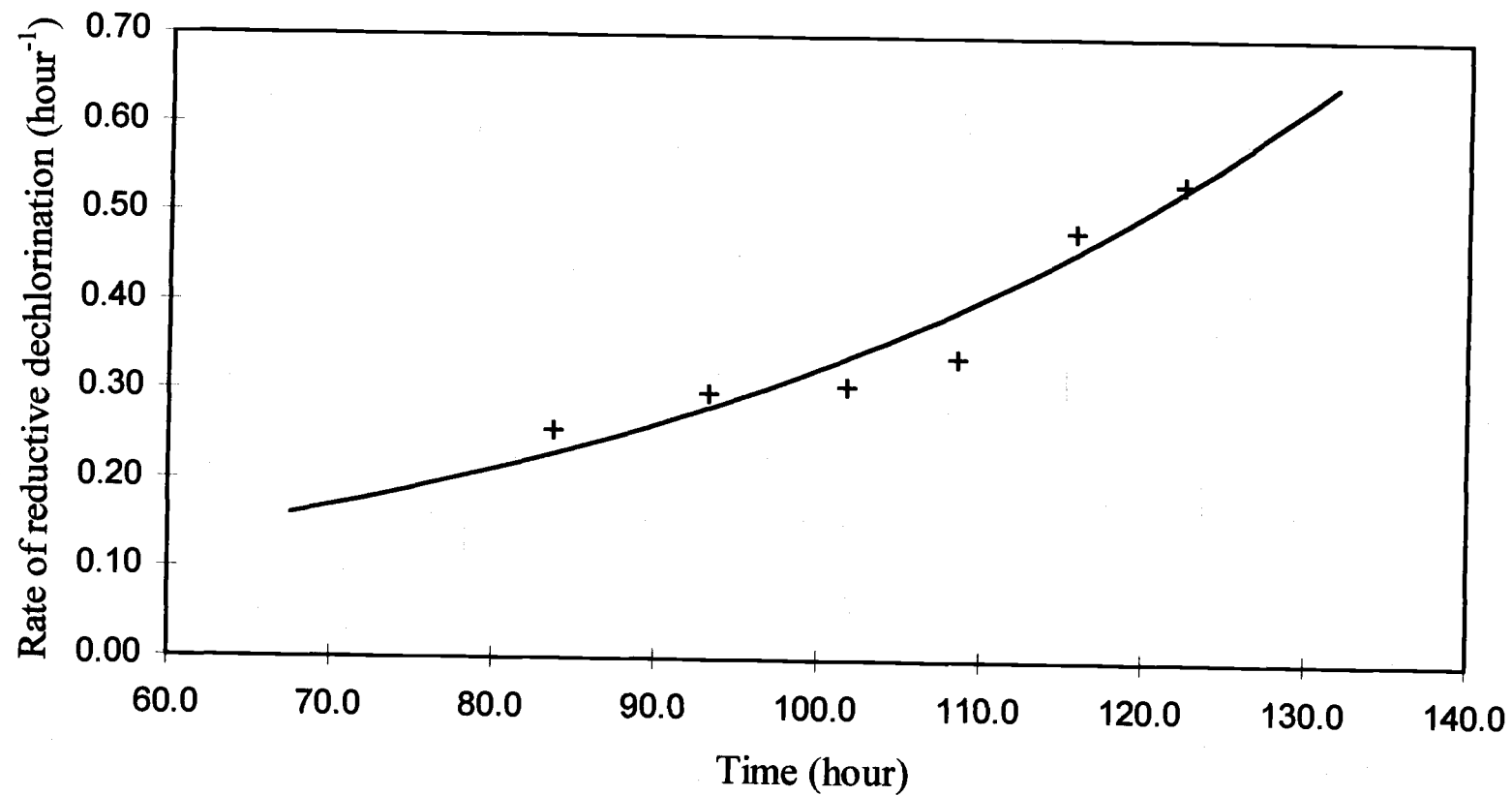


Figure 3.9: Cell growth estimation based on the acceleration of PCP reductive dechlorination rate (+) at 5.7×10^{-4} atm of hydrogen

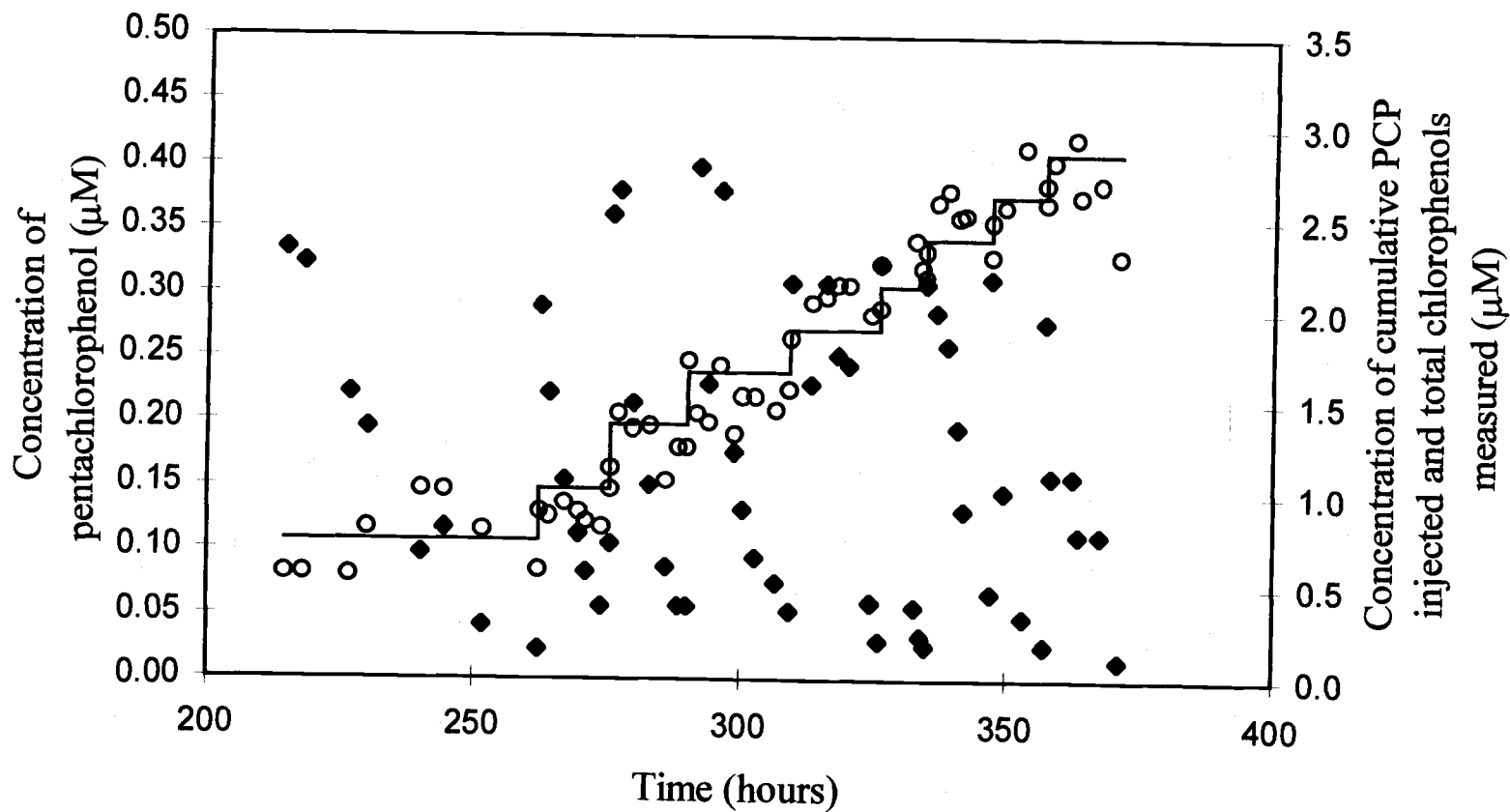


Figure 3.10: Time course study of PCP (◆) reductive dechlorination, sum of measurable chlorophenol congeners (○), and cumulative PCP addition (—) under 7.8×10^{-3} atm of hydrogen

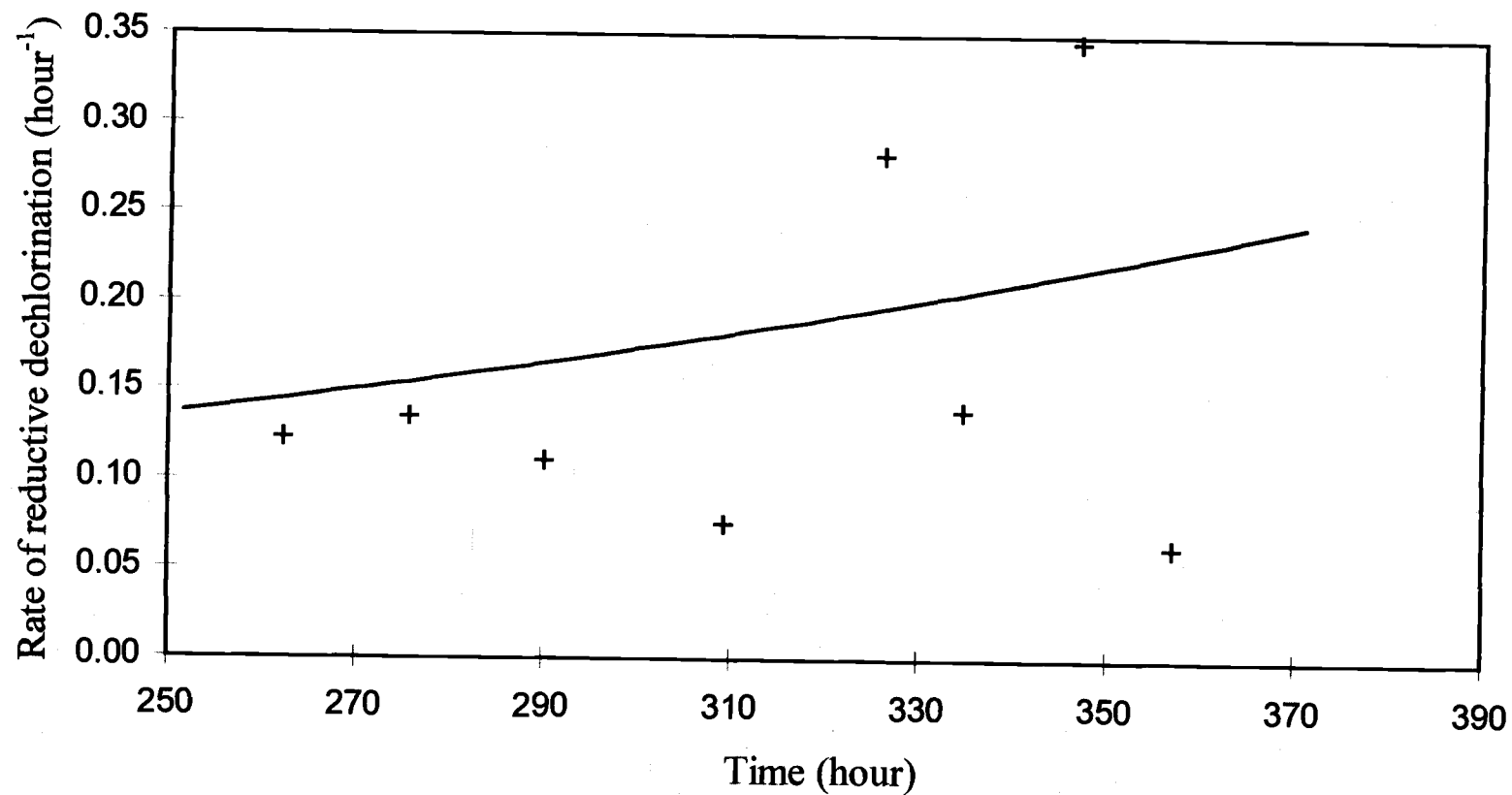


Figure 3.11: Cell growth estimation based on the acceleration of PCP reductive dechlorination rate (+) at 7.8×10^{-3} atm of hydrogen

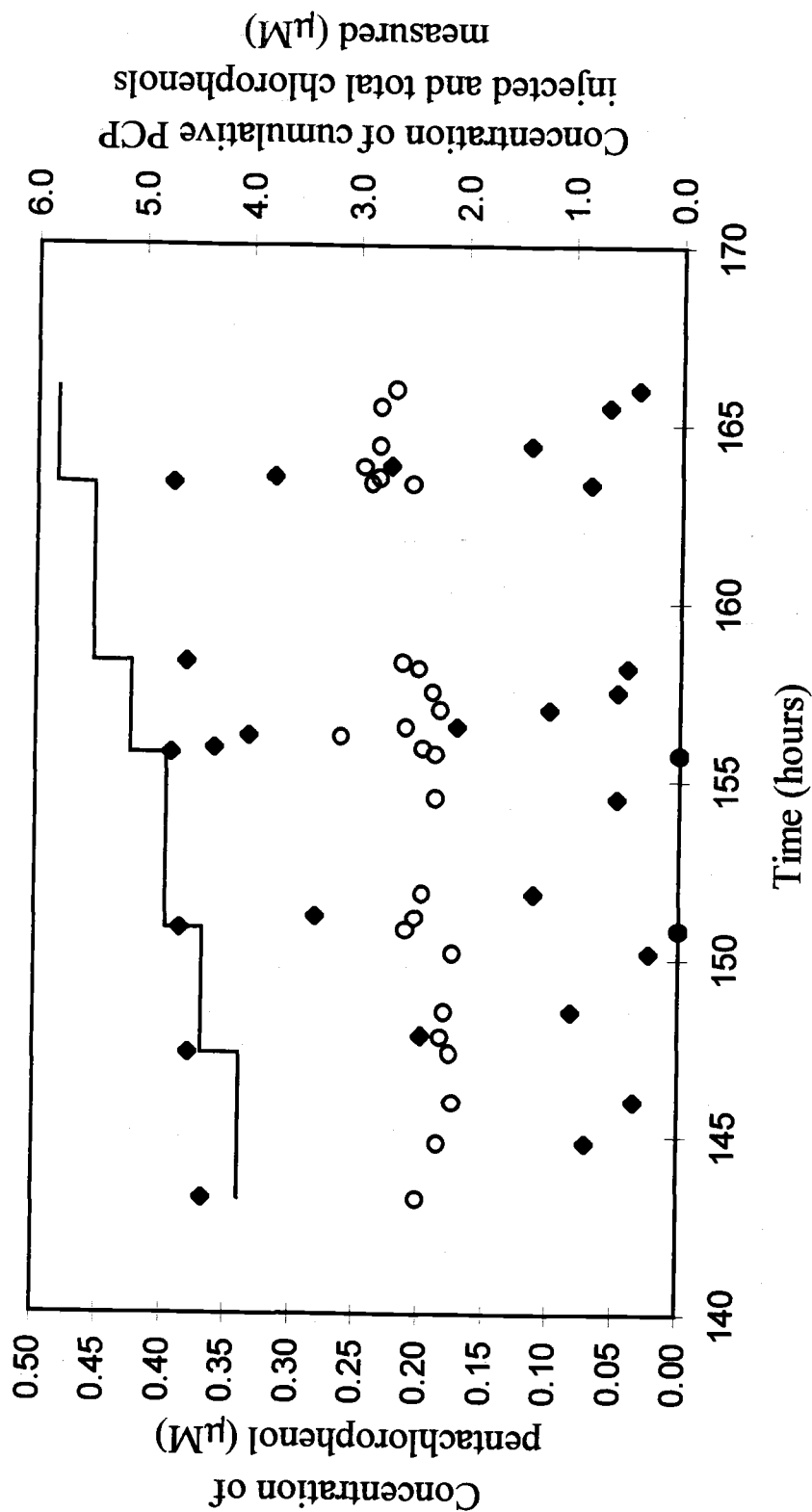


Figure 3.12: Time course study of PCP (◆) reductive dechlorination, sum of measurable chlorophenol congeners (O), and cumulative PCP addition (—) under 3.9×10^{-2} atm of hydrogen

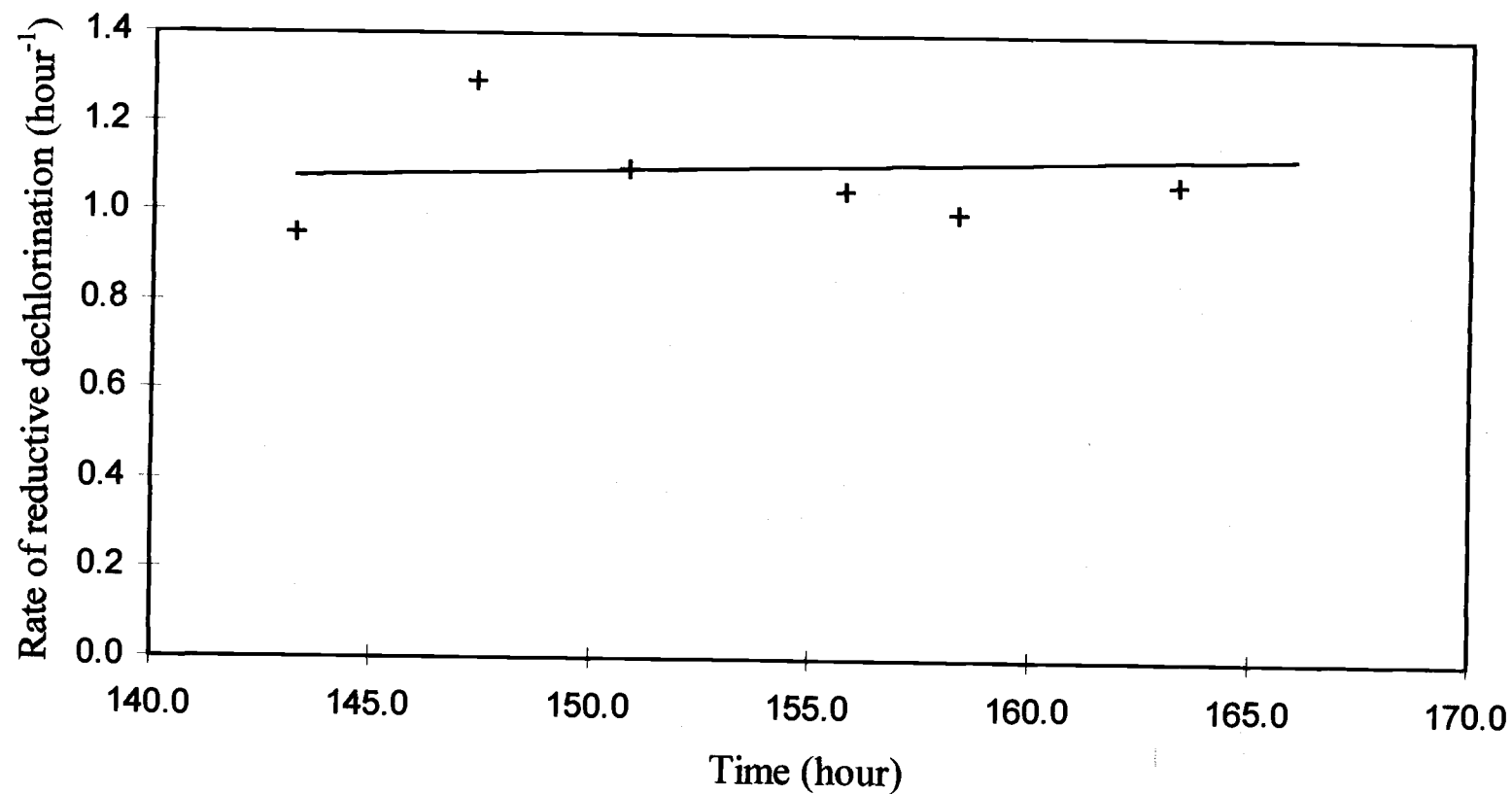


Figure 3.13: Cell growth estimation based on the acceleration of PCP reductive dechlorination rate (+) at 3.9×10^{-2} atm of hydrogen

Acceleration rates were calculated for PCP dechlorinating cultures that were incubated at different hydrogen partial pressures as shown in Table 3.3. The values were reasonable and compared well with vinyl chloride experiments in the literature that showed an exponential increase of 0.019 hour^{-2} (64). These values are used to correlate the competitiveness of reductively dechlorinating bacteria in a mixed culture at different hydrogen partial pressures. Stuart's exponential curve fits were used to determine the activity doubling times at each of the hydrogen concentrations. All values were determined using S-Plus statistical software (MathSoft, Inc.; 1997-98). Degrees of freedom, 2-sided p-values, and standard errors are reported in Table 3.3. The standard error represents the error associated with predicting one dependent value at an individual independent value. It shows the range within the determined value may lie with certainty.

Table 3.3: A comparison of doubling time and hydrogen concentration

H ₂ (atm)	9.4×10^{-5}	2.2×10^{-4}	2.9×10^{-4}	5.7×10^{-4}	7.8×10^{-3}	3.9×10^{-2}
Stuart's α	0.0011	0.0056	0.0302	0.0216	0.0054	0.0020
standard error	0.0048	0.0010	0.0012	0.0034	0.0076	0.0173
df ¹	1	3	2	4	6	2
2-sided p-value	0.8616	0.0097	0.0015	0.0032	0.5068	0.9171
τ_{double} (days) ²	27	5.1	0.96	1.3	5.4	14

¹ degrees of freedom

² doubling time

The two sided p-values are used to help determine the significance of a conclusion. As the p-value decreases the analysis is considered more reliable while a p-value of 1 means that the number was determined by random chance. Most researchers consider a p-value < 0.05 good (5.0% chance) and any value below 0.01

is considered very good. These statistics help in determining how well the experimental data fit to the exponential growth model. The experiments performed at the highest and lowest hydrogen concentration show very poor p-values. This is reasonable because of a low number of points used to fit the curve and the very slow acceleration of the rate data during these experiments (Figure 3.5 and Figure 3.10). The experiment performed at a hydrogen partial pressure of 7.8×10^{-3} atm showed a better but still uncertain relation with a p-value of 0.5068 that could be attributed to scatter in the data. The three estimations made at a more moderate hydrogen concentration showed a very good correlation all with p-values below 0.01.

Hydrogen and the Growth of Reductively Dechlorinating Bacteria

The theoretical growth rate of PCP reductively dechlorinating bacteria with respect to hydrogen was calculated assuming a dual Monod relationship between growth and both PCP and hydrogen concentration. Calculations based on this relationship estimated the theoretical growth response of a culture that grows on hydrogen and PCP. The resulting curve, shown in Figure 3.14, was generated by equating: PCP concentration to 0.06 mg/L, Yield to 0.039 mg/mg-L, decay to 0.002 hour⁻¹, $K_s(\text{PCP})$ to 0.12 mg/L, $K_s(\text{H}_2)$ to 0.0005 atm, and k_{\max} to 3.42 mg/mg-hour and varying hydrogen partial pressure between 1×10^{-5} and 1×10^{-2} atm as based on preliminary results described in Appendix A. All values were based on those in the literature and used for other simulated experiments (Appendix Table A.2). A more complete explanation of the model is described in Appendix H. At low hydrogen concentrations, hydrogen limits the rate of reductive dechlorination, and at high hydrogen concentrations, PCP is rate limiting. The inflection point in the curve representing acceleration showed the point where the growth rate of the bacteria change from first-order to zero-order with respect to hydrogen. The hydrogen level at which an inflection point in this data occurred was at 5×10^{-4} atm as determined by the model fit and shown in Figure 3.14.

The dual Monod model shown in Figure 3.14 assumes that one bacterial population was being maintained. When more than one bacterial species is present, competition for substrate determines which species grow and which are dormant. For example, methanogens can compete for hydrogen and reduce the effectiveness of added electron donors (30). Other studies showed the possibility of uncoupling reductive dechlorination from growth (49). While the dual Monod model showed that at low hydrogen partial pressures the growth of reductively dechlorinating bacteria slowed, competition for substrates provides one reason that growth may

slow at higher hydrogen partial pressures, and changes in metabolism provides another.

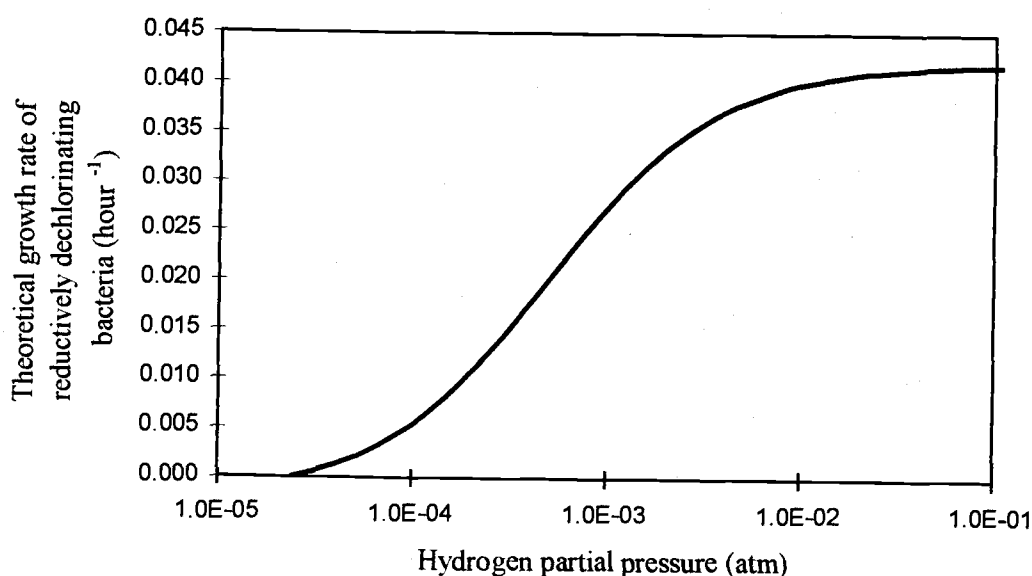


Figure 3.14: Computer simulation of growth rate as a function of hydrogen partial pressure based on dual Monod kinetics

Some substrates inhibit bacteria with increasing concentration. Those substrate kinetics can be explained with an adjustment to the Monod kinetic model. This model implies that at low substrate concentrations there is no inhibition, but as the concentration increases, the inhibition term becomes important. The dual Monod model described above was combined with a substrate inhibition model resulted in Figure 3.15. The growth rate of the organisms increase with increasing substrate until the inhibition term becomes large and begins to slow growth. As the substrate inhibition term declines from 0.0020 atm to 0.0005 atm the inhibition occurs at lower hydrogen partial pressures.

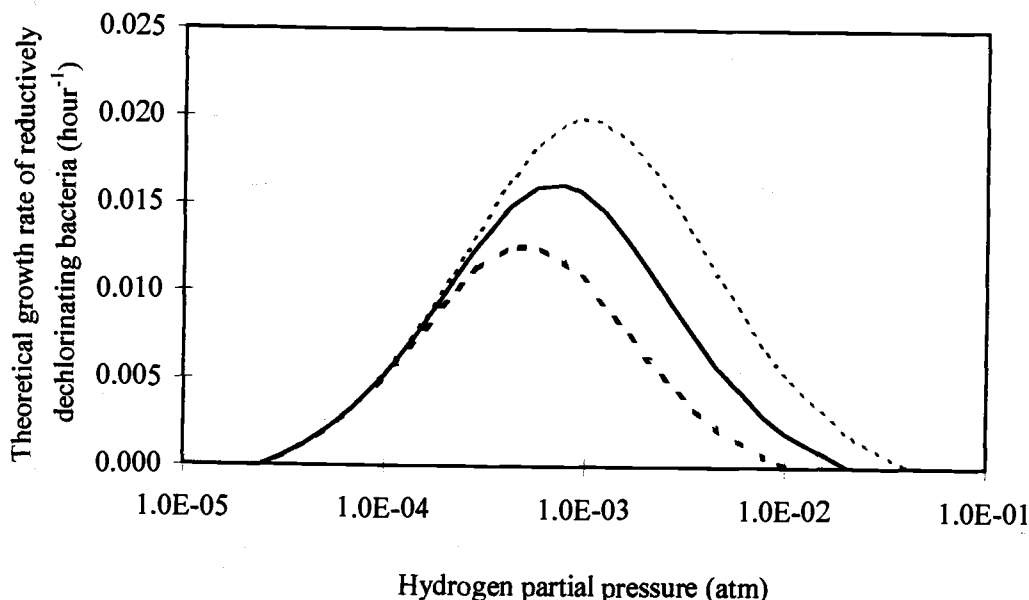


Figure 3.15: Computer simulation of growth rate as a function of hydrogen partial pressure based on dual Monod kinetics with substrate inhibition term of 0.0020 (· · ·), 0.0010 (—), and 0.0005 (— —) atm

The correlation between hydrogen and observable growth was shown by change in the reductive dechlorination acceleration with hydrogen as shown in Figure 3.16. The experimental data was plotted with the substrate inhibition model for comparison. The data and model provided the similar results even when confidence intervals were large. The acceleration of culture activity increased with increasing hydrogen until a maximum experimental value of 2.9×10^{-4} atm (Figure 3.16). The acceleration of reductive dechlorination and the estimated growth changed as a function of the hydrogen partial pressure. The theoretical curve (Figure 3.15) and actual data (Figure 3.16) shared a similar maximum growth rate of about 0.02 hour^{-1} at a hydrogen partial pressure of about 1.0×10^{-3} atm. Above the hydrogen partial pressure of 1.0×10^{-3} atm, the theoretical curve shows a peak and decline in growth rate like the experimental data. The observed relationship suggested that the system and substrate inhibition model were similar.

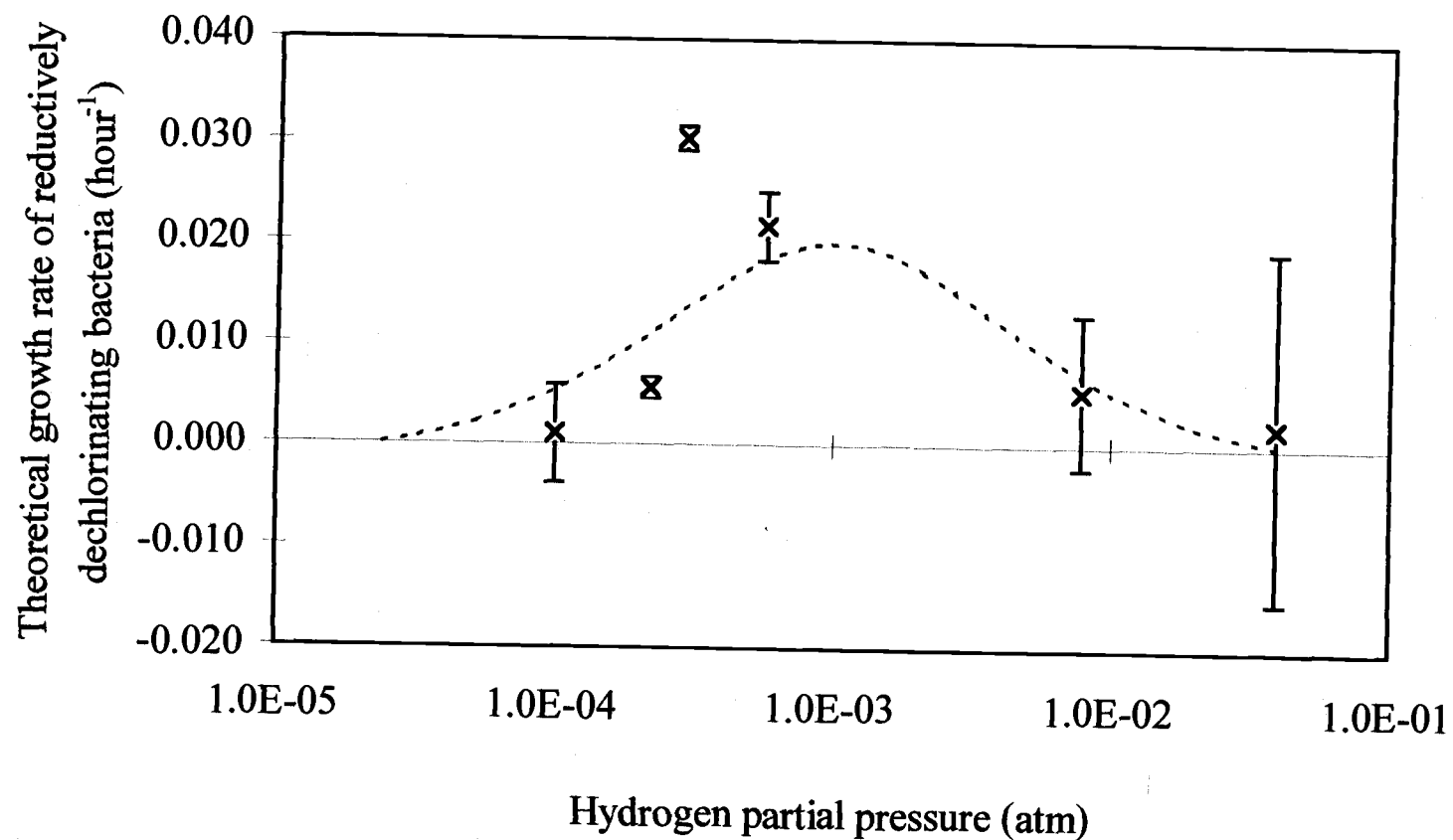


Figure 3.16: Apparent growth rates of reductive dechlorination \pm one standard error estimated compared with a substrate inhibition model when $K_i = 0.0020$ atm and $K_H = 0.0005$ atm (---)

This could be because hydrogen was inhibitory or other organisms began to compete with reductively dechlorinating bacteria at high partial pressures.

Cell Growth

The acceleration of the reductive dechlorination rate was used to estimate the activity increase of reductively dechlorinating bacteria at each of the established hydrogen partial pressures. The α value can be used to calculate an activity doubling time for the sub-population – equal to the natural log of 2 divided by the α value Equation 3.6. There was an increase in the apparent growth rate of the reductively dechlorinating organisms with an increase in the hydrogen concentration as shown by the decrease in the doubling times in Figure 3.17. Because growth of cells was the only factor that could be attributed to the acceleration of reductive dechlorination, the change in rate of reductive dechlorination could be assumed to represent culture doubling time. The partial pressure of hydrogen of each time course study, was compared with the estimated doubling times for the reductively dechlorinating bacteria (Table 3.3). The doubling times ranged between 0.94 and 27 days. The minimum doubling time of 0.94 occurred at a hydrogen partial pressure of 2.9×10^{-4} atm.

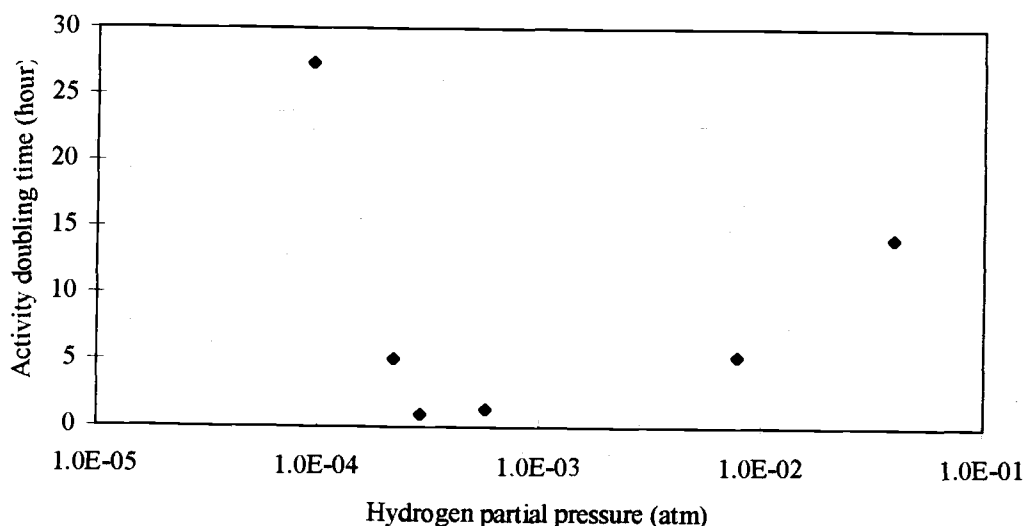


Figure 3.17: Activity doubling times calculated from apparent growth rates.

Measured doubling times of reductively dechlorinating bacteria agree with values reported in literature as shown in Table 3.4. Stuart determined an average doubling time of PCP reductively dechlorinating bacteria in mixed methanogenic cultures of 1.7 days (1.3 - 2.4 days) (74). *Desulfomonile teidjei* cultures show a doubling time between 1.1 and 3.2 days (16). *Desulfitobacterium hafniense* has a doubling time of about 2 days when grown with pyruvate and yeast extract (46). A 2-chlorophenol reductively dechlorinating population shows a doubling time of 3.7 days (10).

Table 3.4: Doubling times of reductively dechlorinating organisms

Culture	Doubling time	Reference
<i>Desulfomonile teidjei</i>	1.1 and 3.2 days	(16)
<i>Desulfitobacterium hafniense</i>	2 days	(46)
2-chlorophenol reductively dechlorinating population	3.7 days	(10)
PCP reductively dechlorinating mixed methanogenic culture	1.3 - 2.4 days	(74)

Cell Decay

Cell decay was estimated as described in the Data Analysis section. The reactor proved effective at measuring the decay rate of reductively dechlorinating bacteria. Using Equation 3.7, the decay rate, b , was determined by experiments performed in the reactor. An initial PCP reductive dechlorination rate was determined for the reactor system just prior to a pause in PCP additions. After some time, t , PCP was added and a new PCP reductive dechlorination rate was measured. The difference in the two rates was used to calculate a decay rate based on an exponential growth equation. After two reactor experiments, the decay was determined to be $0.07\text{-}0.22\text{ day}^{-1}$ as shown in Table 3.5. Because the decay rate of specific cultures should be higher than that of a general mixed culture, this agrees well with literature values that estimate cell decay to be 0.05 day^{-1} for mixed microbial cultures.

Table 3.5: Decay rate analysis

Hydrogen Partial Pressure (atm)	Initial k (estimated) (hour^{-1})	Final k (measured) (hour^{-1})	Time (hours)	Decay Rate (day^{-1})
2.2×10^{-4}	0.18	0.13	33	0.22
7.8×10^{-3}	0.20	0.08	305	0.07

Discussion

PCP Reductive Dechlorination

In the fed-batch reactor system, PCP is sequentially dechlorinated while consuming hydrogen. The predominant pathway followed the removal of an *ortho*-positioned chlorine molecule on PCP to form 2,3,4,5-TeCP. The second *ortho*-positioned chlorine was removed to form 3,4,5-TCP. To a small degree, subsequent dechlorination at the *meta*- and *para*-positions produced 3,5-DCP and 3,4-DCP, which appeared to be further dechlorinated.

This study showed the effects of hydrogen concentration on reductive dechlorination as catalyzed by a population of soil bacteria in a mixed culture. Changes in the rate of reductive dechlorination and growth of reductively dechlorinating bacteria as a function of hydrogen partial pressure were examined by measuring substrate utilization.

When supplied hydrogen as the electron donor and PCP as the electron acceptor, the mixed soil bacterial cultures showed the sustained ability to reductively dechlorinate PCP. Experiments ran for up to 400 hours and continued to show accelerated reductive dechlorination until the experiments were ended. The consortia demonstrated this ability under an array of hydrogen concentrations including those much higher than previously examined. This mixed soil bacterial culture reductively dechlorinated PCP and 2,3,4,5-TeCP at hydrogen partial pressures between 9×10^{-5} and 4×10^{-2} atm. All hydrogen partial pressures examined stimulated reductive dechlorination.

The growth of these organisms on exogenously supplied hydrogen showed that this electron donor effectively supported growth of reductively dechlorinating bacteria. Research showed that H₂-PCE enrichment cultures can be transferred

indefinitely with hydrogen as the electron donor (50). Stuart et al. showed that PCP reductive dechlorination by methanogenic cultures is limited by the accumulation of toxic metabolites like 3,4,5-TCP rather than the loss of a metabolic process due to the use of exogenous hydrogen (74). In this study, experiments were completed before 3,4,5-TCP toxicity was observed.

Pseudo-first-order Removal

The removal curves and the theoretical assumptions made to develop the reductive dechlorination rate model agreed well with this analysis. The reductive dechlorination of each PCP spike conformed to pseudo-first-order kinetics at these concentrations. Experimental design kept the substrate concentration within the limits of the first-order region. Subsequently, the reactor system acted in the first-order region as expected.

The concentration of hydrogen, the preferred electron donor, affected the rate of reductive dechlorination. Qualitative comparisons of reductive dechlorination rates before and after an increase in hydrogen partial pressure showed rate increases. This agreed with other observations that show reductive dechlorination of PCE follows Michaelis-Menten enzymatic kinetics at hydrogen concentrations between 1×10^{-5} and 5×10^{-4} atm (4). Other researchers agree that the addition of hydrogen increases the rate of reductive dechlorination (5, 6, 59). For cellular systems, Monod kinetics explains the relationship between substrate and rate such that an increase in substrate, like hydrogen, produces an increase in rate until some maximum value is reached.

Acceleration of Reductive Dechlorination

In the reactor system, environmental conditions that affect the rate of reductive dechlorination were held constant except for PCP concentration and cell growth. It was assumed that over the course of one PCP spike, cell growth remained negligible. Despite measurable changes, the PCP concentration over the course of an entire reactor experiment was treated as a constant average value. With these assumptions, acceleration of the rate of reductive dechlorination successfully estimated the growth rate of reductively dechlorinating bacteria in a mixed culture. Over the course of an experiment, the rate of reductive dechlorination increased, and this acceleration showed a correlation with the partial pressure of hydrogen.

There is a measurable increase in the rate of reductive dechlorination with substrate additions that fit an exponential growth model. By keeping other environmental factors such as E_H , pH, acetate, and temperature constant, the major change accountable for the rate of reductive dechlorination accelerating is growth of reductively dechlorinating bacteria. The apparent growth rate increases, until a maximum value, with increasing amounts of hydrogen in the headspace. Above that optimum hydrogen value apparent growth rates decrease while reductive dechlorination rates continue to increase. For a qualitative example, an increase in hydrogen concentration above 1×10^{-3} atm during one incubation resulted in a dramatic rise in the reductive dechlorination rate, but the subsequent acceleration of PCP reductive dechlorination rates observed was decreased.

While the optimal hydrogen partial pressure may differ with experimental systems, the trend is significant. The relationship between rates of reductive dechlorination and substrate is important to the design of a bioremediation strategy. There is an optimal hydrogen concentration, approximately 1.0×10^{-3} atm, above which there will not be an appreciable increase in reductive dechlorination rates, and the growth rate of reductively dechlorinating bacteria decline.

Experimentally, the observed acceleration of reductive dechlorination decreased as the hydrogen concentration increased above 2.9×10^{-4} atm. Importantly, while the apparent growth rates observed above that hydrogen concentration decreased, rates of reductive dechlorination continued to increase. The dominance of other organisms at higher hydrogen partial pressures such as methanogens reduce the effectiveness of added electron donors (30). In addition, by raising the hydrogen concentration and allowing the growth of other organisms, nutrient limitation in the reactor could have become an issue. This is not believed to be significant because the rates of reductive dechlorination continued to increase with time and the experiments were performed over a short enough period in a nutrient rich medium to prevent limitations.

Other studies showed the uncoupling of reductive dechlorination and growth (49). At high hydrogen partial pressures cell growth may be inhibited even if enzymatic function remains high. Other anaerobic bacteria show decreased yield with increased hydrogen concentrations even when cell activity is stimulated. Research on anaerobic bacteria shows that an acetogenic organism produced fewer cells even though hydrogenase activity increased when the dissolved hydrogen concentration was raised above 28,000 nM (56). At a hydrogen partial pressure of 2.0×10^{-3} atm, equal to a dissolved concentration of 1600 nM, *Methanotarcina thermophila* TM-1 ceased to grow. The isolate DCB-1 consumed hydrogen during reductive dechlorination only when hydrogen partial pressure was below 2.64×10^{-2} atm (38). The decrease in observable growth rates with increasing hydrogen concentration indicated an effect of high hydrogen concentration on cell yield.

This effect can be described by a substrate inhibition model. When compared with the experimental data, this kinetic model fit well. Like the observed growth rate estimates, the substrate inhibition model shows an increase and then decrease in cell growth with increasing substrate concentration.

Activity Doubling Times

The acceleration of PCP reduction with time indicates growth of a sub-population able to catalyze reductive dechlorination. Other important environmental factors like E_H , pH, and temperature were kept constant leaving cell growth to account for the acceleration. In all of the experiments performed, the acceleration of PCP reductive dechlorination follows an exponential increase like a growth curve. One hydrogen concentration, 9.4×10^{-5} atm, resulted in unusually long doubling times (27 days), but the high standard error and large p-value (Table 3.3) suggest the possibility of experimental error. All other acceleration rate measurements are reasonable and agree with growth rates mentioned in the literature. Previous results show that the doubling time of PCP reductively dechlorinating bacteria ranges between 1.3 and 2.4 days when studied in mixed cultures (74). *Desulfomonile tiedjei* cultures show a doubling time between 1.1 and 3.2 days (16). A 2-chlorophenol reductively dechlorinating population shows a doubling time of 3.7 days (10), and a population of vinyl chloride dechlorinating organisms exhibited a doubling time of about 36 hours (64). These literature values agree well with the observed doubling times of 1 to 14 days seen by this study.

Cell Decay

The cell decay coefficient determines the rate at which a viable cell dies. This rate is related to cell biology, cell age, and environmental conditions. During the reactor studies, the PCP reductively dechlorinating culture displayed a comparable decay rate to literature values. While decay did not appear to be very significant during these studies, the ability to separate cell growth from cell decay is valuable for toxicity studies and culture evaluation.

Conclusions

The research supports several conclusions:

1. The reductive dechlorination of PCP was dechlorinated at the two *ortho* positions to produce 2,3,4,5-TeCP and 3,4,5-TCP,
2. A PCP reductively dechlorinating soil population can be maintained for extended periods with addition of PCP and exogenously supplied hydrogen,
3. The apparent growth rate of a PCP reductively dechlorinating soil population was effectively estimated based on the acceleration of the PCP reductive dechlorination rate,
 - Doubling times of 1 to 14 days agreed well with other values observed for the growth of reductively dechlorinating bacteria,
 - The observed apparent growth rates include cell decay rates,

4. The apparent growth of reductively dechlorinating bacteria correlates to the hydrogen partial pressure,
 - Estimates for growth increase with hydrogen partial pressure until a maximum value of 2.9×10^{-4} atm at which point the growth rate declines with increasing hydrogen,
 - The observed results are modeled well by a substrate inhibition model with $K_H = 0.0005$ atm, $K_i = 0.0020$ atm, $K_{PCP} = 0.4509$ μ M, $k_{max} = 0.0910$, and $Y = 0.1448$,
5. And the cell decay measured for the mixed microbial culture was about 0.07-0.22days⁻¹.

Chapter Four: The Reductive Dechlorination of 2,3,4,5-TeCP and 3,4,5-Trichlorophenol by a Mixed Soil Culture

Introduction

During reductive dechlorination reactor experiments, there were two primary metabolites observed from PCP reductive dechlorination: 2,3,4,5-TeCP and 3,4,5-TCP. The congener 2,3,4,5-TeCP was reductively dechlorinated at the *ortho* position with kinetics similar to PCP reductive dechlorination. The resulting metabolite, 3,4,5-TCP, was reductively dechlorinated at either the *meta* or *para* position and proved more recalcitrant than both PCP and 2,3,4,5-TCP. The work in this paper examines and compares the reductive dechlorination of these two major metabolites of PCP reductive dechlorination.

Many studies of PCP reductive dechlorination have shown the production of 2,3,4,5-TeCP (31, 45, 52, 58). This congener was quickly reductively dechlorinated to produce 3,4,5-TCP. This frequently observed pathway proceeds via two *ortho* positioned reductive dechlorination reactions. Stuart et al. (1996) showed that both congeners supported growth and were reductively dechlorinated at comparable first-order rates (74).

PCP reductive dechlorination often results in the accumulation of the recalcitrant congener 3,4,5-TCP (46). Therefore, reductive dechlorination of the metabolic byproduct 3,4,5-TCP is necessary to completely degrade PCP contaminated sites. Research shows that 3,4,5-TCP is toxic to some reductively dechlorinating bacteria complicating the biodegradation process (31, 44, 65, 72). When degraded, the reductive dechlorination of 3,4,5-TCP begins at the *para* position to produce 3,5-DCP (35, 45, 46, 52, 58). Some researchers have shown the production of 3,4-DCP as a result of reductive dechlorination at the *meta* position (47, 48).

The energies provided from a single chlorine removal from PCP, 3,4,5-TCP, and 2,3,4,5-TeCP are nearly identical. Compared to 157 kJ of energy produced per mole of PCP reductively dechlorinated to 2,3,4,5-TeCP, the reductive dechlorination of 3,4,5-TCP produces 156 kJ when reductively dechlorinated at the *para* position or 142 kJ when reductively dechlorinated at the *meta* position. This suggests that, energetically, 3,4,5-TCP is a comparable substrate to PCP, and bacteria should grow equally well when provided either PCP or 3,4,5-TCP. This research studies the effects of hydrogen on reductive dechlorination of 2,3,4,5-TeCP and 3,4,5-TCP by a PCP degrading soil culture and compares those results with PCP studies described earlier in this paper.

The objectives of this research are to:

1. Evaluate 2,3,4,5-TeCP and 3,4,5-TCP reductive dechlorination in a mixed soil culture by PCP additions,
2. Determine reductive dechlorination rates for 2,3,4,5-TeCP and PCP,
3. Evaluate the pathway by which PCP and 2,3,4,5-TeCP are reductively dechlorinated,
4. Contrast the pathway of 3,4,5-TCP reductive dechlorination with that of PCP and 2,3,4,5-TeCP,
5. Correlate the 3,4,5-TCP reductive dechlorination rate and hydrogen partial pressure, and
6. Evaluate the effect of 3,4,5-TCP additions on the growth of reductively dechlorinating bacteria.

Materials and Methods

Time course studies were performed in a computer-monitored/feedback-controlled bioreactor designed to monitor and hold constant temperature, pH,

acetate concentration, redox potential, and hydrogen concentration while PCP transformation occurred. The batch reactor is described in Chapter 2. The use of this reactor has been explained previously by Sheryl L. Stuart (75). Incubations were conducted at 31°C and a pH of 6.81 (± 0.27) according to the protocol in Chapter 2 with any exceptions noted in the results.

Results

Six fed-batch multiple addition reactor studies were performed by adding spikes of PCP to a reductively dechlorinating soil culture. Each incubation was performed under a specific hydrogen partial pressure. Liquid samples were analyzed for the concentration of PCP and the products of reductive dechlorination.

Pathway

In each of the multiple addition reactor studies, 2,3,4,5-TeCP was produced and reductively dechlorinated to produce 3,4,5-TCP as shown earlier in Figure 3.1. The reductive dechlorination of 2,3,4,5-TeCP did not show any lag period between its production and degradation. This observation held true for the reductive dechlorination of 2,3,4,5-TeCP after each of the PCP additions including the very first PCP addition. The addition shown in Figure 3.1 is representative of the earlier PCP additions into the reactor. During the multiple PCP addition experiments, the production and disappearance of 2,3,4,5-TeCP was measured and modeled according to Equation 3.2.

In six fed-batch reactor studies, 3,4,5-TCP was the major metabolite of PCP reductive dechlorination. Sequential additions of PCP were reductively dechlorinated to 3,4,5-TCP via 2,3,4,5-TeCP production and reductive

dechlorination. The accumulation of 3,4,5-TCP while incubated at a hydrogen partial pressure of 5.7×10^{-4} is representative of the observed 3,4,5-TCP accumulation during the reactor experiments as shown in Figure 4.1. 3,4,5-TCP concentration peaked at $1.8 \mu\text{M}$ after which it began to decline. Similar results were observed for reactor study experiments performed at different hydrogen partial pressures as shown in Figure 4.2 - Figure 4.5. 3,4-DCP was included in figures only when it was observed at concentrations above background.

The initial 3,4,5-TCP in the reactor prior to hour 50 was residual from PCP reductive dechlorination during the soil preparation. Production of 3,4,5-TCP appeared to begin after 56 hours as a function of PCP and 2,3,4,5-TeCP reductive dechlorination (Figure 4.1). The production of 3,5-DCP after 90 hours indicated the reductive dechlorination of 3,4,5-TCP. By 100 hours, the reductive dechlorination rate of 3,4,5-TCP appeared to equal that of PCP as shown by the end of 3,4,5-TCP accumulation in the reactor. 3,4,5-TCP was reductively dechlorinated at both the *para* and *meta* positions.

The production of dichlorophenol congeners was not observed during any experiment until the conclusion of an extended lag period. This lag ranged between 90 and 300 hours as shown in Table 4.1. At a hydrogen partial pressure of 9.4×10^{-5} atm the production of dichlorophenols was not observed until after 200 hours at which time 3,4,5-TCP concentration in the reactor rapidly declined (Figure 4.2).

Table 4.1: Reductive dechlorination of 3,4,5-TCP

Hydrogen Partial Pressure	Lag period before reductive dechlorination of 3,4,5-TCP	Lag period before reductive dechlorination of PCP	Initial observed metabolite
9.4×10^{-5}	170	70	3,5-DCP
2.9×10^{-4}	300	150	3,5-DCP
5.7×10^{-4}	90	56	3,5-DCP
9.8×10^{-4}	200	75	3,5-DCP
7.8×10^{-3}	300	200	3,5-DCP

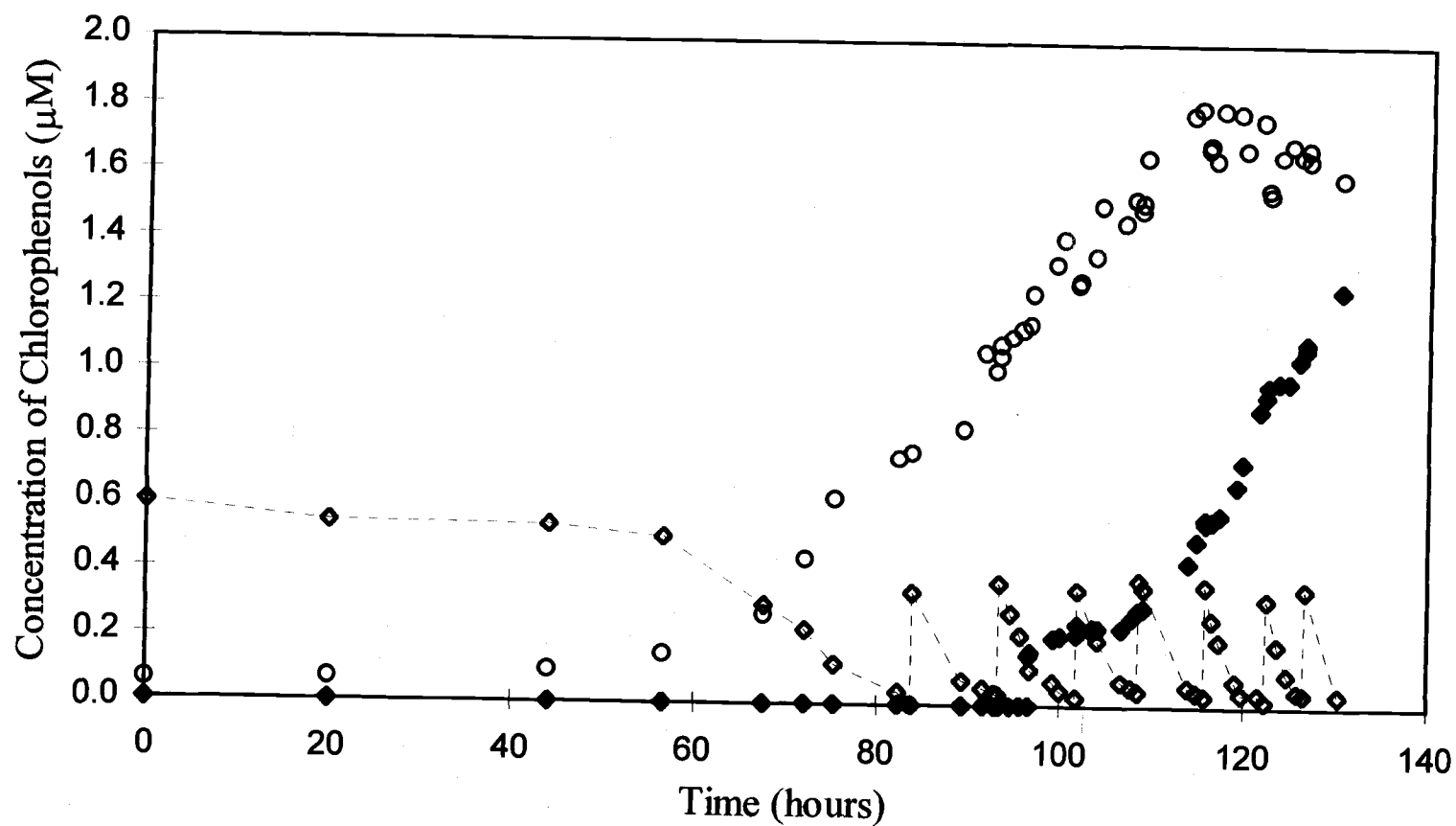


Figure 4.1: A time course study of PCP (◇); 3,4,5-TCP (O); and 3,5-DCP (◆); incubated at 5.7×10^{-4} atm of hydrogen

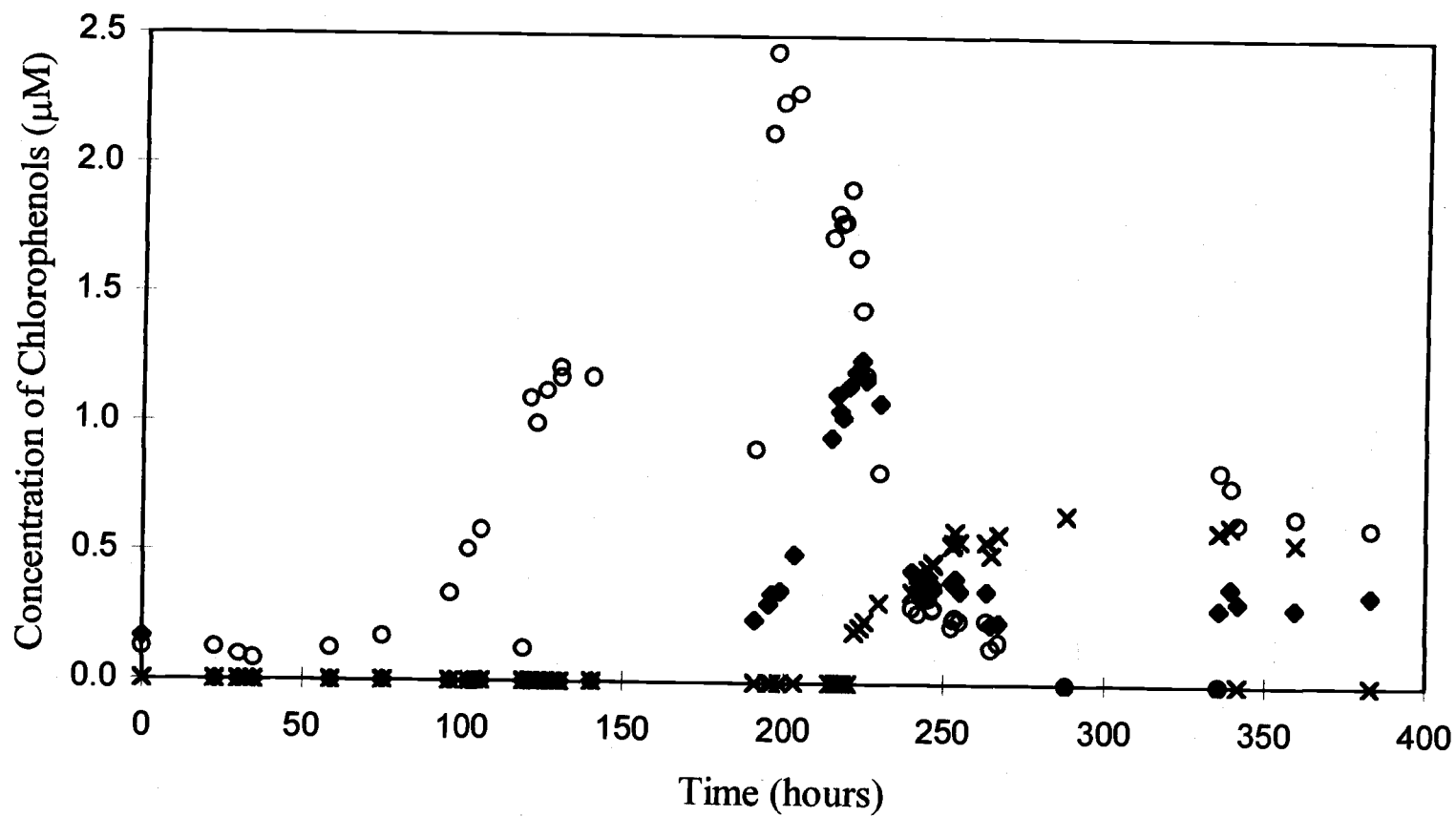


Figure 4.2: A time course study of 3,4,5-TCP (○); 3,5-DCP (◆); and 3,4-DCP (×) incubated at 9.8×10^{-4} atm of hydrogen

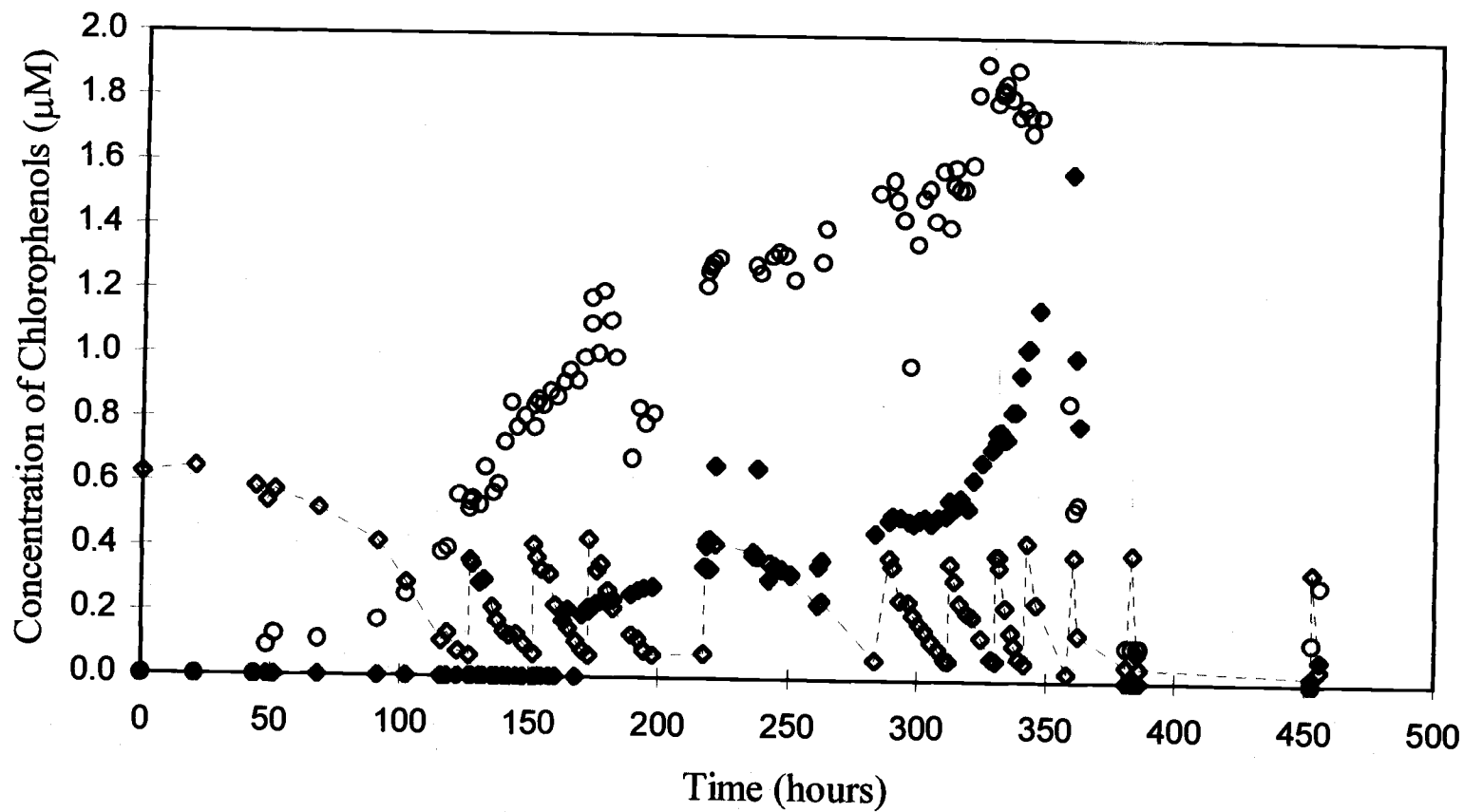


Figure 4.3: A time course study of PCP (◇); 3,4,5-TCP (○); and 3,5-DCP (◆); incubated at 9.4×10^{-5} atm of hydrogen

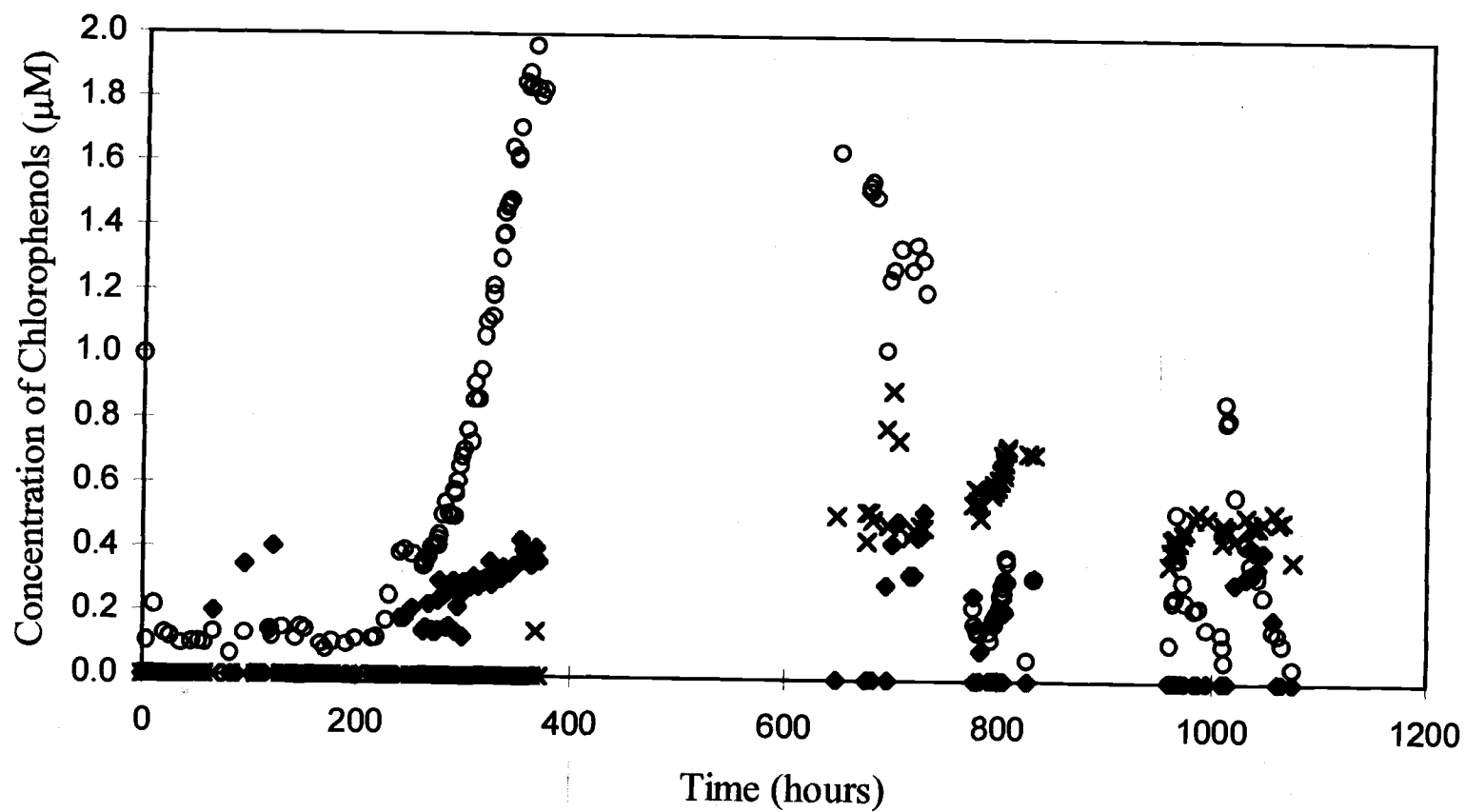


Figure 4.4: A time course study of 3,4,5-TCP (●); 3,5-DCP (◆); and 3,4-DCP (×) incubated at 7.8×10^{-4} atm of hydrogen

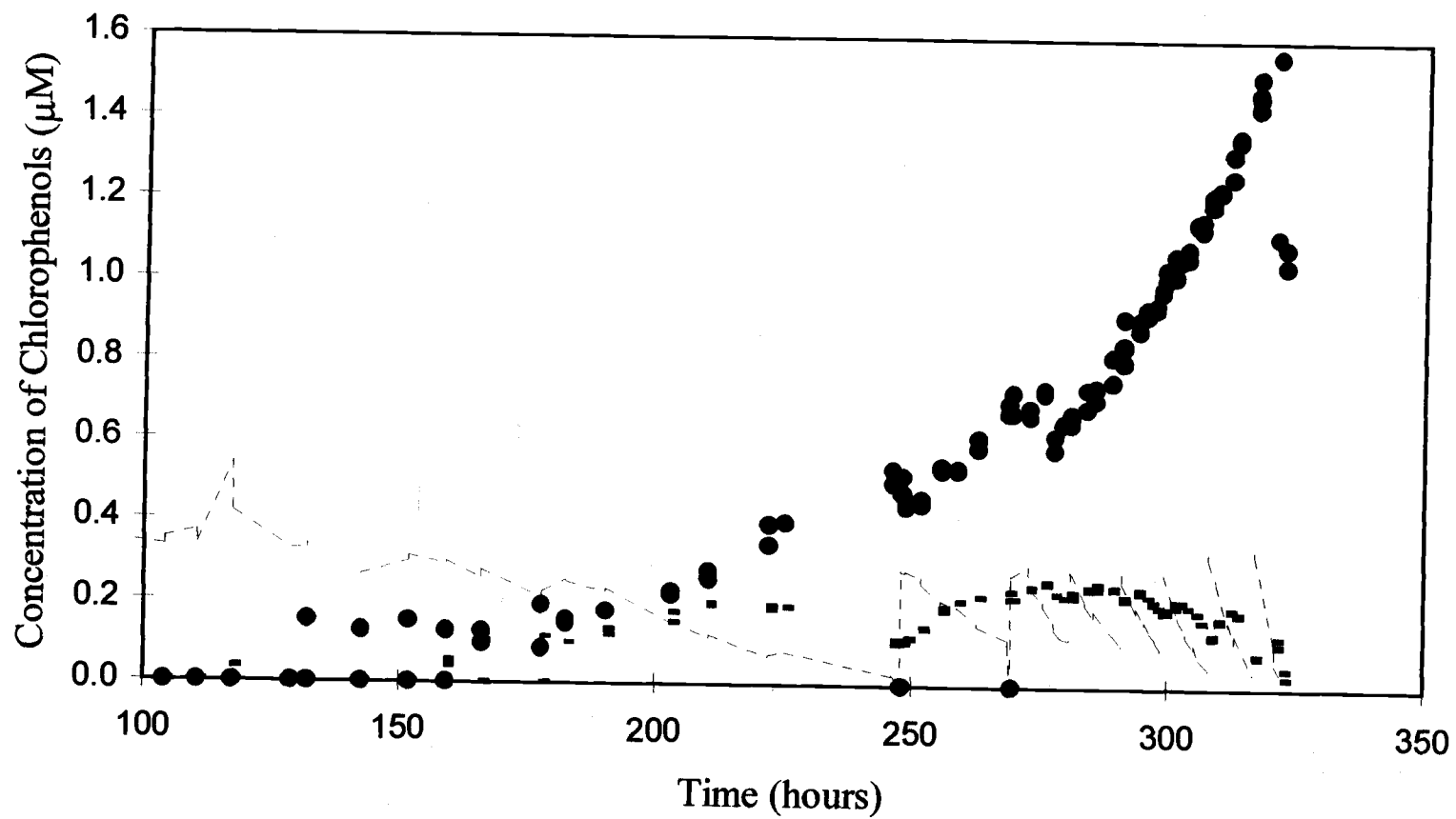


Figure 4.5: A time course study of PCP (---); 2,3,4,5-TeCP (■); and 3,4,5-TCP (●) incubated at 2.9×10^{-4} atm of hydrogen

Large blank spaces of time without sample points in Figure 4.2 and Figure 4.4 represent times between experiments in the reactor. The incubation at 5.7×10^{-4} atm showed very high concentrations of 3,4,5-TCP in the reactor. After the reactor was kept dormant for 200 hours rapid 3,4,5-TCP reductive dechlorination was stimulated by the addition of PCP into the reactor. (Figure 4.4) After a PCP degradation experiment was finished, PCP addition ceased and organisms metabolized remaining chlorophenol congeners. Other studies show that complete mineralization occurred in reactors after PCP additions cease (52). After all the chlorophenolic congeners were degraded, another study was begun to examine the reductive dechlorination of 3,4,5-TCP.

The production of 3,4-DCP was only occasionally observed. The *meta* positioned reductive dechlorination of 3,4,5-TCP may not have been initiated during all incubations. The production of 3,5-DCP via a *para* positioned reductive dechlorination was more consistent between incubations.

2,3,4,5-Tetrachlorophenol

Rate

In the reactor, 2,3,4,5-TeCP was produced by the reductive dechlorination of PCP and removed by reductive dechlorination. For reductive dechlorination rate calculations both the production and removal of 2,3,4,5-TeCP were examined. First-order 2,3,4,5-TeCP reductive dechlorination rates were calculated for each addition of PCP by simultaneously curve fitting PCP and 2,3,4,5-TeCP time course data as explained in Chapter 4. The measured PCP and 2,3,4,5-TeCP reductive dechlorination rates calculated for any PCP addition were very similar across the entire range of hydrogen partial pressures examined (Appendix Table E).

Acceleration and Growth

During the PCP multiple addition experiments, the measured 2,3,4,5-TeCP reductive dechlorination rates increased with PCP additions. First-order 2,3,4,5-TeCP reductive dechlorination rates were calculated. An acceleration rate of 2,3,4,5-TeCP reductive dechlorination was based on the reductive dechlorination rate increase. During the multiple addition experiment performed at a hydrogen partial pressure of 2.2×10^{-4} atm, the first-order rates of 2,3,4,5-TeCP reductive dechlorination increased from 0.05 to 0.13 hour^{-1} as shown in Figure 4.6. Stuart's method was used to fit the exponential increase in 2,3,4,5-TeCP reductive dechlorination rates to a growth model as earlier done for PCP reductive dechlorination (Chapter 3). At the hydrogen partial pressure of 2.2×10^{-4} atm, the acceleration of 2,3,4,5-TeCP was 0.0066 hour^{-2} (\pm a standard error of 0.0022), compared to 0.0056 hour^{-2} for PCP reductive dechlorination. The first-order 2,3,4,5-TeCP reductive dechlorination rates measured during multiple addition reactions are shown with the resulting acceleration curves in Figure 4.6 - Figure 4.11. Each figure corresponds to experiments performed at a different hydrogen partial pressure. The exponentially increasing model matched the data very well when the hydrogen partial pressure was maintained at values between 2.2×10^{-4} and 5.7×10^{-4} atm. The reductive dechlorination rates measured at a hydrogen partial pressures of 9.4×10^{-5} atm and 3.9×10^{-2} atm, Figure 4.11 and respectively, did not conform well to the exponentially increasing model, and those values should be considered carefully.

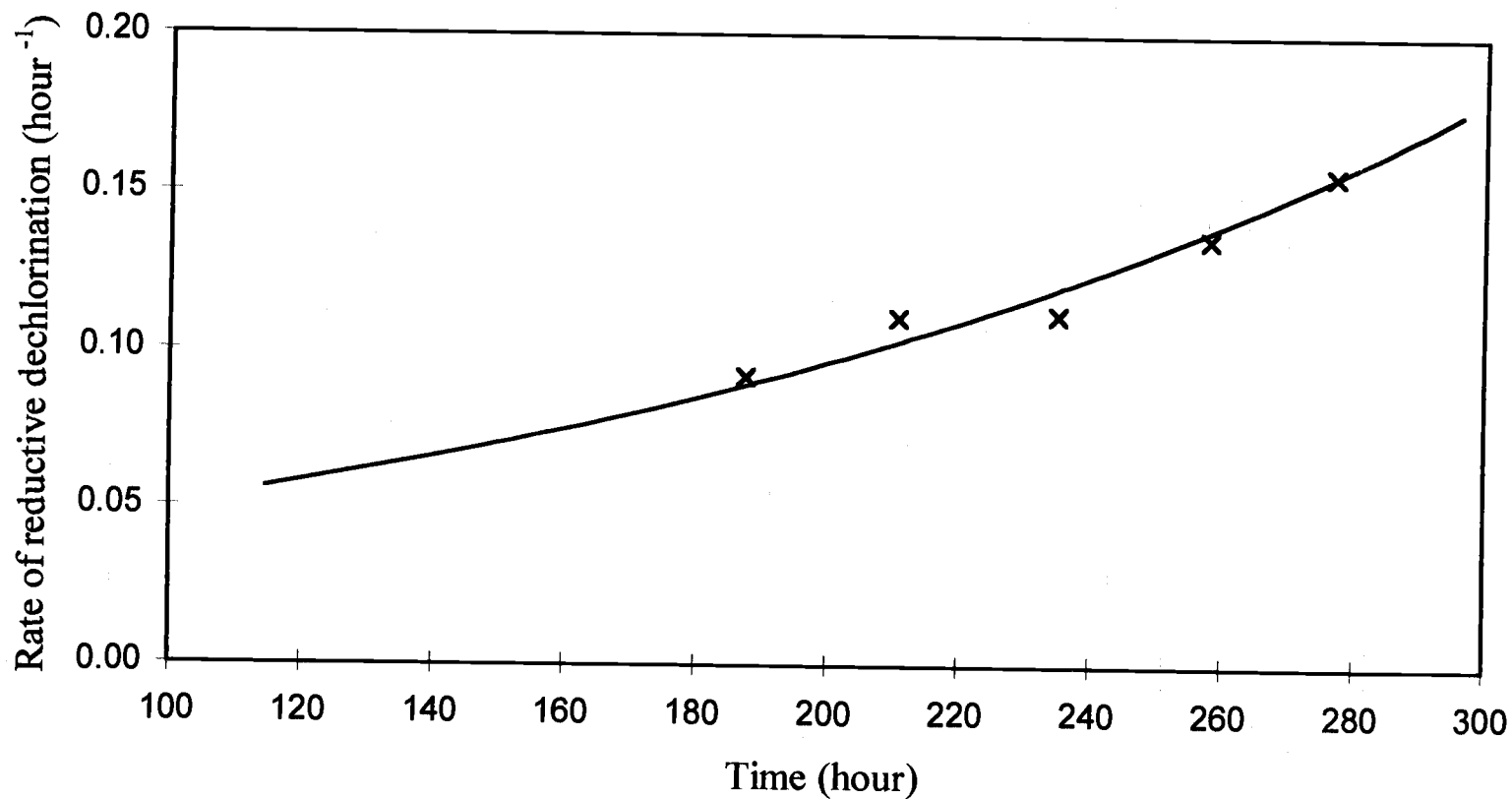


Figure 4.6: Time course study of 2,3,4,5-TeCP (+) first-order reductive dechlorination and derived exponential growth curve (—) at 2.2×10^{-4} atm of hydrogen

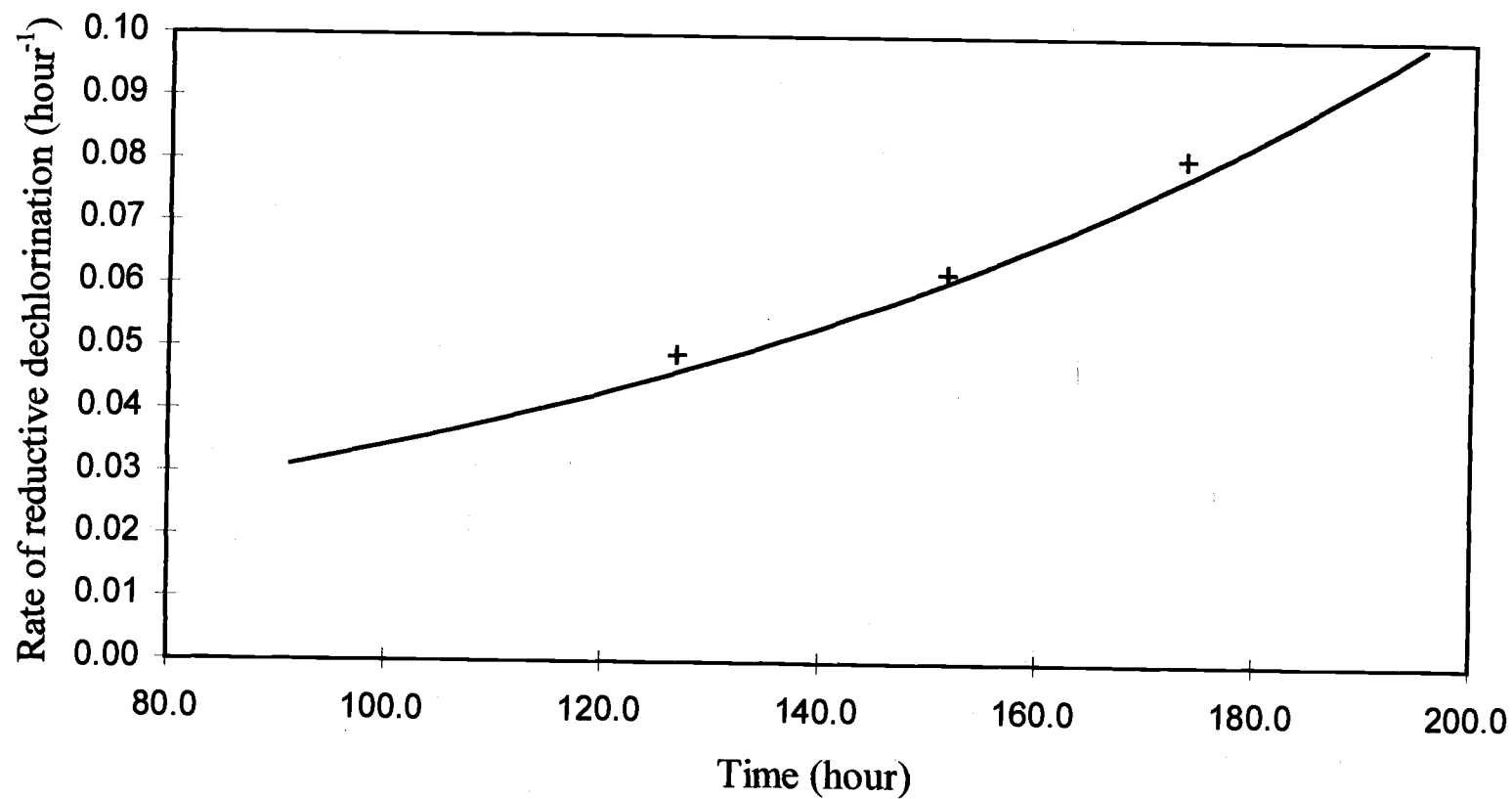


Figure 4.7: Time course study of 2,3,4,5-TeCP (+) first-order reductive dechlorination and derived exponential growth curve (—) at 9.4×10^{-5} atm of hydrogen

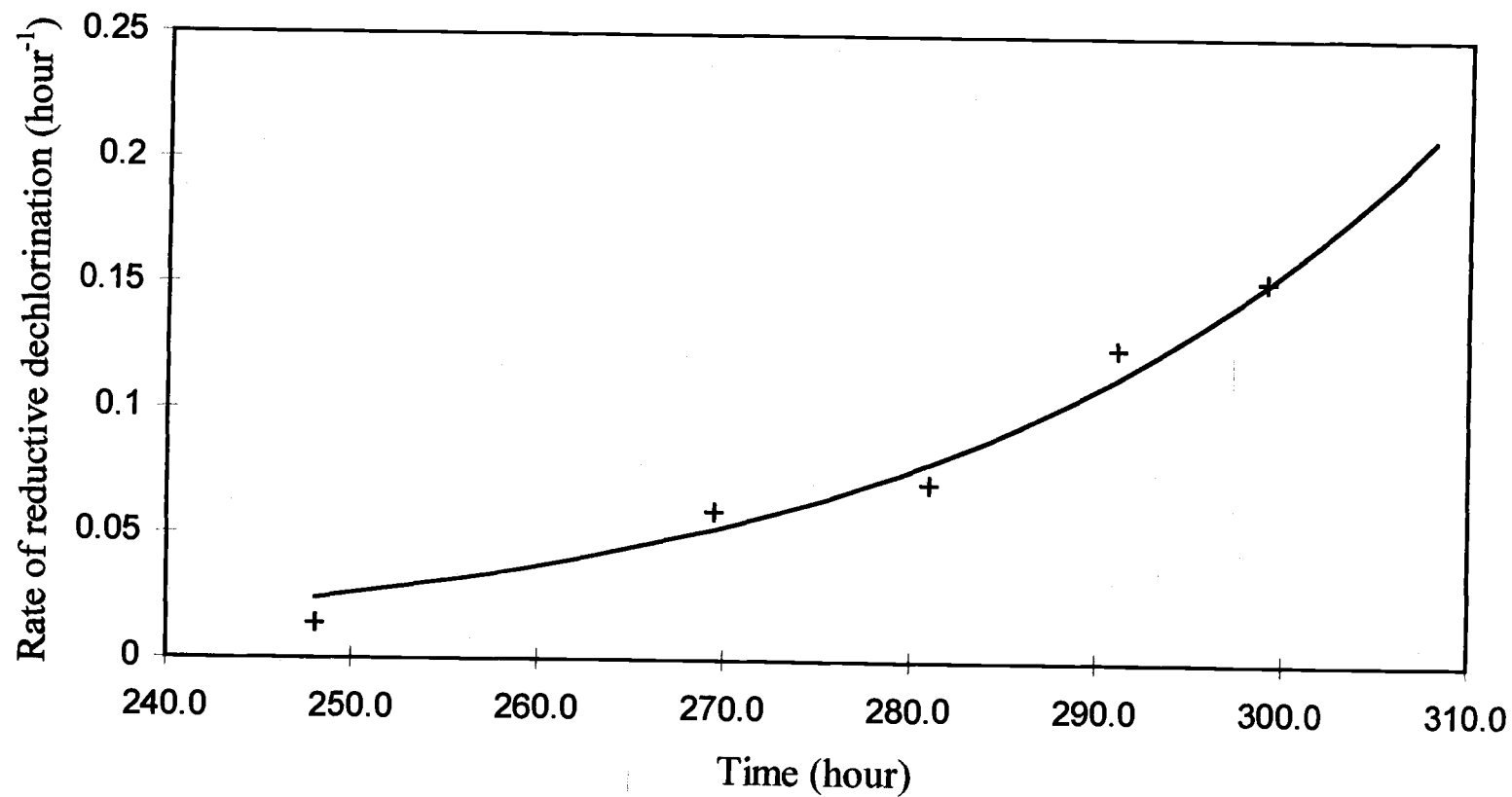


Figure 4.8: Time course study of 2,3,4,5-TeCP (+) first-order reductive dechlorination and derived exponential growth curve (—) at 2.9×10^{-4} atm of hydrogen

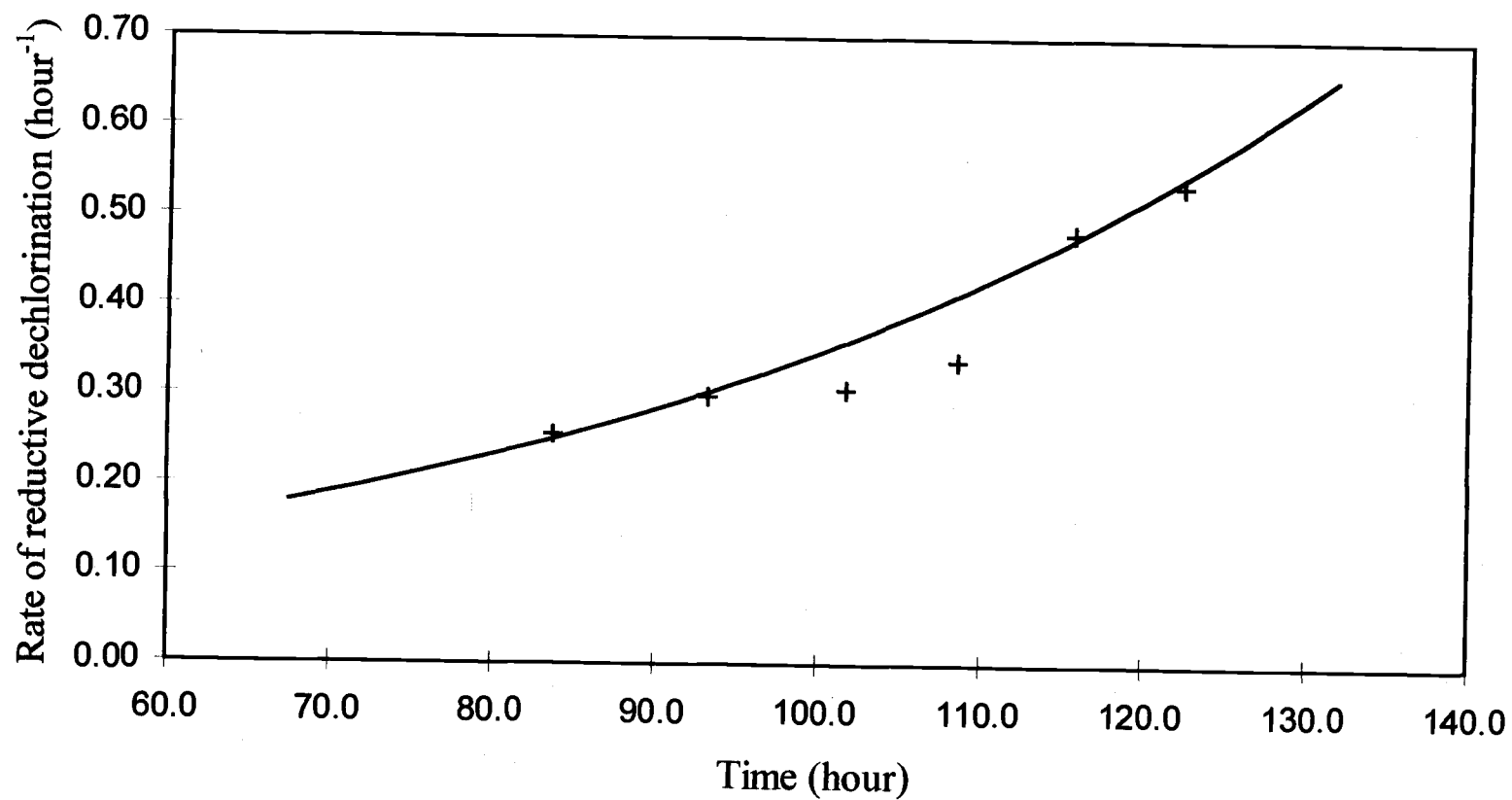


Figure 4.9: Time course study of 2,3,4,5-TeCP (+) first-order reductive dechlorination and derived exponential growth curve (—) at 5.7×10^{-4} atm of hydrogen

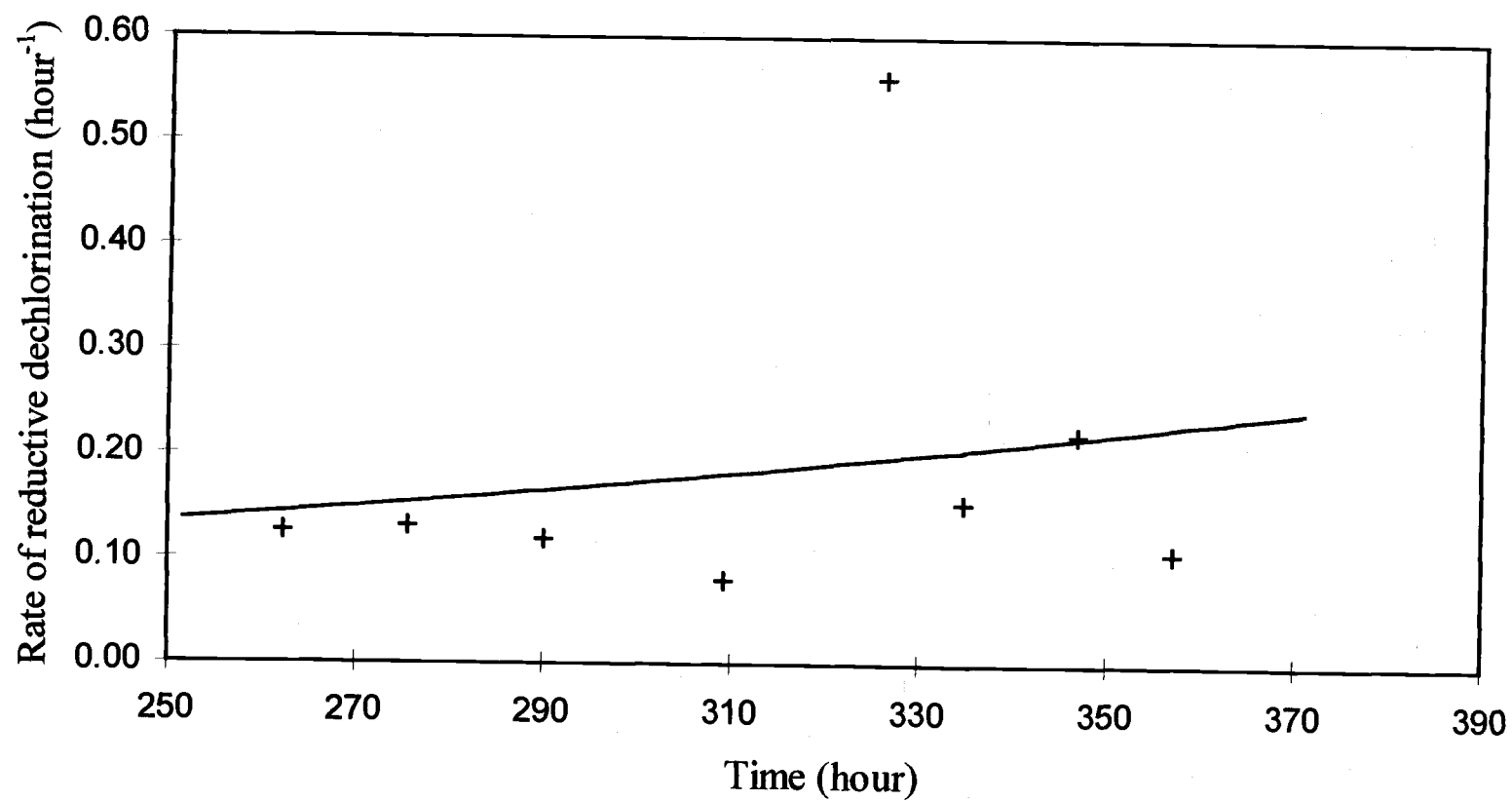


Figure 4.10: Time course study of 2,3,4,5-TeCP (+) first-order reductive dechlorination and derived exponential growth curve (—) at 7.8×10^{-3} atm of hydrogen

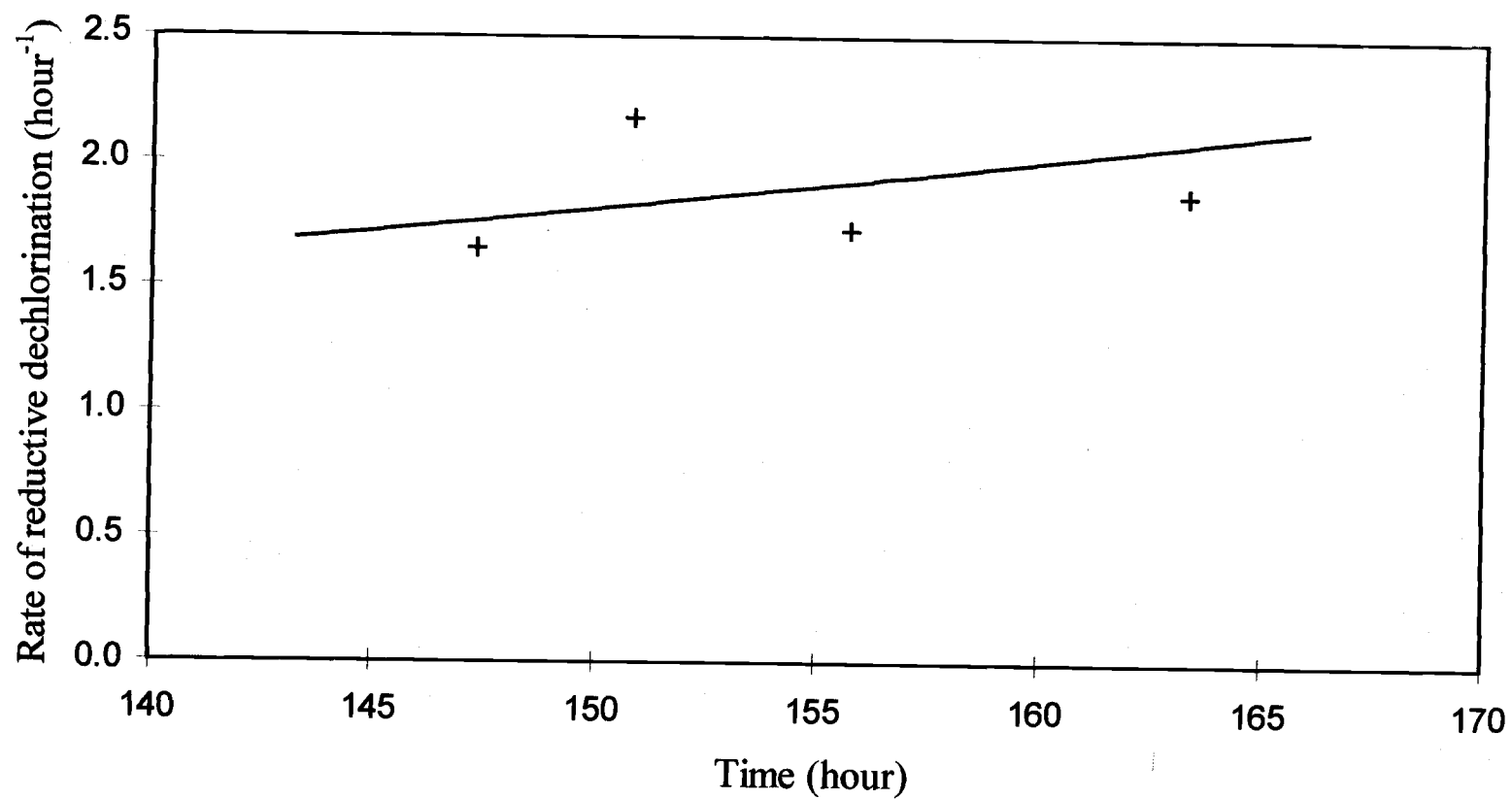


Figure 4.11: Time course study of 2,3,4,5-TeCP (+) first-order reductive dechlorination and derived exponential growth curve (—) at 3.9×10^{-2} atm of hydrogen

The apparent acceleration rates and doubling times as estimated from 2,3,4,5-TeCP reductive dechlorination data were compared with hydrogen partial pressure as shown in Table 4.2. The PCP apparent acceleration rates and doubling times from Chapter 3 are included for comparison. The experiments were performed in accordance with the assumptions based on Stuart's model, and the calculated acceleration rate values measured for 2,3,4,5-TeCP reductive dechlorination agreed well with those for PCP. The maximum apparent acceleration rate calculated by analysis of 2,3,4,5-TeCP data was 0.0352 hour^{-2} for a doubling time of 0.82 days at a hydrogen partial pressure of $2.9 \times 10^{-4} \text{ atm}$. At that same partial pressure of hydrogen, the PCP reductive dechlorination acceleration rate reached a maximum of 0.0302 hour^{-2} . The growth rates approximated by analysis of PCP reductive dechlorination increased to a value that corresponded to a 0.94 day half life at partial pressure of $2.9 \times 10^{-4} \text{ atm}$, and then declined. The approximated half lives of 2,3,4,5-TeCP ranged between 0.80 and 6 days. Similarly, the half lives of PCP ranged between 0.94 days and 6 days (the 26 day doubling time of PCP does not have a reliable corresponding 2,3,4,5-TeCP value).

Table 4.2: A comparison of apparent acceleration rates as measured by PCP and 2,3,4,5-TeCP reductive dechlorination

Hydrogen Partial Pressure atm	PCP		2,3,4,5-TeCP	
	Acceleration Rate (\pm standard error) hour ⁻²	Doubling Time day	Acceleration Rate (\pm standard error) hour ⁻²	Doubling Time day
9.4×10^{-5}	0.0011 (\pm 0.0608)	27	0.0111 (\pm 0.0111)	2.6
2.2×10^{-4}	0.0056 (\pm 0.0030)	5.1	0.0066 (\pm 0.0071)	4.4
2.9×10^{-4}	0.0302 (\pm 0.0050)	0.96	0.0352 (\pm 0.0247)	0.82
5.7×10^{-4}	0.0216 (\pm 0.0095)	1.3	0.0201 (\pm 0.0116)	1.4
7.8×10^{-3}	0.0054 (\pm 0.0186)	5.4	0.0048 (\pm 0.0249)	6.0
3.9×10^{-2}	0.0020 (\pm 0.0074)	14	0.0102 (\pm 0.0783)	2.8

The apparent acceleration rates of PCP and 2,3,4,5-TeCP increased with increasing hydrogen partial pressure until a maximum value and then decrease as shown in Figure 4.12. The estimations of PCP and 2,3,4,5-TeCP reductive dechlorination acceleration were similar and were within \pm one standard error. The apparent acceleration values determined for hydrogen partial pressures around 2.9×10^{-4} atm had small standard errors indicating more certainty. The 2,3,4,5-TeCP apparent acceleration rate rises and then decreases after the maximum value of 0.0360 hour^{-2} at 2.9×10^{-4} atm of hydrogen (Figure 4.12). The 2,3,4,5-TeCP acceleration rates follow a substrate inhibition curve with hydrogen like the PCP acceleration rates earlier examined in Chapter 3.

3,4,5-Trichlorophenol

During the reductive dechlorination studies on PCP and 2,3,4,5-TeCP the acclimation of the bacterial culture, the rate of reductive dechlorination, the influence of hydrogen partial pressure, and the apparent growth rate of the bacterial culture were examined. The reductive dechlorination of 3,4,5-TCP differed from the two congeners previously discussed in several ways. 3,4,5-TCP reductive dechlorination did not occur rapidly like that of PCP and 2,3,4,5-TeCP during the PCP reactor studies. Reductive dechlorination rates slowed and in some cases ceased. Furthermore, the reductive dechlorination rates of 3,4,5-TCP did not appear to increase with sequential additions 3,4,5-TCP like 2,3,4,5-TeCP and PCP incubations. This section again examines those issues previously discussed and considers the differences specific to this substrate.

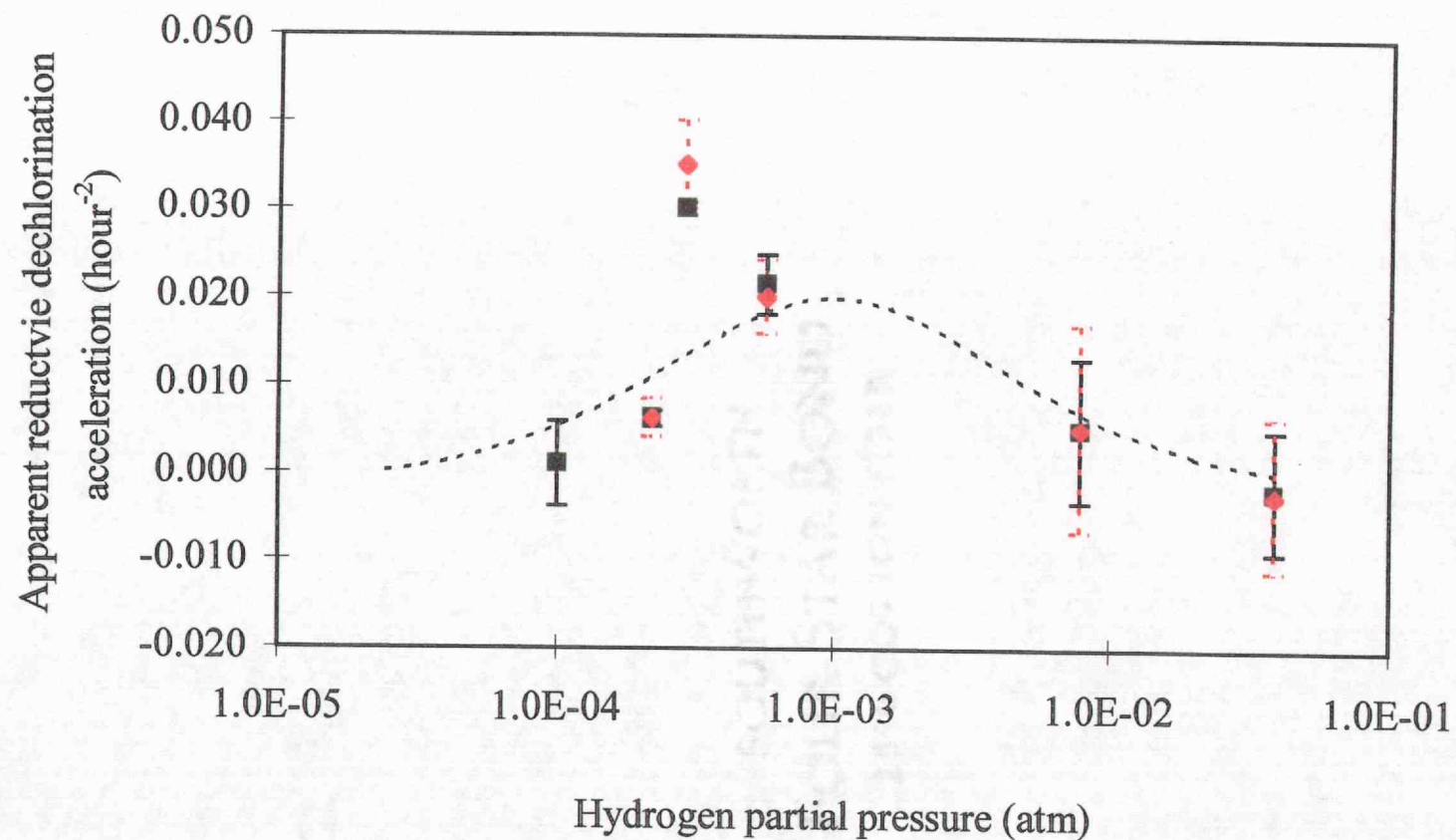


Figure 4.12: Comparison of the acceleration calculated from PCP (■) and 2,3,4,5-TeCP(♦) reductive dechlorination with hydrogen partial pressure (the hydrogen substrate inhibition model (- -) from Chapter 3 is included)

Lag Periods

Unlike the 2,3,4,5-TeCP that was produced and rapidly degraded, 3,4,5-TCP reductive dechlorination was slow and often followed a long lag time. After the dechlorination of 2,3,4,5-TeCP, no *ortho* positioned chlorine molecules remain, and 3,4,5-TCP reductive dechlorination must occur at a different ring position. There is research that suggests different enzymes are required for reductive dechlorination at different ring positions (8, 14, 48, 52); therefore, incubation with PCP may not induce the enzymes necessary for 3,4,5-TCP reductive dechlorination. This is shown by long lag periods and slow degradation rates of 3,4,5-TCP during the reactor experiments.

Reductive dechlorination of both PCP and 3,4,5-TCP showed an extended lag period during each of the reactor studies. The lag periods before PCP and 3,4,5-TCP reductive dechlorination were measured at each hydrogen partial pressure (Table 4.1). Correlation between hydrogen partial pressure and observed lag periods were tested as shown in Figure 4.13. There did not appear to be a correlation between hydrogen partial pressure and measured lags for either PCP or 3,4,5-TCP reductive dechlorination. However, analysis of the lag period prior to the reductive dechlorination of 3,4,5-TCP and the lag period prior to the reductive dechlorination of PCP at the same hydrogen partial pressure showed an interesting result. Both the lag periods of PCP and 3,4,5-TCP followed the same trend. Longer delays before PCP reductive dechlorination correlated with longer lags before 3,4,5-TCP reductive dechlorination. The observed lag periods before PCP and 3,4,5-TCP reductive dechlorination appeared related as shown by the relatively constant ratio between the two at any one hydrogen partial pressure (Figure 4.13). This suggested that the lag periods observed were related to the initial cell inoculum, and growth of 3,4,5-TCP reductively dechlorinating bacteria was not induced by PCP.

All measured lag periods were within a factor of four – between 50 and 200 hours for PCP and 100 and 300 for 3,4,5-TCP. During simulations, the PCP lag between 50 and 200 hours before first-order degradation corresponded to a factor of 10 difference between cell concentration. Observed lag periods within this range before PCP reductive dechlorination indicated that the procedure for inoculation sufficiently established a constant culture concentration between experiments.

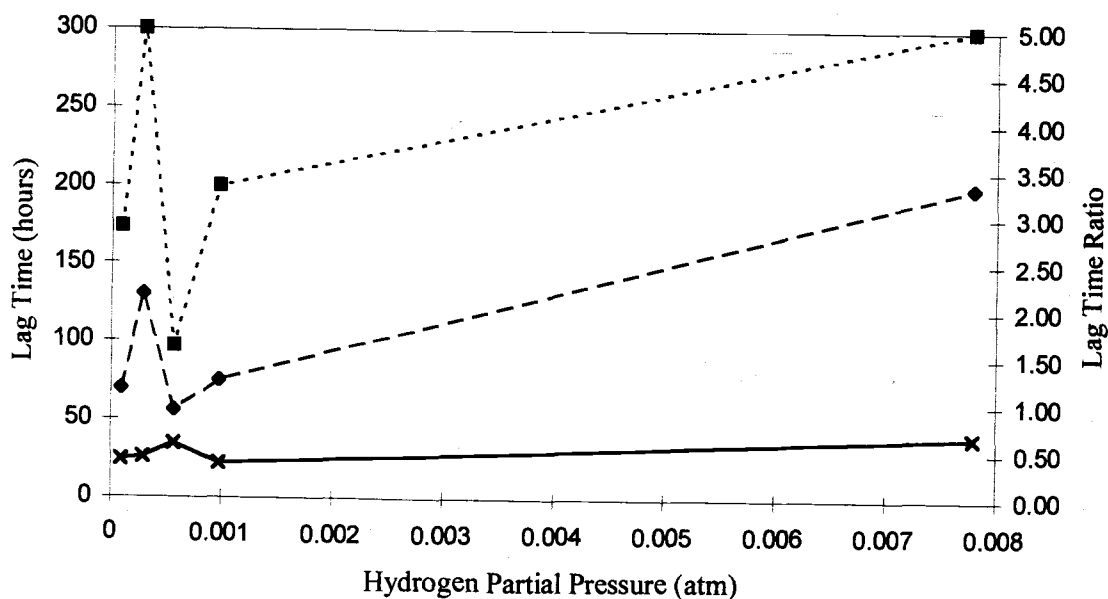


Figure 4.13: Correlation between lag time before reductive dechlorination of PCP (—◆—), 3,4,5-TCP (- - ■ - -), the ratio of PCP/TCP lag (—×—) and hydrogen partial pressure

Effect of H_2 Partial Pressure

Hydrogen serves as an electron donor for 3,4,5-TCP reductive dechlorination and can affect the rate of reductive dechlorination like it does for other reductive dechlorination processes. One experiment was performed to analyze

the effect of hydrogen concentration on 3,4,5-TCP reductive dechlorination. Following continued reductive dechlorination of PCP, the remaining chlorophenol congeners were completely degraded with exogenous hydrogen in the reactor. At that point, a spike of PCP was added and degraded to 3,4,5-TCP. A supplemental addition of 3,4,5-TCP was added to the reactor to raise the concentration of 3,4,5-TCP to $0.53 \mu\text{M}$. The rate of reductive dechlorination was measured to be 0.095 hour^{-1} under a hydrogen partial pressure of 9.76×10^{-2} as shown in Table 4.3. The hydrogen partial pressure was lowered to $4.26 \times 10^{-3} \text{ atm}$, and the measured rate of reductive dechlorination slowed to 0.024 hour^{-1} . The hydrogen partial pressure was returned to the higher level of $1.60 \times 10^{-1} \text{ atm}$, and the rate of reductive dechlorination increased. A second 3,4,5-TCP addition was made, and the rate of reductive dechlorination was measured. The two rates measured at the hydrogen concentration of 1.6×10^{-1} were dramatically different. The second was much lower than the first (Table 4.3). Again, measured reductive dechlorination rates increased and decreased with increasing and decreasing hydrogen.

Table 4.3: Reductive dechlorination rate of 3,4,5-TCP at varying hydrogen partial pressures measured during one reactor experiment

Hydrogen Partial Pressure (atm)	Change	First-order Reductive Dechlorination Rate (hour^{-1})	Change
9.76×10^{-2}		0.095	
4.26×10^{-3}	Decrease	0.024	Decrease
1.60×10^{-1}	Increase	0.352	Increase
1.60×10^{-1}		0.042	
8.98×10^{-3}	Decrease	0.031	Decrease
1.25×10^{-2}	Increase	0.085	Increase

Sustained 3,4,5-TCP Reductive Dechlorination

The reductive dechlorination of PCP provides enough energy to sustain a microbial population able to perform reductive dechlorination of PCP, 2,3,4,5-TeCP, and 3,4,5-TCP. In the reactor experiments studying PCP reductive dechlorination, 3,4,5-TCP was completely reductively dechlorinated to dichlorophenol congeners. The ability to sustain reductive dechlorination of 3,4,5-TCP with additions of 3,4,5-TCP was tested.

During successive additions of PCP, 3,4,5-TCP accumulated in the reactor and was then reductively dechlorinated as shown in Figure 4.14. Following the complete disappearance of 3,4,5-TCP at hour 288, the reactor was allowed to completely degrade the remaining chlorophenol congeners for 47 hours with only 3,4-DCP measurable in the reactor (data not shown). After hour 355, a spike of 3,4,5-TCP was added to the reactor (Figure 4.14). The measured concentration of 3,4,5-TCP initially dropped from 0.83 μM to 0.77 μM in 3.5 hours, but the concentration stabilized at 0.625 μM and no additional degradation was observed after forty hours. Unlike during the PCP reactor experiments, when 3,4,5-TCP was the initial substrate, reductive dechlorination did not continue until completion. While 3,4,5-TCP was completely degraded in the presence of PCP between hours 200 and 300, when 3,4,5-TCP was added without PCP as a substrate, 3,4,5-TCP reductive dechlorination was not maintained in the reactor.

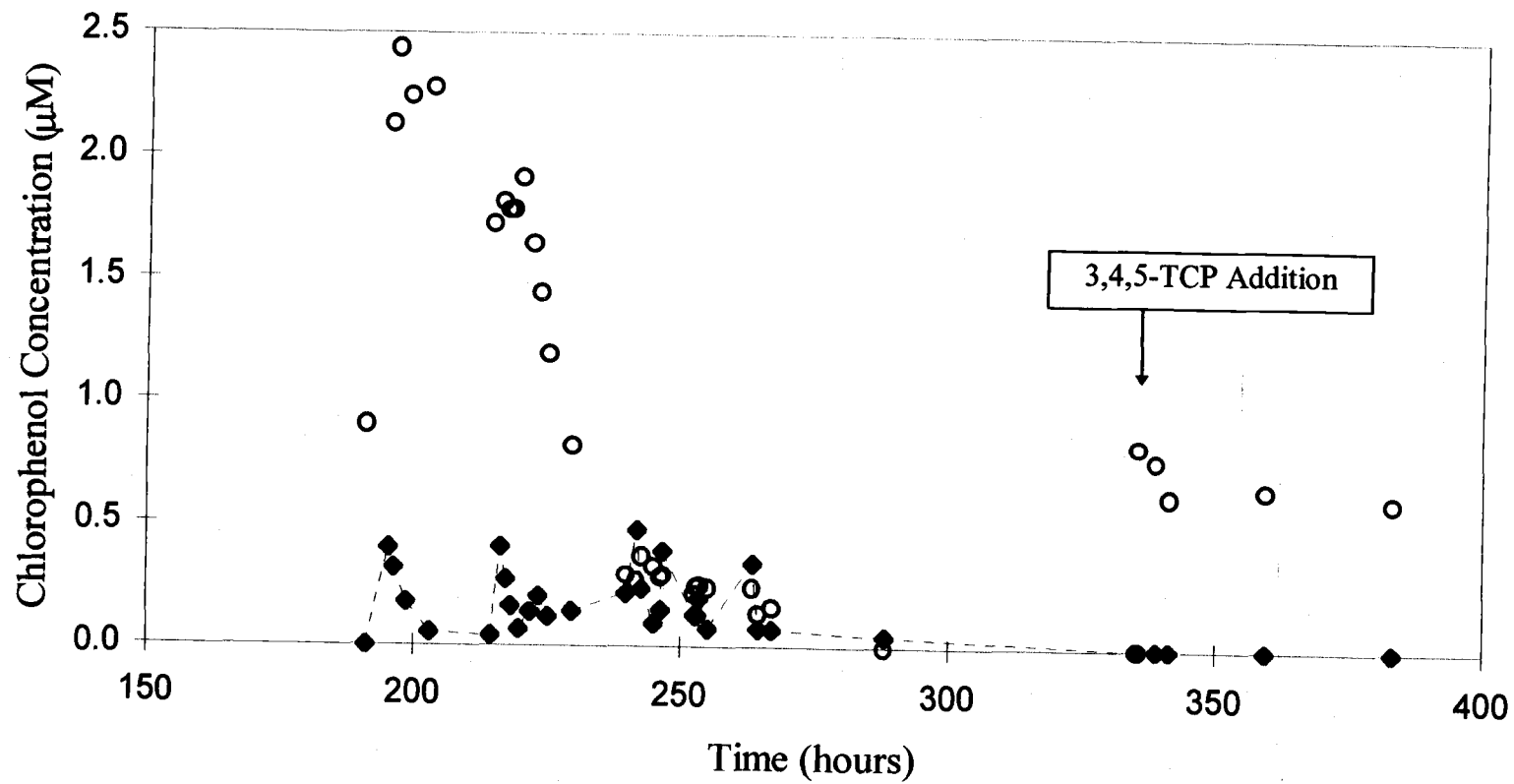


Figure 4.14: Long term reductive dechlorination of 3,4,5-TCP (○) and PCP (◆)

Discussion

2,3,4,5-Tetrachlorophenol

The reductive dechlorination of 2,3,4,5-TeCP occurred in PCP reactor studies concurrently with PCP reductive dechlorination. There was no observable acclimation period required for the organisms to reductively dechlorinate 2,3,4,5-TeCP. 3,4,5-TCP accumulated during the reactor studies as a result of PCP and 2,3,4,5-TeCP reductive dechlorination. The production of 3,4,5-TCP indicated that PCP was reductively dechlorinated at both *ortho* positions. The two substrates are similar and both have *ortho* positioned chlorine molecules available for reductive dechlorination. Because of similar energetics and structure, the reductive dechlorination rate for each should be similar provided that the number of reductive dechlorinating organisms were the same. The measured PCP and 2,3,4,5-TeCP reductive dechlorination rates calculated for any one PCP addition were very similar to one another across the entire hydrogen range (Appendix Table E). This suggests that the same enzyme system and possibly the same bacteria catalyzed both PCP and 2,3,4,5-TeCP observed reductive dechlorination reactions.

Both the reductive dechlorination of PCP and of 2,3,4,5-TeCP shows an acceleration with sequential additions of PCP. The acceleration of reductive dechlorination rates suggests the increase in the reductively dechlorinating enzyme system.

The apparent acceleration rates with hydrogen concentration are similar between the PCP and 2,3,4,5-TeCP analysis. The acceleration calculations derived using Stuart's model agree very well at all hydrogen concentrations as shown in Table 4.2. The trends between apparent acceleration rates and hydrogen partial

pressure are similar for both substrates. This also suggests that the same bacteria are involved in both dechlorination steps.

3,4,5-Trichlorophenol

3,4,5-TCP formed as the early metabolite of PCP and 2,3,4,5-TeCP reductive dechlorination agrees with observations made by other researchers studying the reductive dechlorination of PCP (35, 45, 46, 48, 52, 58). 3,4,5-TCP accumulated as a product of PCP reductive dechlorination in six separate reactor studies, like results shown in earlier research (52).

Reductive dechlorination at the *meta* position of 3,4,5-TCP and 3,4-DCP may not be catalyzed by *ortho* degrading cultures. During the reactor experiment with a hydrogen partial pressure of 3.9×10^{-2} atm, 3,4-DCP began accumulating in the reactor. The observed recalcitrance of this compound agreed with previous research (46). In chlorophenol competition studies, Magar et al. did not observe inhibition between *ortho* and *meta* dechlorinated chlorophenols suggesting that the two reactions are independent (47). Similarly, the PCP reductive dechlorination rate studies explained in Chapter 3 did not indicate competitive inhibition between *para* and *ortho* positioned reductive dechlorination. The accumulation and subsequent reductive dechlorination of 3,4,5-TCP at the *para* and *meta* positions did not have a measurable effect on the *ortho* positioned reductive dechlorination rate of PCP. The inconsistent production of 3,4-DCP suggests that *meta* positioned reductive dechlorination of 3,4,5-TCP may not have been stimulated in all reactor studies.

Cultures acclimated to different mono and dichlorophenol congeners follow different reductive dechlorination pathways when incubated with PCP. When incubated on 2,4-DCP or 3,4-DCP, cultures preferentially dechlorinated at the *ortho* and *meta* positions respectively (8). Another study used 2-CP, 3-CP, and 4-CP acclimated cultures to completely reductively dechlorinate PCP (52). Separate

enzymes or populations are responsible for the reductive dechlorination of these two compounds. This supports early findings that reductive dechlorination of PCP to 3,5-DCP involved at least two different populations (35). Studies of reductive dechlorination of 2,4-DCP also suggested a minimum of two separate organisms to reductively dechlorinate this congener (33).

The observed lag period prior to reductive dechlorination of 3,4,5-TCP better correlated with the observed lag before PCP reductive dechlorination than hydrogen partial pressure. This suggests adaptation rather than induction of the culture. Induction of enzymatic function is only one step in the adaptation process that can include cell growth, substrate deficits, enzyme induction, or genetic exchanges (37). The lag period observed before 3,4,5-TCP reductive dechlorination was primarily due to low initial cell numbers. The PCP reductive dechlorination experiments were designed to begin with a low inoculum. The correlation between the PCP and 3,4,5-TCP lag periods suggests that the lag periods were a function of population dynamics.

There is a correlation between the rate of 3,4,5-TCP reductive dechlorination and hydrogen concentration. Twice during a fed-batch reactor study the rate of reductive dechlorination was decreased and then increased by lowering and raising hydrogen partial pressure in the reactor. The results show that the rate of 3,4,5-TCP is immediately affected by changes in hydrogen partial pressure. The dynamics of cell growth and decay made quantitative growth measurements of 3,4,5-TCP reductively dechlorinating bacteria difficult.

Sustained 3,4,5-TCP reductive dechlorination was not observed without PCP additions. Reductive dechlorination rates decreased after subsequent additions of 3,4,5-TCP during the hydrogen partial pressure study. As shown in Table 4.3 the second measured rate of reductive dechlorination at 1.60×10^{-1} atm of hydrogen was significantly lower than the first. This could be due to decay of reductively dechlorinating organisms without additional growth or loss of reductive dechlorination activity. The toxicity of 3,4,5-TCP and its tendency to act as a proton

dissipater provide one reason that it does not support microbial growth (72). This agrees with observations made by Stuart et al. that concluded 3,4,5-TCP could be metabolized, but did not sustain growth (74).

3,4,5-TCP acts as a proton dissipater (73)—disrupts the energy producing hydrogen transport chain. Unlike PCP and 2,3,4,5-TeCP, 3,4,5-TCP does not support the growth of reductively dechlorinating bacteria. Because 3,4,5-TCP does not support bacterial growth, multiple spike reactor experiments do not show the acceleration effect demonstrated during PCP and 2,3,4,5-TeCP incubations.

Conclusions

This research suggested a number of conclusions:

1. The reductive dechlorination at both *ortho* positions on the PCP congener and on the 2,3,4,5-TeCP congener are catalyzed by the same bacteria in a PCP acclimated soil culture,
 - The reductive dechlorination of PCP and 2,3,4,5-TeCP begins simultaneously in the reactor system,
 - Reductive dechlorination rates for any one incubation were comparable for PCP and 2,3,4,5-TeCP,
 - The reductive dechlorination of both substrates increases at the same apparent acceleration rate with PCP additions,
 - And the observed accelerations of reductive dechlorination respond the same to hydrogen partial pressure increases; therefore, the doubling times of reductively dechlorinating bacteria are similar,
2. 3,4,5-TCP is reductively dechlorinated at the *meta* position by different enzymes than the *ortho* positioned reductive dechlorination of PCP and 2,3,4,5-TeCP as shown by long lag periods,

3. The rate of 3,4,5-TCP reductive dechlorination correlates directly with increases and decreases in hydrogen partial pressure,
4. And successive additions of 3,4,5-TCP does not support growth of the reductively dechlorinating soil culture like PCP as shown by long term experimental trials.

Chapter Five: Conclusions and Engineering Significance

This chapter summarizes the main findings of this research, discusses its significance to the design of remediation systems, and presents suggestions for future work.

Stuart's growth estimation model can be applied to low cell density soil bacterial cultures.

Conclusions: Stuart et al. originally tested her model with a concentrated population from a PCP acclimated sludge. This study showed that a soil culture with a very low cell density can also be examined by reactor study experiments. By analyzing the reactor study data, the apparent growth of reductively dechlorinating bacteria can be determined within a mixed cell culture of high or low cell density. When the initial cell concentration is very low, the number of cells grown is much larger than the initial cell mass; therefore, the initial cell concentration of the culture does not need to be known. Because of this, many scenarios and environmental conditions can be tested to determine the effectiveness of reductively dechlorinating bacteria without the need to discover and isolate a pure culture.

Engineering Significance: While pure culture bacterial studies are important to understanding microbial processes, they do not effectively predict complex *in situ* systems faced by the engineer. Environmental samples better predict real world systems, but they are difficult to understand and analyze. This model provides a valuable tool to measure the viability of environmentally significant subcultures within a complex consortium. The model can be used to determine nutritional needs of a particular consortia.

Research Needs: A simulation performed with the PCP concentration in the zero-order range showed a situation when Stuart's model failed. Stuart's model needs to be tested outside the first-order kinetics region with reactor experiments.

Hydrogen partial pressure affects the apparent growth rate of PCP and 2,3,4,5-TeCP reductively dechlorinating bacteria.

Conclusions: PCP and 2,3,4,5-TeCP reductive dechlorination reactions are coupled to the growth of reductively dechlorinating bacteria. Reductive dechlorination rates accelerate with PCP additions indicating growth of a reductively dechlorinating culture. The apparent growth rate correlates to the partial pressure of hydrogen. Reactor experiments show that the apparent growth rate of PCP reductively dechlorinating microorganisms increases with increasing hydrogen until approximately 2.9×10^{-4} atm with doubling times of 0.94 days as estimated by PCP removal. Beyond that hydrogen partial pressure, the apparent growth rate declines. The correlation between apparent growth rate and hydrogen partial pressure fits well with a substrate inhibition model. The demonstration of hydrogen substrate inhibition on cell growth suggests that there is some optimal hydrogen concentration to stimulate PCP reductively dechlorinating bacteria. A substrate inhibition model of the PCP reductive dechlorination data suggests that the optimal hydrogen partial pressure for this PCP reductively dechlorinating subculture is about 1.0×10^{-3} atm.

Engineering Significance: Hydrogen can be used to stimulate reductively dechlorinating bacteria in mixed culture systems. PCP reductive dechlorination by a mixed soil culture shows that native bacteria can be stimulated to reductively dechlorinate chlorinated hydrocarbons with the addition of hydrogen. The hydrogen substrate inhibition model, suggested here, helps to explain why some researchers observe either reduced yields or inactivation of bacterial cultures at high hydrogen partial pressures. Stimulating reductively dechlorinating bacteria with hydrogen is effective provided the correct hydrogen concentration is provided. This information is important for the efficient design of bioremediation treatment systems of chlorinated hydrocarbons. Prior to the design of a reductive dechlorination strategy, substrate optimization studies for hydrogen need to be performed. In addition,

environmental mixed cultures from the contaminated site should be studied to ensure that the hydrogen concentration selected stimulates the native bacteria rather than environmental isolates or other opportunistic species. This study shows that the optimal hydrogen partial pressure for PCP reductively dechlorinating bacteria in this soil is between 2.9×10^{-4} atm and 1.0×10^{-3} atm.

Research Needs: Reasons for the observed decline in cell growth with increasing hydrogen concentration is not well defined. Hydrogen may inhibit reductive dechlorination at high concentrations as predicted by the substrate inhibition model. However, increased hydrogen concentrations may be toxic and increase the cell decay rate. Reductive dechlorination could be uncoupled from growth as bacteria shift from cell production to energy production when the concentration of hydrogen becomes very high. A better understanding of this relationship will further the understanding of reductively dechlorinating bacteria.

The reductive dechlorination of PCP and 2,3,4,5-TeCP is different from that of 3,4,5-TCP.

Conclusions: The PCP fed reductively dechlorinating soil culture effectively degrades 3,4,5-TCP, but not as the sole electron acceptor. After a longer lag period, the culture degraded 3,4,5-TCP; 3,5-DCP; and 3,4-DCP. Lag periods between *ortho* positioned reductive dechlorination and *meta* or *para* positioned reductive dechlorination combined with the lack of observable inhibition between PCP and 3,4,5-TCP reductive dechlorination suggest that different enzymes or organisms are responsible for reductive dechlorination of PCP and 3,4,5-TCP. The rate of 3,4,5-TCP increases and decreases with increasing and decreasing hydrogen partial pressure, but sequential additions of 3,4,5-TCP did not result in measurable growth like that observed during PCP experiments. Unlike PCP, sequential additions of 3,4,5-TCP do not support bacterial growth of reductively dechlorinating organisms.

Engineering Significance: 3,4,5-TCP is a common metabolite of PCP reductive dechlorination and an environmental contaminant. This begins to distinguish the similarities and differences between PCP and 3,4,5-TCP reductive dechlorination. Hydrogen affects the reductive dechlorination of 3,4,5-TCP, but it may not stimulate bacterial growth. This research indicates several areas of consideration when attempting to mineralize PCP via 3,4,5-TCP production and degradation.

Research Needs: The reductive dechlorination of 3,4,5-TCP provides nearly that same amount of energy as PCP. It is still not clear why 3,4,5-TCP does not support a reductive dechlorinating population. Continued 3,4,5-TCP incubations to study rate, inhibition, toxicity and yield are needed.

Bibliography

1. **Ahring, B. K., P. Westermann, and R. A. Mah.** 1991. Hydrogen Inhibition of Acetate Metabolism and Kinetics of Hydrogen Consumption by *Methanosarcina thermophila* TM-1. *Archives of Microbiology*. **157**:38-42.
2. **Anandarajah, K., P. M. K. Jr, B. S. Donohoe, and S. D. Copley.** 2000. Recruitment of a Double Bond Isomerase to Serve as a Reductive Dehalogenase During Biodegradation of Pentachlorophenol. *Biochemistry*. **39**(18):5303-5311.
3. **Atlas, R. M., and R. Bartha.** 1993. *Microbial Ecology Fundamentals and Applications*, 3 ed. The Benjamin/Cummings Publishing Company, Inc., New York.
4. **Ballapragada, B. S., H. D. Stensel, J.A.Puhakka, and J. F. Ferguson.** 1997. Effect of Hydrogen on Reductive Dechlorination of Chlorinated Ethenes. *Environmental Science and Technology*. **31**:1728-1734.
5. **Bhatnagar, L., J. A. Krzycki, and J. G. Zeikus.** 1987. Analysis of Hydrogen Metabolism in *Methanocarcina barkeri*: Regulation of Hydrogenase and Role of CO-Dehydrogenase in H₂ Production. *FEMS Microbiology Letters*. **41**:337-343.
6. **Bjornstad, B. N., J. P. McKinley, T. O. Stevens, S. A. Rawson, J. K. Fredrickson, and P. E. Long.** 1994. Generation of Hydrogen Gas as a Result of Drilling within the Saturated Zone. *Ground Water*.
7. **Breznak, J. A.** 1994. Acetogenesis from Carbon Dioxide in Termite Guts, p. 303-330. *In* H. L. Drake (ed.), *Acetogenesis*. Chapman and Hall, New York.
8. **Bryant, F. O., D. D. Hale, and J. E. Rogers.** 1991. Regiospecific Dechlorination of Pentachlorophenol by Dichlorophenol-Adapted Microorganisms in freshwater, Anaerobic Sediment Slurries. *Applied and Environmental Microbiology*. **57**(8):2293-2301.
9. **Carr, C. S., and J. B. Hughes.** 1998. Enrichment of High-Rate PCE Dechlorination and Comparative Study of Lactate, Methanol, and Hydrogen as Electron Donors to Sustain Activity. *Environmental Science and Technology*. **32**:1817-1824.

10. **Cole, J. R., A. L. Cascarelli, W. W. Mohn, and J. M. Tiedje.** 1994. Isolation and Characterization of a Novel Bacterium Growing via Reductive Dehalogenation of 2-Chlorophenol. *Applied and Environmental Microbiology*. **60**(10):3536-3542.
11. **Colwell, R. R., P. R. Brayton, D. J. Grimes, D. B. Roszak, S. A. Huq, and L. M. Palmer.** 1985. Viable but Non-culturable *Vibrio cholerae* and Related Pathogens in the Environment: Implications for Release of Genetically Engineered Microorganisms. *Bio/Technology*. **3**.
12. **Conrad, R.** 1996. Soil Microorganisms as Controllers of Atmospheric Trace Gases (H_2 , CO , CH_4 , OCS , N_2O , and NO). *Microbiological Reviews*. **60**:609-640.
13. **Cord-Ruwisch, R., H.-J. Seitz, and R. Conrad.** 1988. The Capacity of Hydrogenotrophic Anaerobic Bacteria to Compete for Traces of Hydrogen Depends on the Redox Potential of the Terminal Electron Acceptor. *Archives of Microbiology*. **149**:350-357.
14. **Dennie, D., I. Gladu, F. Lépine, R. Villemur, J. G. Bisailon, and R. Beaudet.** 1998. Spectrum of the Reductive Dehalogenation Activity of *Desulfitobacterium frappieri* PCP-1. *Applied and Environmental Microbiology*. **64**(11):4603-4606.
15. **DeWeerd, K. A., F. Concannon, and J. M. Suflita.** 1991. Relationship Between Hydrogen Consumption, Dehalogenation, and the Reduction of Sulfur Oxyanions by *Desulfomonile tiedjei*. *Applied and Environmental Microbiology*. **57**(7):1929-1934.
16. **DeWeerd, K. A., L. Mandelco, R. S. Tanner, C. R. Woese, and J. M. Suflita.** 1990. *Desulfomonile tiedjei* gen. nov. and sp. nov., a Novel Anaerobic Dehalogenating, Sulfate-Reducing Bacterium. *Archives of Microbiology*. **154**:23-30.
17. **DiStefano, T. D., J. M. Gossett, and S. H. Zinder.** 1992. Hydrogen as an Electron Donor for Dechlorination of Tetrachloroethene by an Anaerobic Mixed Culture. *Applied and Environmental Microbiology*. **58**(11):3622-3629.
18. **Dolfing, J.** 1990. Reductive Dechlorination of 3-Chlorobenzoate is Coupled to ATP Production and Growth in an Anaerobic Bacterium, Strain DCB-1. *Archives of Microbiology*. **153**:264-266.

19. **Dolfing, J., and K. B. Harrison.** 1992. Gibbs Free Energy of Formation of Halogenated Aromatic Compounds and Their Potential Role as Electron Acceptors in Anaerobic Environments. *Environmental Science and Technology*. **26**(11):2213-2218.
20. **Dolfing, J., and J. M. Tiedje.** 1987. Growth Yield Increase Linked to Reductive Dechlorination in a Defined 3-Chlorobenzoate Degrading Methanogenic Coculture. *Archives of Microbiology*. **149**:102-105.
21. **Fantroussi, S. E., H. Navaeu, and S. N. Agathos.** 1998. Anaerobic Dechlorinating Bacteria. *Biotechnology Progress*. **14**(2):167-188.
22. **Fennell, D. E., and J. M. Gossett.** 1997. Comparison of Butyric Acid, Ethanol, Lactic Acid, and Propionic Acid as Hydrogen Donors for the Reductive Dechlorination of Tetrachloroethene. *Environmental Science and Technology*. **31**:918-926.
23. **Fennell, D. E., and J. M. Gossett.** 1998. Modeling the Production of and Completion for Hydrogen in a Dechlorination Culture. *Environmental Science and Technology*. **32**:2450-2460.
24. **Gibson, S. A., and J. M. Suflita.** 1986. Extrapolation of Biodegradation Results to Groundwater Aquifers: Reductive Dechlorination of Aromatic Compounds. *Applied and Environmental Microbiology*. **52**(4):681-688.
25. **González, J. M., W. B. Whitman, R. E. Hodson, and M. A. Moran.** 1996. Identifying Numerically Abundant Culturable Bacteria from Complex Communities: an Example from a Lignin Enrichment Culture. *Applied and Environmental Microbiology*. **63**(12):4433-4440.
26. **Hale, D. D., J. E. Rogers, and J. Wiegel.** 1991. Environmental Factors Correlated to Dichlorophenol Dechlorination in Anoxic Freshwater Sediments. *Environmental Toxicology and Chemistry*. **10**:1255-1265.
27. **Heijnen, J. J., and J. P. v. Dijken.** 1992. In Search of a Thermodynamic Description of Biomass Yields for the Chemotrophic Growth of Microorganisms. *Biotechnology and Bioengineering*. **39**:833-858.
28. **Heijnen, J. J., M. C. M. v. Loosdrecht, and L. Tijhuis.** 1992. A Black Box Mathematical Model to Calculate Auto- and Heterotrophic Biomass Yields Based on Gibbs Energy Dissipation. *Biotechnology and Bioengineering*. **40**:1139-1154.

29. **Horowitz, A., J. M. Suflita, and J. M. Tiedje.** 1983. Reductive Dehalogenation of Halobenzoates by Anaerobic Lake Sediment Microorganisms. *Applied and Environmental Microbiology*. **45**(5):1459-1465.
30. **Isalou, M., B. E. Sleep, and S. N. Liss.** 1998. Biodegradation of High Concentrations of Tetrachloroethene in a Continuous Flow Column System. *Environmental Science and Technology*. **32**:3579-3585.
31. **Kennes, C., W.-M. Wu, L. Bhatnagar, and J. G. Zeikus.** 1996. Anaerobic Dechlorination and Mineralization of Pentachlorophenol and 2,4,6-Trichlorophenol by Methanogenic Pentachlorophenol-Degrading Granules. *Applied Microbiology and Biotechnology*. **44**:801-806.
32. **Kohring, G.-W., J. E. Rogers, and J. Wiegel.** 1989. Anaerobic Biodegradation of 2,4-Dichlorophenol in Freshwater Lake Sediments at Different Temperatures. *Applied and Environmental Microbiology*. **55**(2):348-353.
33. **Kohring, G.-W., X. Zhang, and J. Wiegel.** 1989. Anaerobic Dechlorination of 2,4-Dichlorophenol in Freshwater Sediments in the Presence of Sulfate. *Applied and Environmental Microbiology*. **55**(10):2735-2737.
34. **Krone, U. E., K. Laufer, R. K. Thauer, and H. P. Hogenkamp.** 1989. Coenzyme F430 as a Possible Catalyst for the Reductive Dehalogenation of Chlorinated C1 Hydrocarbons in Methanogenic Bacteria. *Biochemistry*. **28**(26):10061-10065.
35. **Larsen, S., H. V. Hendriksen, and B. K. Ahring.** 1991. Potential for Thermophilic (50°C) Anaerobic Dechlorination of Pentachlorophenol in Different Ecosystems. *Applied and Environmental Microbiology*. **57**(7):2085-2090.
36. **Lasdon, L. S., A. D. Waren, A. Jain, and M. Ratner.** 1978. Design and Testing of a Generalized Reduced Gradient Code for Nonlinear Programming. *ACM Transaction on Mathematical Software*. **4**(1):34-50.
37. **Linkfield, T. G., J. M. Suflita, and J. M. Tiedje.** 1989. Characterization of the Acclimation Period before Anaerobic Dehalogenation of Halobenzoates. *Applied and Environmental Microbiology*. **55**(11):2773-2778.

38. **Linkfield, T. G., and J. M. Tiedje.** 1990. Characterization of the Requirements and Substrates for Reductive Dehalogenation by Strain DCB-1. *Journal of Industrial Microbiology*. **5**(1):9-15.
39. **Liu, S.-M., C.-E. Kuo, and T.-B. Hsu.** 1996. Reductive Dechlorination of Chlorophenols and Pentachlorophenol in Anoxic Estuarine Sediments. *Chemosphere*. **32**(7):1287-1300.
40. **Löffler, F. E., J. M. Tiedje, and R. A. Sanford.** 1999. Fraction of Electrons Consumed in Electron Acceptor Reduction and Hydrogen Thresholds as Indicators of Halorespiratory Physiology. *Applied and Environmental Microbiology*. **65**(9):4049-4056.
41. **Lovley, D. R.** 1985. Minimum Threshold for Hydrogen Metabolism in Methanogenic Bacteria. *Applied and Environmental Microbiology*. **49**:1530-1531.
42. **Lovley, D. R., F. H. Chapelle, and J. C. Woodward.** 1994. Use of Dissolved H₂ Concentrations to Determine Distribution of Microbially Catalyzed Redox Reactions in Anoxic Groundwater. *Environmental Science and Technology*. **28**(7):1205-1210.
43. **Lovley, D. R., and S. Goodwin.** 1988. Hydrogen Concentrations as an Indicator of the Predominant Terminal Electron-accepting Reactions in Aquatic Sediments. *Geochimica et Cosmochimica Acta*. **52**:2993-3003.
44. **Madsen, T., and J. Aamand.** 1992. Anaerobic Transformation and Toxicity of Trichlorophenols in a Stable Enrichment Culture. *Applied and Environmental Microbiology*. **58**(2):557-561.
45. **Madsen, T., and J. Aamand.** 1991. Effects of Sulfuroxy Anions on Degradation of Pentachlorophenol by a Methanogenic Enrichment Culture. *Applied and Environmental Microbiology*. **57**(9):2453-2458.
46. **Madsen, T., and D. Licht.** 1992. Isolation and Characterization of an Anaerobic Chlorophenol-Transforming Bacterium. *Applied and Environmental Microbiology*. **58**(9):2874-2878.
47. **Magar, V. S., H. D. Stensel, J. A. Puhakka, and J. F. Ferguson.** 1999. Sequential Anaerobic Dechlorination of Pentachlorophenol: Competitive Inhibition Effects and a Kinetic Model. *Environmental Science and Technology*. **33**(10):1604-1611.

48. **Masunaga, S., S. Susarla, J. L. Gundersen, and Y. Yonezawa.** 1996. Pathway and Rate of Chlorophenol Transformation in Anaerobic Estuarine Sediment. *Environmental Science and Technology*. **30**:1253-1260.
49. **Maymo-Gatell, X., Y.-t. Chien, J. M. Gossett, and S. H. Zinder.** 1997. Isolation of a Bacterium that Reductively Dechlorinates Tetrachloroethene to Ethene. *Science*. **276**:1568-1571.
50. **Maymo-Gatell, X., V. Tandoi, J. M. Gossett, and S. H. Zinder.** 1995. Characterization of an H₂-Utilizing enrichment Culture That Reductively Dechlorinates Tetrachloroethene to Vinyl Chloride and Ethene in the Absence of Methanogenesis and Acetogenesis. *Applied and Environmental Microbiology*. **61**(11):3928-3933.
51. **McCarty, P. L.** 1993. *In situ* Bioremediation of Chlorinated Solvents. *Current Opinion in Biotechnology*. **4**:232-330.
52. **Mikesell, M. D., and S. A. Boyd.** 1986. Complete Reductive Dechlorination and Mineralization of Pentachlorophenol by Anaerobic Microorganisms. *Applied and Environmental Microbiology*. **52**(4):861-865.
53. **Mohn, W. W., and K. J. Kennedy.** 1992. Reductive Dehalogenation of Chlorophenols by *Desulfomonile tiedjei* DCB-1. *Applied and Environmental Microbiology*. **58**(4):1367-1370.
54. **Mohn, W. W., and J. M. Tiedje.** 1992. Microbial Reductive Dehalogenation. *Microbiological Reviews*. **56**(3):482-507.
55. **Mohn, W. W., and J. M. Tiedje.** 1990. Strain DCB-1 Conserves Energy for Growth from Reductive Dechlorination Coupled to Formate Oxidation. *Archives of Microbiology*. **153**:267-271.
56. **Morinaga, T., and N. Kawada.** 1990. The Production of Acetic Acid from Carbon Dioxide and Hydrogen by an Anaerobic Bacterium. *Journal of Biotechnology*. **14**:187-194.
57. **Nastainczyk, W., H. Ahr, and V. Ulrich.** 1981. The Mechanism of the Reductive Dehalogenation of Polyhalogenated Compounds by Microsomal Cytochrome P-450. *Advances in Experimental Medical Biology*. **136**:799-808.

58. **Nicholson, D. K., S. L. Woods, J. D. Istok, and D. C. Peek.** 1992. Reductive Dechlorination of Chlorophenols by a Pentachlorophenol-Acclimated Methanogenic Consortium. *Applied and Environmental Microbiology*. **58**(7):2280-2286.
59. **Novak, P. J., L. Daniels, and G. F. Parkin.** 1998. Enhanced Dechlorination of Carbon Tetrachloride and Chloroform in the Presence of Elemental iron and *Methanosarcina barkeri*, *Methanosarcina thermophila*, or *Methanosaeta concillii*. *Environmental Science and Technology*. **32**:1438-1443.
60. **Owen, W. F., D.C.Stuckey, J. B. Heal, L.Y.Young, and P. L. McCarty.** 1979. Bioassay for Monitoring Biochemical Methane Potential and Anaerobic Toxicity. *Water Research*. **13**:485-492.
61. **Press, W. H., B. P. Flannery, S. A. Teukolsky, and W. T. Vetterling.** 1989. Numerical Recipes: The Art of Scientific Computing (FORTRAN Version). Cambridge University Press, Cambridge.
62. **Robinson, J. A., and W. G. Characklis.** 1984. Simultaneous Estimation of V_{max} , K_m , and the Rate of Endogenous Substrate Production (R) from Substrate Depletion Data. *Microbial Ecology*. **10**:165-178.
63. **Robinson, J. A., and J. M. Tiedje.** 1983. Nonlinear Estimation of Monod Growth Kinetic Parameters from a Single Substrate Depletion Curve. *Applied and Environmental Microbiology*. **45**(5):1453-1458.
64. **Rosner, B. M., P. L. McCarty, and A. M. Spormann.** 1997. In Vitro Studies on reductive Vinyl Chloride Dehalogenation by an Anaerobic Mixed Culture. *Applied and Environmental Microbiology*. **63**(11):4139-4144.
65. **Ruckdeschel, G., G. Renner, and K. Schwarz.** 1987. Effects of Pentachlorophenol and Some of Its Known and Possible Metabolites on Different Species of Bacteria. *Applied and Environmental Microbiology*. **53**(11):2689-2692.
66. **Schmidt, S. K.** 1992. A Substrate-Induced Growth-Response Method for Estimating the Biomass of Microbial Functional Groups in Soil and Aquatic Systems. *FEMS Microbiology Ecology*. **101**:197-206.
67. **Scow, K. M., S. Simkins, and M. Alexander.** 1986. Kinetics of Mineralization of Organic Compounds at Low Concentrations in Soil. *Applied and Environmental Microbiology*. **51**(5):1028-1035.

68. **Simkins, S., and M. Alexander.** 1984. Models for Mineralization Kinetics with the Variables of Substrate Concentration and Population Density. *Applied and Environmental Microbiology*. **47(6):1299-1306.**
69. **Simkins, S., R. Mukherjee, and M. Alexander.** 1986. Two Approaches to Modeling Kinetics of Biodegradation by Growing Cells and Application of a Two-Compartment Model for Mineralization Kinetics in Sewage. *Applied and Environmental Microbiology*. **51(6):1153-1160.**
70. **Smatlak, C. R., and J. M. Gossett.** 1996. Comparative Kinetics of Hydrogen Utilization for Reductive Dechlorination of Tetrachloroethene and Methanogenesis in an Anaerobic Enrichment Culture. *Environmental Science and Technology*. **30(9):2850-2858.**
71. **Smith, D. P., and P. L. McCarty.** 1989. Energetic and Rate Effects on Methanogenesis of Ethanol and Propionate in Perturbed CSTRs. *Biotechnology and Bioengineering*. **34:39-54.**
72. **Steiert, J. G., J. J. Pignatello, and R. L. Crawford.** 1987. Degradation of Chlorinated Phenols by a Pentachlorophenol-Degrading Bacterium. *Applied and Environmental Microbiology*. **53(5):907-910.**
73. **Steiert, J. G., W. J. Thomas, K. Ugurbil, and R. L. Crawford.** 1988. ³¹P Nuclear Magnetic Resonance Studies of Effects of Some Chlorophenols on *Escherichia coli* and a Pentachlorophenol-Degrading Bacterium. *Journal of Bacteriology*. **170(10):4954-4957.**
74. **Stuart, S. L.** 1996. Doctor of Philosophy. Oregon State University, Corvallis.
75. **Stuart, S. L., and S. L. Woods.** 1998. Kinetic Evidence for Pentachlorophenol-Dependent Growth of a Dehalogenating Population in a Pentachlorophenol- and Acetate-Fed Methanogenic Culture. *Biotechnology and Bioengineering*. **57(4):420-429.**
76. **Stuart, S. L., S. L. Woods, T. L. Lemmon, and J. James D. Ingle.** 1999. The Effect of Redox Potential Changes on Reductive Dechlorination of Pentachlorophenol and the Degradation of Acetate by a Mixed Methanogenic Culture. *Biotechnology and Bioengineering*. **63(1):69-78.**

77. **Stumm, W., and J. J. Morgan.** 1995. Aquatic Chemistry: Chemical Equilibria and Rates in Natural Waters, 3rd Edition, 3 ed. John Wiley and Sons.
78. **Sufliita, J. M., A. Horowitz, D. R. Shelton, and J. M. Tiedje.** 1982. Dehalogenation: A Novel Pathway for the Anaerobic Biodegradation of Haloaromatic Compounds. *Science*. **218**:1115-1117.
79. **Sufliita, J. M., W. J. Smolenski, and J. A. Robinson.** 1987. Alternative Nonlinear Model for Estimating Second-Order Rate Coefficients for Biodegradation. *Applied and Environmental Microbiology*. **53**(5):1064-1068.
80. **Takazawa, R. S., and H. J. Strobel.** 1986. Cytochrome P-450 Mediated Reductive Dechlorination of the Perhalogenated Aromatic Compound Hexachlorobenzene. *Biochemistry*. **25**(17):4804-4809.
81. **Tchobanoglous, G., and F. L. Burton.** 1991. Wastewater Engineering Treatment, Disposal, and Reuse / Metcalf & Eddy, Inc., 3 ed. McGraw-Hill, Inc., San Francisco.
82. **Utkin, I., D. D. Dalton, and J. Wiegel.** 1995. Specificity of Reductive Dehalogenation of Substituted *ortho*-Chlorophenols by *Desulfitobacterium dehalogenans* JW/IU-DC1. *Applied and Environmental Microbiology*. **61**(1):346-351.
83. **Utkin, I., C. R. Woese, and J. Wiegel.** 1994. Isolation and Characterization of *Desulfitobacterium dehalogenans* gen. nov., sp. nov., an Anaerobic Bacterium which Reductively Dechlorinates Chlorophenolic Compounds. *International Journal of Systematic Bacteriology*. **44**(4):612-619.
84. **Vogel, T. M., C. S. Criddle, and P. L. McCarty.** 1987. Transformations of Halogenated Aliphatic Compounds. *Environmental Science and Technology*. **21**(8):722-736.
85. **Vogel, T. M., and P. L. McCarty.** 1985. Biotransformation of Tetrachloroethylene to Trichloroethylene, Dichloroethylene, Vinyl Chloride, and Carbon Dioxide Under Methanogenic Conditions. *Applied and Environmental Microbiology*. **49**(5):1080-1083.

86. **Wang, Y.-T., S. Muthukrishnan, and Z. Wang.** 1998. Reductive Dechlorination of Chlorophenols in Methanogenic Cultures. *Journal of Environmental Engineering*. **124**(3):231-238.
87. **Wiegel, J., X. Zhang, and Q. Wu.** 1999. Anaerobic Dehalogenation of Hydroxylated Polychlorinated Biphenyls by *Desulfitobacterium dehalogenans*. *Applied and Environmental Microbiology*. **65**(5):2217-2221.
88. **Wiggins, B. A., S. H. Jones, and M. Alexander.** 1987. Explanations for the Acclimation Period Preceding the Mineralization of Organic Chemicals in Aquatic Environments. *Applied and Environmental Microbiology*. **53**(4):791-796.
89. **Yang, Y., and P. L. McCarty.** 1998. Competition for Hydrogen within a Chlorinated Solvent Dehalogenating Anaerobic Mixed Culture. *Environmental Science and Technology*. **32**:3591-3597.

Appendices

Appendix A: Activity of a PCP Reductively Dechlorinating Mixed Soil Culture

This appendix outlines computer simulations of multiple addition reactor experiments. The simulations were used to evaluate the effects of initial cell number and hydrogen concentration on substrate utilization data and to help design the reactor experiments. Reactor simulations were used to test substrate utilization constants, cell yield, and half velocity coefficients on the observable doubling time of a culture that reductively dechlorinates PCP. This study also presents a newly developed substrate utilization model (Lotrario's) and compares it with a similar model derived by Stuart et al. (74). It should be noted that Lotrario's model, as presented here, incorporates large errors as time steps between concentration measurements get larger than one hour.

The methods in this appendix enable the study of small sub-populations of environmentally relevant bacteria. While specific organisms cannot be identified from within the bulk population, their metabolic functions can. Substrate utilization and metabolite production can be measurable representations of bacterial activity. The methods described in this paper explain two comparable models that use substrate utilization data to estimate cell growth of PCP reductively dechlorinating bacteria within a mixed soil culture.

An array of mathematical models of varying complexity is available to evaluate cell growth as a function of substrate utilization. Studies show that nonlinear regression with Monod based models are a valuable tool to estimate microbial mineralization kinetics (68). Studies using simulated data sets show the ability to estimate Monod growth kinetic parameters using nonlinear least squares analysis (63). Nonlinear estimations of progress curve data is superior to linear methods when the initial substrate concentration estimate is not free from error (62). Progress curves of substrate depletion are used as indirect indicators of growth (66), and biomass estimates of organisms that catalyze a specific metabolic function in a

complex system are possible by nonlinear regressions of substrate mineralization curves (66).

While non-linear batch study estimations of growth parameters can provide accurate results, limitations linked to cell growth, inoculum history, and maintenance requirements can introduce large errors (63). Violations to the no-growth assumption leads to an underestimation of substrate utilization rates (79). Models based on the second-order rate coefficient derived from the differential form of the Monod equation can underestimate the time required for the degradation of a contaminant by not considering cell growth over the course of the experiment (79). A diversity of shapes of mineralization curves result from the interactions of substrate and population density (68), and the mineralization kinetics of organic compounds at low concentrations are often not effectively modeled by Monod kinetic models (67).

The models described above are limited to batch reactions where there is an assumption of no cell growth and substrate is added to the culture once. This study incorporates an experimental design that enables the study of bacterial viability and competition under mixed microbial conditions. The proposed method of analysis estimates the development of a specific sub-population in the presence of other organisms by measuring substrate degradation. When reductively dechlorinating bacteria are provided discrete additions of PCP and monitored for their rate of reductive dechlorination, the rate of dechlorination increases exponentially as the culture grows (75). In one study, microbial activity increases with the addition of substrate at a rate analogous to the rate of substrate addition. This study also shows that activity growth rates could be linear or exponential depending on the pattern of PCP addition (74).

The objectives established for this appendix are to:

1. Simulate reactor experiments with a simple computer program,
2. Examine the effect of initial cell mass and hydrogen concentration on PCP reductive dechlorination, and

3. Compare a newly developed model with Stuart's (used in Chapter 3) as they are used to estimate the apparent growth rates of PCP reductively dechlorinating bacteria using simulated substrate depletion data.

Theory

Model Derivation

Lotrario's strategy was an adjustment to Stuart's model. The reactor system was similar for both, and the different assumptions of each model were satisfied by adjustments to the experimental procedures. A derivation of Lotrario's model follows.

This derivation did not require the first-order degradation rate assumption, therefore, allowing the reactor to be used for a wider variety of reactions. Lotrario's derivation also enabled data to be analyzed after a single curve fit rather than the two fold process required by Stuart's method. By simplifying and numerically solving the mass balance equations on cells and substrate, (Appendix Equation A.1 and Appendix Equation A.2, respectively) an activity coefficient comparable to Stuart's was derived. One assumption made during Lotrario's derivation was that the concentration of PCP in the reactor was constant. In practice the PCP concentration was kept at a nearly constant value with an allowably small variation between high and low concentrations. This assumption was satisfied experimentally by shortening the interval along which the PCP spikes were allowed to degrade before injecting an additional spike and thereby maintaining a pseudo-constant PCP concentration. The ability to simulate constant conditions in the reactor was tested and compared to experiments with variable PCP concentrations. Computer simulations were used to determine a sufficiently small variation in PCP concentration that could simulate constant PCP concentration. The PCP concentration in the reactor was, therefore,

assumed constant for the purpose of the model derivation. If the assumption is not maintained through careful experimentation, it can result in large errors.

Appendix Equation A.1
$$\frac{dX}{dt} = Yk_m \frac{S}{K_s + S} X - bX$$

Appendix Equation A.2
$$\frac{dS}{dt} = k_m \frac{S}{K_s + S} X$$

Where

X = cell mass of reductively dechlorinating bacteria, mg/L

k_m = the maximum substrate utilization rate, $\mu\text{M}_{\text{substrate}}/\text{mg}_{\text{cells present}}\text{-hour}$

Y = the cell yield, $\text{mg}_{\text{cells produced}}/\mu\text{M}_{\text{substrate}}$

K_s = the half velocity coefficient, μM

S = the chlorinated phenol, μM

When the PCP concentration in the reactor is assumed constant, the quantity, $Yk_m S/(K_s + S) - b$ reduces to a constant, α' that is comparable to the constant α presented by Stuart (75). The pseudo-constant PCP concentration assumption made the first-order assumption of Stuart's model unnecessary. Integrating Appendix Equation A.1 for constant substrate, S , with respect to time solved for X as an exponential function of α' as shown in Appendix Equation A.3.

Appendix Equation A.3
$$X_t = X_{t=0} (e^{\alpha' t})$$

Appendix Equation A.3 was substituted into Appendix Equation A.2 to establish the measurable disappearance of substrate with time ($\Delta S/\Delta t$) as a function of the exponential constant α' as shown in Appendix Equation A.4. The differential,

dS/dt , was replaced with the measurable quantity, $\Delta S/\Delta t$, and a numerical solution was used to solve Appendix Equation A.4 for the "activity" growth constant. This solution is only a good approximation for the two differentials over small time increments.

Appendix Equation A.4
$$\frac{\Delta S}{\Delta t} = k_m \frac{S}{K_s + S} X_{t=0} (e^{\alpha' t})$$

Discrete measurements of PCP taken during the experiment were used to calculate $\Delta S/\Delta t$. Those data were then graphed according to the time of the second sample and fit to a first-order growth curve. The first-order growth rate equaled α' . As expected, when substrate utilization was linked to growth, the acceleration of substrate degradation was equal to the culture's growth rate. Non-linear estimation was used to solve for the first-order growth coefficient (α') and initial reductive dechlorination rate ($X_{t=0} k_m S / (K_s + S)$). The difference between α' and α from Equation 3.4 is due to the difference in the two derivations and their respective assumptions. Both terms represent an apparent growth rate term of a specific population of bacteria able to metabolize the substrate in question.

Appendix Table A.1: Summary of Lotrario's and Stuart's models

Comparisons	Lotrario	Stuart
Kinetic Model	Monod	1 st order
Decay term	Explicit	Implicit
Substrate concentration	Assumed constant	Allowed to decline
Pros	One regression necessary	Not affected by concentration fluctuations
	Includes data from first PCP addition	
Cons	Sensitive to PCP concentration fluctuations in the reactor	Requires two separate regressions
	Large errors are possible from small deviations from assumptions	Only applicable to first-order degradation reactions

Computer Simulations

The computer simulation was designed to model the degradation of PCP to 2,3,4,5-TeCP in the reactor according to dual Monod kinetics. Using Excel for Windows 95 (Version 7.0, Microsoft), a simple numerical solution by serially stepping through Monod growth equations calculated PCP reductive dechlorination and cell growth. The program simulated multiple PCP additions analogous to the reactor protocol. By setting a PCP addition concentration and a minimum concentration at which a new addition was made, the PCP concentration range in the reactor was established. This also established an average concentration of PCP in the reactor. The effect of initial cell mass and hydrogen partial pressure on reductive dechlorination rates and growth rates were tested with simulations. The computer simulations were used in the design of the final reactor experiment. Numerous PCP concentration ranges were tested to compare the ability of each model to estimate the growth rate of reductively dechlorinating bacteria. The model

estimation of apparent growth is compared to the curve fit cell concentration data calculated by the computer simulation.

The models developed for this research were based on Monod kinetics. Computer simulations of reactor experiments were performed using Monod coefficient values obtained from the literature and displayed in Appendix Table A.2. Values were obtained from a number of sources and based on research with different bacteria and methods. These values from the literature were used to provide a basis for coefficients used in the reactor simulations. Pure culture and mixed consortia studies are compared. Numbers used in the model are near the median of literature values.

The half velocity coefficient of PCP was observed by Magar et al. to be 0.41 μM (47). Stuart et al. observed a half velocity coefficient of 0.5 μM (75). In incubations with the soil consortia used for these experiments show that at PCP concentrations between 0.4 and 0.04 μM PCP resulted in first-order reductive dechlorination kinetics. Those results suggested a value of 0.45 μM as the PCP half velocity coefficient as discussed in the results section.

Yield of reductively dechlorinating bacteria on PCP was estimated mathematically based on energetic equations to be 6 g VSS/mole (19, 27, 28, 75) and measured to be between 3 and 11 g VSS/mole of electron acceptor (20, 53). Calculations of yield coefficients with varying hydrogen concentrations showed that 6 g VSS/mole of electron acceptor was a good approximation for both PCP and 2,3,4,5-TeCP at hydrogen partial pressures between 10^{-4} and 1 atm (19, 27, 28).

The maximum substrate utilization coefficient varied widely with the experimental system. The value used by Stuart et al., 24 mmol $\text{Cl}^-/\text{g protein-h}$, was calculated from energetics equations (75). All others were determined experimentally. The value chosen, 11.3 mmol $\text{Cl}^-/\text{g protein-h}$, was between the very low and very high numbers presented in the literature. This range may be due to differences in experimental methods and microbial cultures.

The hydrogen half velocity coefficients presented in Appendix Table A.2 were measured for other reductively dechlorinating systems and may or may not represent PCP reductively dechlorinating bacterial systems.

The apparent lag period, shape of reductive dechlorination curves, and the shape of cell growth curves of simulated data were all compared with preliminary experiments. From these data, values for Monod kinetic coefficients were chosen in conjunction with experimental initial cell number values that best simulate experimental results.

Appendix Table A.2: Monod kinetic coefficients and estimated values

Constants	Available Values	References
PCP half velocity coefficient $\mu\text{mol/L}$ ($K_s(\text{PCP})$)	0.41	(47)
	0.50	(75)
Yield (Y) g VSS/mol e^- acceptor (PCP to 2,3,4,5-TeCP)	3-6	(55)
	6	(75)
	11	(18)
Maximum substrate utilization coefficient (k_{max}) mmol $\text{Cl}^-/\text{g protein-h}$	0.0075	(48)
	0.029	(47)
	0.054	(54)
	24	(75)
	114	(86)
Cell decay (b) day^{-1}	0.05	(81)
	0.02-0.08	Experimental estimate
Hydrogen half velocity coefficient ($K_s(\text{H}_2)$) nM {atm}	9	(4)
	$\{1.13 \times 10^{-5}\}$	
	100	(70)
	$\{1.26 \times 10^{-4}\}$	

Results

Two sets of computer simulations were performed, the first was a variable study of the computer model. The second set was composed of reactor experiment simulations. Variable study experiments were used to determine appropriate ranges for initial cell mass and H_2 concentration. Computer simulations of the reactor experiments were performed to test the growth models under a wide array of situations. Laboratory reactor experiments were time and supply intensive and computer simulations allowed the experimental design to be efficiently optimized prior to laboratory experiments. The simulations also allowed the two models to be compared before laboratory experiments were performed. Each model was tested for its ability to estimate calculated growth coefficients under a variety of concentration ranges. While the reactor experiment studies examined mixed cultures the computer studies assumed that all bacteria were PCP reductive dechlorinators.

Variable Study

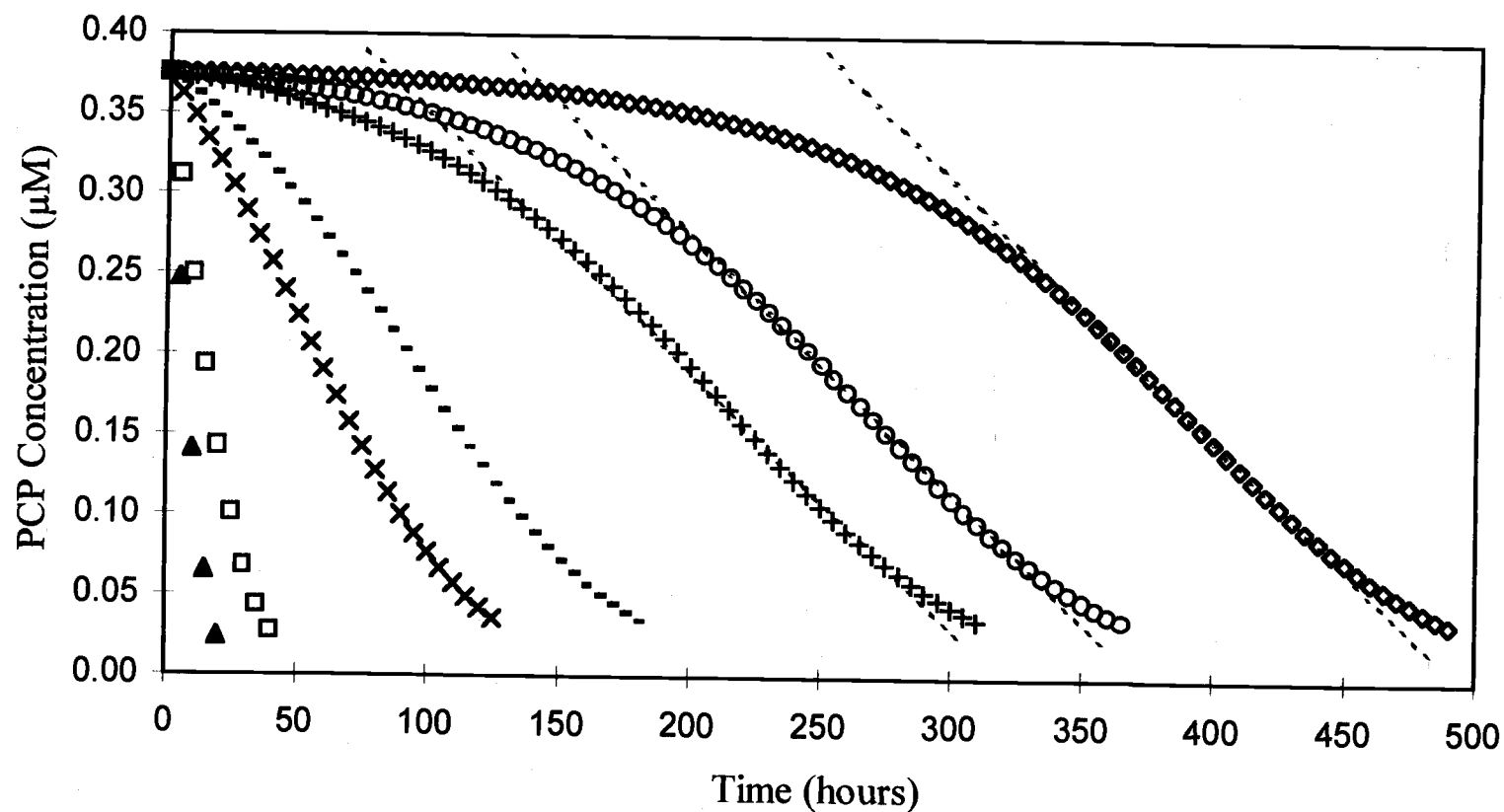
The variable studies were conducted to evaluate the importance of H_2 and initial cell mass of reductively dechlorinating bacteria on the rate of reductive dechlorination of PCP. These were done by entering kinetic constants and initial variables into a program that simulates Monod based kinetic systems. Each time the program was run, one of either initial cell mass or H_2 gas was varied and all other variables remained constant. A computer simulation of PCP reductive dechlorination was developed based on Monod kinetics to compare the sensitivity and robustness of the two theoretical models. The kinetic constants used in the simulations were based on those presented in literature and early experimental results as listed in

Appendix Table A.3. When more than one value was available from the literature, the value was chosen that produced data which best fit the observed lag time, curve shape, and growth trend of preliminary experimental data. A number of simulations were run according to the parameters shown in Appendix Table A.3 to understand the working of the model and to design the reactor experiment.

Appendix Table A.3: Parameters used during computer simulations to test the effect of initial cell concentration

Constants used during simulation	Values	Units
Initial Values		
Initial cells (X_0)	Variable	mg cells L^{-1}
Initial substrate (PCP_0)	3.8×10^{-1}	μM
Hydrogen partial pressure	1.0×10^{-4}	atm
Monod Constants		
PCP Half velocity coefficient - $K_s(PCP)$	4.5×10^{-1}	μM
Yield - Y	6.13×10^{-3}	mg cells $L^{-1} \mu M^{-1}$
Degradation rate - k_m	11.3	μM CI mg cells ⁻¹ hour ⁻¹
Cell decay rate - b	2.0×10^{-3}	hours ⁻¹
Hydrogen Half Velocity coefficient - $K_s(H_2)$	1.0×10^{-4}	atm
Simulation variables		
At what S concentration re-spike	3.8×10^{-2}	μM
Spike stock concentration, Ssp	3.42×10^{-1}	μM
Duration of experiment	1.2×10^2	hours
Delta time	5	hours

The effects of initial cell number of reductively dechlorinating bacteria on the rate of reductive dechlorination and the shape of the dechlorination curve was examined. A time course of simulated PCP dechlorination data was plotted for different initial cell concentrations as shown in Appendix Figure A.1. Initial PCP reductive dechlorinator concentration affected both the apparent lag times before first-order reductive dechlorination began and the reductive dechlorination rates. For a large range of initial cell concentrations, 5×10^{-4} mg/L and lower, the eventual first-order degradation rates were approximately 1.6 μ M Cl/hour. The degradation rates begin differently, but converge on a similar value during the period of zero-order degradation. The amount of substrate provided during the first addition is sufficient to grow approximately 3.2×10^{-3} mg of PCP reductively dechlorinating bacteria so that when a low number of cells is initially added to the reactor the final concentration of cells in the reactor following PCP consumption is determined by the mass of PCP consumed. The time prior to observable reductive dechlorination was not dependent on true acclimation - defined by Linkfield et al. as a "period of no degradation followed by initiation and acceleration of degradation," (37) - but rather, a function of low cell number similar to that observed in other studies (88). At low initial cell numbers, the degradation curve does not approximate first-order kinetics until a minimum cell concentration is achieved. After that time the apparent zero-order degradation rates are approximately the same. When a very low number of initial cells was used, the cell growth from one PCP addition was much greater than the initial inoculum. This made the initial concentration negligible so that the relative cell number after one PCP addition could be assumed constant. At cell concentrations greater than 5×10^{-4} mg/L, the cell number affected the slope of the curve and the apparent zero-order degradation rate began to increase with an increase in cell concentration.



Appendix Figure A.1: Progress curves of simulated PCP reductive dechlorination when the initial cell concentration is 0.01 mg/L (▲), 0.005 mg/L (□), 0.001 mg/L (×), 0.0005 mg/L (▪), 0.0001 mg/L (+), 0.00005 mg/L (○), and 0.00001 mg/L (◇) with linearization for a first-order reductive dechlorination rate of $1.6 \mu\text{M Cl}^-/\text{hour}$ (- - -)

A low initial cell concentration ensured that the experiments began with relatively the same number of cells and at the same rate of reductive dechlorination. When a very low number of initial cells was used, the cell growth from one PCP addition was much greater than the initial cell inoculum; therefore, the initial concentration was negligible as shown in Appendix Table A.4. When compared to the difference of the initial number of cells, a 1000 times increase in initial cell concentration only resulted in a 1.6 factor increase in final cell number. This suggests that each reactor experiment was begun with approximately the same number of reductively dechlorinating bacteria within a factor of two even though cell number measurements were not possible.

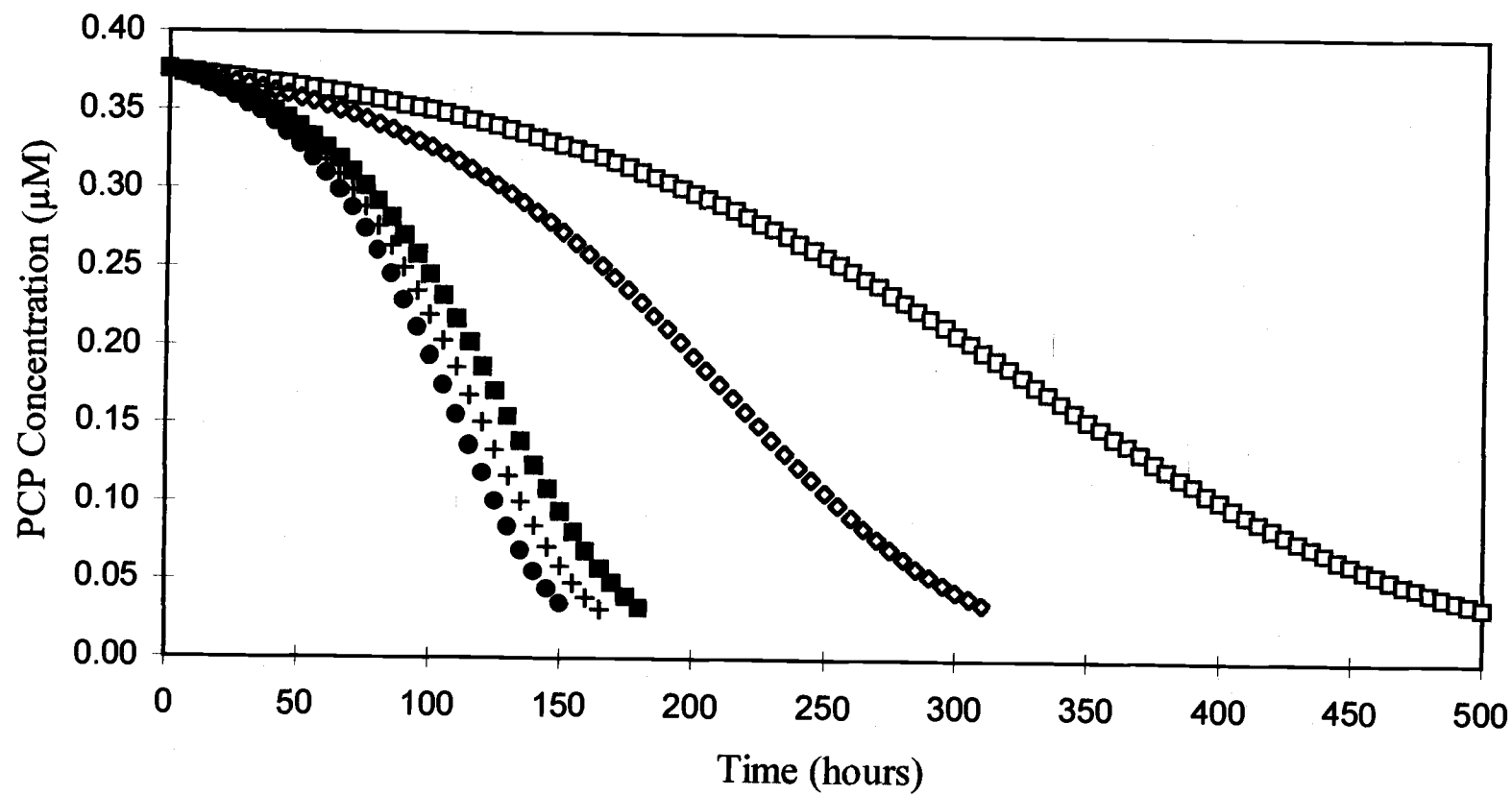
Appendix Table A.4: Cell Concentration after one addition of PCP

Initial Cell Concentration mg/L	Factor of Difference	Cell Concentration After One PCP Spike mg/L
1×10^{-3}	1000	2.6×10^{-3}
5×10^{-3}	500	2.1×10^{-3}
1×10^{-4}	100	1.7×10^{-3}
5×10^{-4}	50	1.6×10^{-3}
1×10^{-5}	1	1.6×10^{-3}

Because the initial rate of dechlorination does not follow first order kinetics (Appendix Figure A.1), data from the first spike of PCP was not used in Stuart's analysis. The assumption of negligible cell growth is not valid during the dechlorination of the first PCP addition because the relatively low number of initial cells at least doubles during the reductive dechlorination of the first PCP addition (Appendix Table A.4). By the second addition of PCP in the reactor, the cell concentration had risen to a level where first-order reductive dechlorination was seen in the simulation. Stuart's derivation of apparent cell growth from measured rates of PCP reductive dechlorination in the reactor is more accurate when the rate

of reductive dechlorination of the first addition of PCP is excluded. Because Lotrario's model did not require first-order kinetics, data from the initial PCP addition was used.

Determining the effect of hydrogen concentration on the rate of PCP reductive dechlorination in a mixed microbial culture was a major goal of this research. A second simulation compared the effects of varying hydrogen concentration on reductive dechlorination. This simulation was run to indicate what trends might be observed during subsequent reactor experiments. This simulation also provided an indication of the range of hydrogen concentration that would be required to observe changes in microbial kinetics. The simulation calculated the rate of dechlorination under varying hydrogen partial pressures. Changes in dechlorination followed a predictable pattern as shown in Appendix Figure A.2. As the concentration of hydrogen increases the reductive dechlorination rate approaches some maximum value as shown in Appendix Figure A.2. This trend is a trait of the Monod kinetics equation and was expected as a result from the simulation. A median hydrogen partial pressure of 1×10^{-4} atm was chosen to test the models.



Appendix Figure A.2: Progress curves of simulated PCP reductive dechlorination when the hydrogen partial pressure is 0.00005 atm (□), 0.0001 atm (◇), 0.0005 atm (■), 0.001 atm (+), and 0.005 atm (●)

Reactor Simulations

Following the variable study, computer simulations of the experimental reactor were performed under different conditions. Simulations of the reactor allowed many scenarios to be examined without the need for lengthy experiments. Lotrario's and Stuart's models were used to analyze the data from each simulation. Comparisons of the two models over a number of simulations were used to evaluate the performance of each model. Simulations showed that reactor conditions affected the accuracy of each model.

The parameters tested by the simulation were used to design the reactor experiments by aiding in the selection of variables like PCP concentration and PCP addition rates. Results from the computer simulations also allowed sampling schedules of substrates and products to be established so that the limited number of samples were not taken during periods of inactivity. The simulated reactor began with an initial reductively dechlorinating cell concentration of 1×10^3 mg cells L^{-1} and substrate. This was selected because variable simulation studies showed that this cell concentration produced the desired Monod kinetics pattern of substrate utilization that quickly entered the first-order region (Appendix Figure A.1). Monod kinetic parameters were used to calculate substrate degradation and cell growth.

PCP concentration in the reactor was maintained by adding discrete amounts of a PCP stock solution at specified times. When the PCP concentration reached some predetermined minimum value, the program simulated an addition and raised the concentration of PCP in the reactor. By adjusting the volume of PCP additions and minimum PCP concentration to initiate PCP addition, the maximum, minimum, and average PCP concentration in the reactor were established. The lowest possible PCP concentration in the reactor before PCP addition was determined by the low end detection ability of the GC/ECD.

Rates of reductive dechlorination were then measured over a specific concentration range. This procedure was duplicated in laboratory experiments and was described as a multiple spike reactor experiment in Chapter 2. PCP was added to the reactor during the simulation in one of two ways: in a pseudo-steady state manner with many small additions and according to a spike decay pattern that allowed larger additions to be degraded over a longer incubation time.

The computer program simulated the multiple spike reactor experiment according to the parameters in Appendix Table A.5. The initial values chosen for cell and hydrogen concentrations were selected based on the variable studies described earlier. The Monod constants were the same as those used during the variable simulations (Appendix Table A.5). Simulation variables determined the duration of the simulation, the concentration of PCP added to the reactor, and the concentration of PCP at which PCP was re-added. Values listed as variable in Appendix Table A.5 were changed according to pseudo-constant PCP or variable PCP simulation protocol.

A simulation of a multiple addition reactor experiment is shown in Appendix Figure A.3. During the course of the simulation, the PCP is added as a spiked concentration and then degraded. The PCP reductively degrading bacteria grow according to the degradation of PCP. The change in PCP concentration with respect to time is also graphed with time to show the acceleration of PCP removal. This analysis and figure were used to compare the growth of PCP reductively dechlorinating bacteria with the acceleration of PCP reductive dechlorination.

Appendix Table A.5: Parameters used during computer simulations of multiple PCP addition reactions

Constants used during simulation	Values	Units
Initial Values		
Initial cells (X_0)	1.0×10^{-3}	mg cells L^{-1}
Initial substrate (PCP ₀)	Variable	μM
Hydrogen partial pressure	1.0×10^{-4}	atm
Monod Constants		
PCP Half velocity coefficient - $K_s(PCP)$	4.5×10^{-1}	μM
Yield - Y	6.13×10^{-3}	mg cells $L^{-1} \mu M^{-1}$
Degradation rate - k_m	11.3	μM Cl ⁻ mg cells ⁻¹ hour ⁻¹
Cell decay rate - b	2.0×10^{-3}	hours ⁻¹
Hydrogen Half Velocity coefficient - $K_s(H_2)$	1.0×10^{-4}	atm
Simulation variables		
At what PCP concentration re-spike	Variable	μM
Spike stock concentration, PCP _{sp}	Variable	μM
Duration of experiment	1.2×10^2	hours
Delta time	5	hours

The simulations provided data used to calculate PCP reductive dechlorination and cell growth data as shown in Appendix Figure A.3. PCP concentration during the simulation was maintained between 0.1 mg/L and 0.01 mg/L. The high limit on PCP concentration was selected to maintain the reaction within the first-order kinetics range. The low PCP concentration value, 0.01 mg/L, was based on the sensitivity and accuracy limits of the GC/ECD at low concentrations of PCP. Within the 300-hour time frame of the simulation, five additions of PCP were made and reductively dechlorinated to 0.01 mg/L as shown in Appendix Figure A.3. The data was analyzed by both of the models described in the methods section.

Like in earlier simulations, the first addition of PCP was not degraded according to first-order kinetics. Stuart's model omitted data from the first addition in acknowledgment of this. Lotrario's model did not assume first-order kinetics and provided more accurate results as determined by r^2 values when the initial data was included. The concentration of cells increased in the reactor at a rate proportional to the PCP concentration; overall, concentration of cells increased exponentially according to a first-order growth rate constant. Growth of cells over the period of the experiment was not negligible. An exponential curve fit of the cell data estimated the growth rate equal to $7.0 \times 10^{-3} \text{ hour}^{-2}$ for a cell doubling time of 4.1 days as determined by the growth constants used for the simulation (Appendix Figure A.3).

A 4.1 day doubling time of reductively dechlorinating bacteria meant that the reductive dechlorination rate in the reactor would double about three times over the course of a 300 hour experiment. The rate of PCP reductive dechlorination dramatically increases from one addition to the next. If the degradation of PCP occurred over hours, the growth of cells would not be significant. Because reductive dechlorination occurs slowly, significant cell growth occurs during the reductive dechlorination of each PCP addition, and a first-order degradation assumption may not always be valid. The 4.1 day doubling time is a function of yield (Y), degradation rate (k_m), and decay rate (b). Yield establishes the amount of cells grown as a result of reductive dechlorination, and an increase in yield raises the amount of cells produced from the degradation of each addition of PCP and an increase in acceleration. An increase in the degradation coefficient raises the rate of PCP reductive dechlorination per cell number. Increasing the decay rate will reduce the acceleration because as the death rate increases the number of active cells decreases.

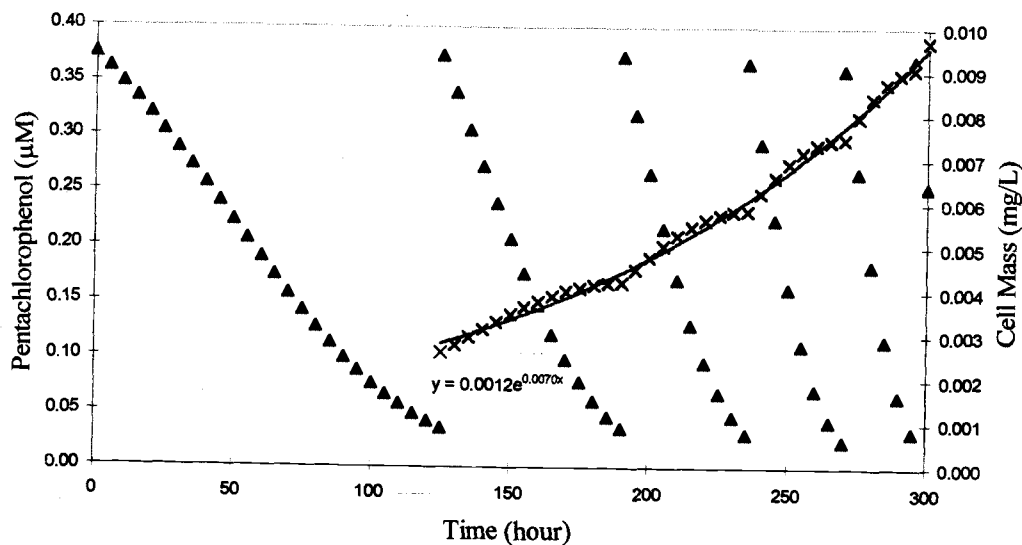
Cell concentration increased significantly (a factor of 10 over 300 hours) during the course of PCP degradation as shown in Appendix Figure A.3. However, during individual PCP additions, this growth was not significant enough to disturb

the first-order shape of the PCP degradation curves. After the first addition of PCP, subsequent additions were effectively modeled by first-order approximations.

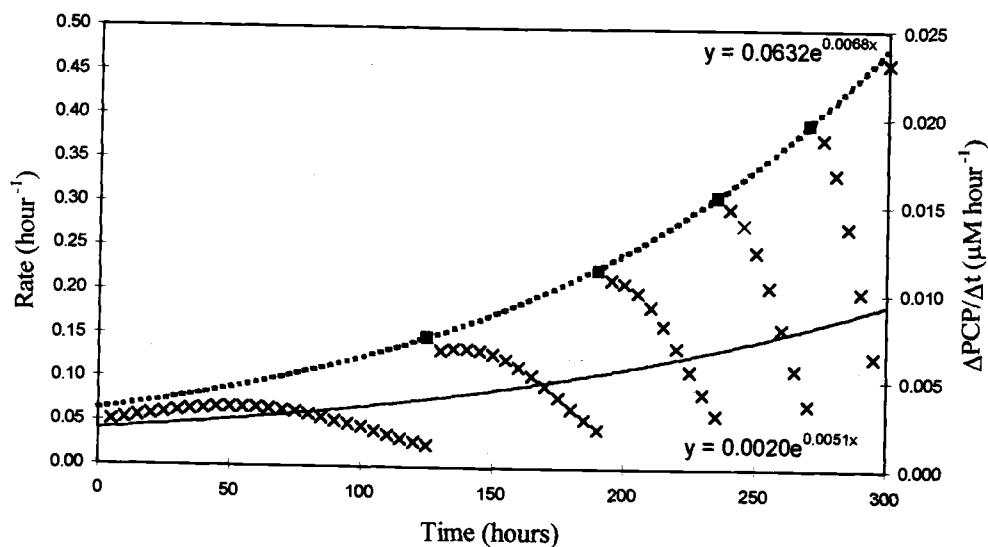
The $\Delta S/\Delta t$ data showed in Appendix Figure A.4 demonstrated the effects of changing substrate concentration in the reactor on the rate of degradation.

According to Monod kinetics, the reductive dechlorination rate of the first PCP addition showed an inflection point at the time when the rate switched from cell limited to substrate limited. Subsequent additions were reductively dechlorinated according to first-order kinetics.

Simulations were modeled using both Stuart's and Lotrario's models as shown in Appendix Figure A.4. Again, initial PCP addition data was not included for Stuart's model but was included for Lotrario's model. The simulated data and Lotrario's acceleration rate estimation and constants calculated during Stuart's analysis with Stuart's acceleration rate estimation are shown in Appendix Figure A.4.



Appendix Figure A.3: Multiple addition simulation of PCP concentration (▲) between 0.04 to 0.4 μM and cell concentration (×) in mg/L



Appendix Figure A.4: Lotrario's (—) and Stuart's (■) estimations of cell growth for computer simulated data when PCP is between 0.04 to 0.4 μM based on $\Delta\text{PCP}/\Delta t$ (×) and first-order rates (■) respectively

Simulated substrate degradation data was analyzed according to the model developed by Stuart et al. to estimate the rate of increase in reductive dechlorination. After omitting the first curve, the data from each of four PCP additions was regressed to determine four first-order degradation constants. Each of the computed degradation constants were plotted according to the time of the corresponding PCP addition as shown in Appendix Figure A.4. The resulting curve was used to calculate the acceleration of reductive dechlorination. Reductive dechlorination acceleration of $6.8 \times 10^{-3} \text{ hours}^{-2}$ was determined by Stuart's analysis (Appendix Table A.6). This was used to estimate the apparent growth rate. The acceleration coefficient determined from a curve fit of the simulated cell growth data shown in Appendix Figure A.3 was very close to the value estimated from Stuart's regression on the substrate data shown in Appendix Figure A.3. The modeled and measured acceleration rates of $6.8 \times 10^{-3} \text{ hours}^{-2}$ and $7.0 \times 10^{-3} \text{ hours}^{-2}$ are nearly the same for the simulation of reductive dechlorination with cell growth.

Appendix Table A.6: Acceleration rates based on determination method

Acceleration Rate (hours^{-2})	Method of Determination
0.0070	Actual as a function of growth constants
0.0068	Stuart's analysis of first-order rates
0.0051	Lotrario's analysis of $\Delta\text{PCP}/\Delta t$

Lotrario's model was also used to analyze the simulated data and to determine a reductive dechlorination "growth" rate. This analysis used all of the data points measured during the incubation. The change in PCP divided by the change in time was used to determine an exponential growth constant according to Lotrario's model as described in Appendix Equation A.4 and shown in Appendix Figure A.4.

As expected, the parameter $\Delta\text{PCP}/\Delta t$ showed a decrease with PCP concentration and an increase with the increase in cell mass (Appendix Figure A.4). The curve regressed through these points was used to determine the acceleration of reductive dechlorination with time.

Because the reductive dechlorination rate and the parameter $\Delta\text{PCP}/\Delta t$ decreased with the decrease of PCP in solution - according to Monod kinetics - exponential curve fit underestimated the growth rate as shown in Appendix Figure A.4. The acceleration rate was estimated at 5.1×10^{-3} by Lotrario's model - much lower than both that estimated by Stuart's model and calculated as a curve fit to the simulated cell growth values (7.0×10^{-3}) as shown in Appendix Figure A.4. The variation of substrate concentration in the reactor introduced the error observed between Lotrario's estimation and the actual value.

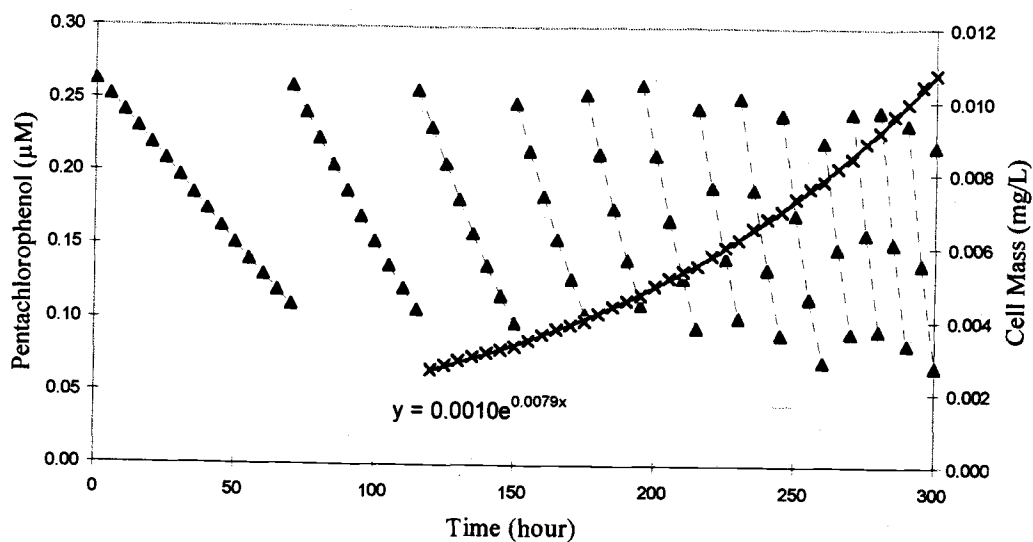
When the constant substrate concentration assumption made during the derivation of Lotrario's model was not satisfied, that analysis underestimated the acceleration of reductive dechlorination and subsequently the growth rate of reductively dechlorinating bacteria. The acceleration curve used to determine Lotrario's acceleration rate, α' , underestimated that value when the change in substrate concentration was large ($0.4 \mu\text{M}$ to $0.04 \mu\text{M}$). Lotrario's model became more accurate as the constant substrate concentration was more nearly satisfied as shown in Appendix Table A.7. The range of PCP concentration in the reactor was controlled so that the average PCP concentration was 0.048 mg/L for each simulation.

Appendix Table A.7: Actual and estimated growth rates as PCP concentration approaches a constant value

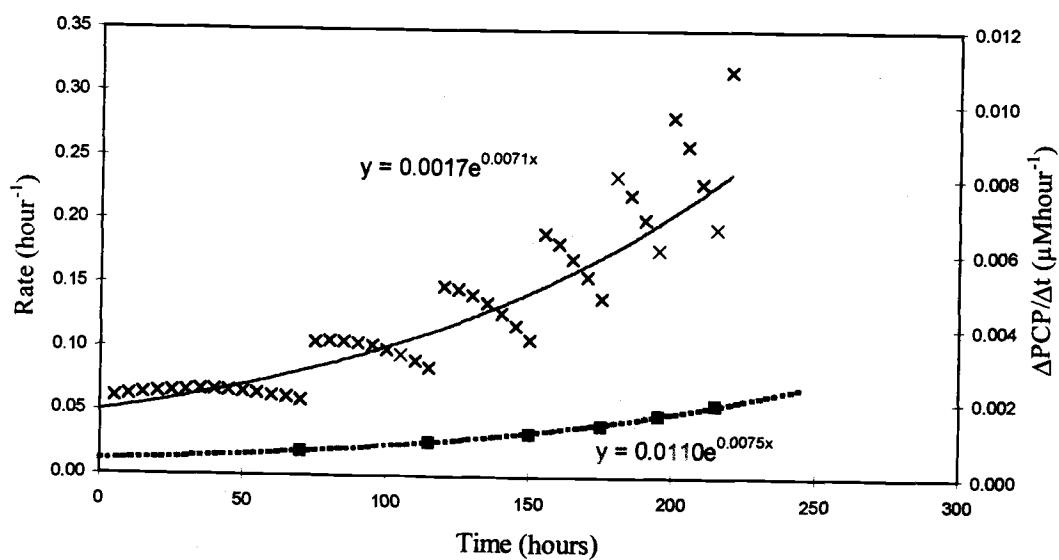
PCP _{high}	PCP _{low}	Average PCP	Growth Rate derived from cell number hours ⁻¹	Growth Rate estimated by Lotrario's model hours ⁻¹
mg/L	mg/L	mg/L		
0.100	0.010	0.048	0.0070	0.0051
0.090	0.013	0.048	0.0068	0.0054
0.080	0.018	0.047	0.0071	0.0063
0.070	0.030	0.048	0.0078	0.0071
0.060	0.035	0.047	0.0076	0.0075
0.048	0.048	0.048	0.0077	0.0077

When the PCP concentration was kept between 0.07 mg/L and 0.03 mg/L, the substrate addition better satisfied the assumptions for Lotrario's model, and that model more nearly estimated the measured growth rate. The regression on the cell concentration was $7.8 \times 10^{-3} \text{ hour}^{-1}$ compared to Lotrario's model estimation of $7.5 \times 10^{-3} \text{ hour}^{-1}$ as shown in Appendix Figure A.5. Stuart's model estimated the acceleration coefficient to be $7.5 \times 10^{-3} \text{ hour}^{-2}$ as shown in Appendix Figure A.6. When the simulation kept the PCP concentration within a small range, Lotrario's model performed better than for the previous simulation. Therefore, when the reactor is run at a near constant PCP concentration Lotrario's model becomes more accurate.

A final simulation was performed for a situation when the PCP concentration within the reactor is outside the first-order range. The simulation began with a PCP concentration of 0.75 μM and maintained the concentration above 0.37 μM . This ensured that the reactor was not within the first-order range and Stuart's assumption does not apply.



Appendix Figure A.5: Multiple addition simulation of PCP concentration (\blacktriangle) between 0.11 to 0.26 μM and cell concentration (\times) in mg/L



Appendix Figure A.6: Lotrario's (—) and Stuart's (\blacksquare) estimations of cell growth for computer simulated data when PCP is between 0.11 to 0.26 μM based on $\Delta\text{PCP}/\Delta t$ (\times) and first-order rates (\blacksquare) respectively

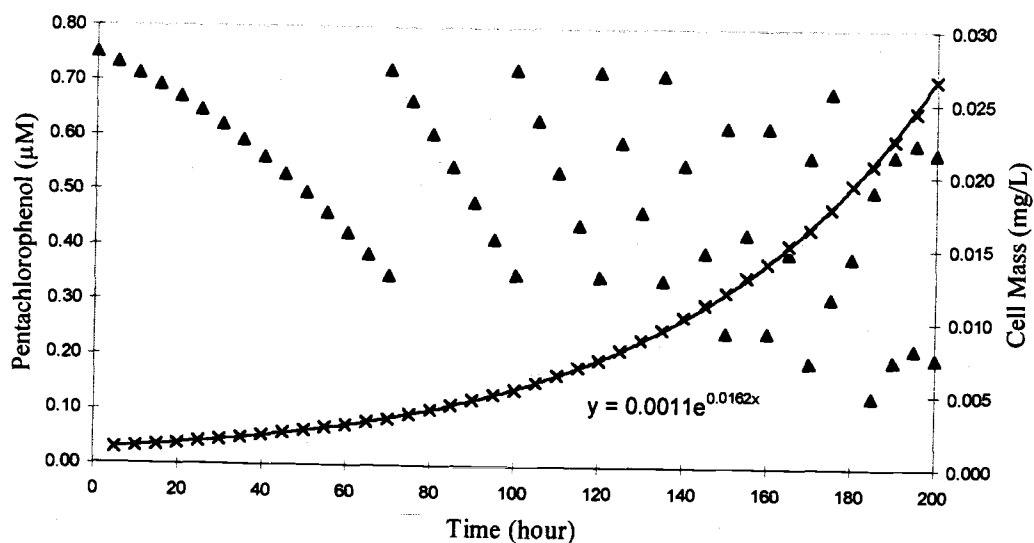
Simulated data supported this conclusion. The reductive dechlorination of PCP additions did not follow first-order degradation curves (Appendix Figure A.7). Compared to the calculated acceleration coefficient based on an exponential curve fit of the cell data (0.0162), Stuart's model overestimated the acceleration to be 0.0262 (Appendix Figure A.8). Lotrario's model performed much better than Stuart's during this simulation and again slightly underestimated the acceleration coefficient to be 0.0156.

Discussion

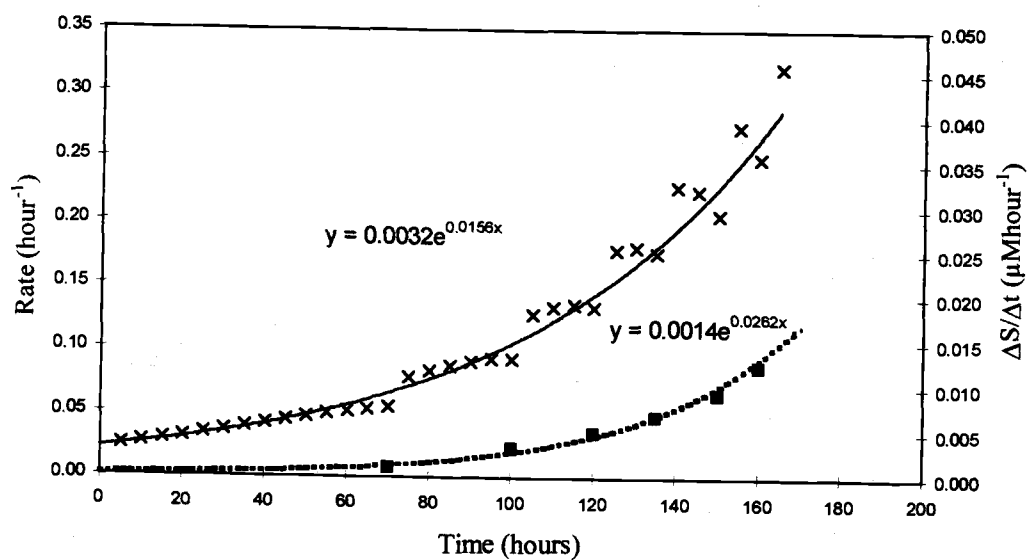
Variable Simulations

Computer simulations proved a valuable tool in the understanding and design of reactor experiments. The simulations were instrumental in the selection of initial inoculum concentration and PCP concentration range. They also provided data used to assess the effectiveness of Stuart's and Lotrario's respective models.

The simulations showed that by beginning with very low numbers of dechlorinating organisms each reactor study had approximately the same number of cells after the first PCP addition. When initial cell number is sufficiently low, the new cells produced during the degradation of the first PCP addition became the approximate concentration in the reactor. Provided the initial concentration is low, the cell concentration enters a range of approximately 10^{-3} mg/L of cells after one PCP addition. Simulations on varying initial cell concentration in the reactor showed that cell concentration did not affect the ability of either model to assess growth from substrate utilization data. This was true provided that the concentration of cells was not so high that the system became substrate limited.



Appendix Figure A.7: Multiple addition simulation of PCP concentration (\blacktriangle) μM and cell concentration (\times) in mg/L with zero-order reductive dechlorination



Appendix Figure A.8: Lotrario's (—) and Stuart's (\blacksquare) estimations of cell growth for computer simulated data when PCP is between 0.30 to 0.75 μM based on $\Delta\text{PCP}/\Delta t$ (\times) and zero-order rates (\blacksquare) respectively

The simulations performed to test hydrogen concentration on the rate of reductive dechlorination and cell growth were limited to the Monod equations by which they were calculated. The simulation only accounted for PCP reductively dechlorinating organisms as they utilized hydrogen. This simulation also did not consider possible toxic effects of high hydrogen concentration. Within its limits, the simulations allowed an estimate of reductive dechlorination with hydrogen concentration and helped in the selection of hydrogen partial pressure used in reactor studies. It was determined that a hydrogen partial pressure of about 2.5×10^{-4} atm would yield good results (Appendix Figure A.2)

Reactor Simulations

Simulations of the reactor studies were a good way of assessing the two models with controlled experiments. The simulations used Monod kinetics to calculate the PCP concentration and cell mass within the reactor with time. Parameters were established to approximate PCP additions like those made during a reactor study experiment. The calculated cell mass data was used to determine an apparent cell growth rate that was estimated by Stuart's and Lotrario's models. Each model was then evaluated on its ability to estimate the calculated value.

Stuart's and Lotrario's models each appeared to be more accurate under the specific conditions that best met the assumptions of the theoretical model. When PCP concentration in the reactor was maintained within the range of first-order degradation, Stuart's model effectively estimated the acceleration rate determined from the simulated data. This was verified by comparing the estimated value with an acceleration coefficient determined from a curve fit of the cell mass data. As the PCP concentration range narrows, Lotrario's model becomes more accurate. Stuart's model is more robust and fit both sets of simulated data within the first-

order range well, but it does require two regressions and first-order degradation rates in order to estimate growth from the substrate utilization data.

When the PCP concentration was outside the range necessary for first-order reductive dechlorination, Stuart's model failed. During the simulation with PCP concentrations in the zero-order range, Stuart's model estimated the acceleration coefficient to be 0.0262 compared with the calculated value of 0.0162. The simulation for PCP concentrations in the zero-order range resulted in a gross overestimation of the acceleration coefficient by Stuart's model.

Lotrario's model was more effective for situations when the assumption of constant substrate concentration was more nearly maintained and it worked for a wide range of PCP concentrations including those in both the first-order and zero-order degradation range. Lotrario's model consistently underestimates the growth rate when the PCP concentration range is both large and small and provides a conservative estimation of the active organisms' growth rate. This conservative estimation approaches the calculated value as the concentration within the reactor approaches a constant value. This was shown by the reactor simulations that compared acceleration values from the cell growth curve generated by the simulation and Stuart's and Lotrario's estimates for different allowable PCP concentration ranges. The competing changes in the reactor result in the underestimate of acceleration by Lotrario's model. The model is much more accurate when the pseudo-constant substrate concentration assumption is held. For experiments that are performed with the concentration of PCP tightly controlled, this model will closely estimate the growth rate. For all others it will provide a conservative estimate.

Lotrario's model can also be used more accurately by estimating a $\Delta\text{PCP}/\Delta t$ during each PCP addition when the reactor concentration reached a set value. In that way, concentration changes in the reactor would be avoided by the estimate and several repetitions could be made by assessing the data at a number of different concentrations. This was done for simulated data and proved successful (data not

shown), but was avoided during these reactor studies because it complicated the experiments. When added accuracy is necessary, this alteration to the data analysis provides an additional option.

Lotrario's model performed similarly for the simulation during which PCP was kept in the zero-order range. For PCP concentrations above $0.4 \mu\text{M}$, Lotrario's model still provided a conservative estimate of 0.0156 for the acceleration coefficient of 0.0162 that was much more accurate than the estimate provided by Stuart's model.

Conclusions

This research suggested a number of conclusions:

1. A very simple computer program based on Monod kinetic equations can simulate the substrate addition and degradation of the PCP reactor experiments,
 - Simulations provide a way of comparing the two models' estimations with exponential cell growth numbers,
 - Simulations can examine a wide array of conditions more quickly and easily than reactor experiments,
2. Simulations showed that beginning reactor experiments with very low initial cell mass allows the reactor experiments to be performed with the same amount of reductively dechlorinating bacteria after one PCP addition,
3. Both Stuart's and Lotrario's models can estimate the apparent growth of a specific sub-population within a mixed microbial culture,
 - Stuart's model is effective under a wide variety of situations,
 - Lotrario's model becomes more precise when the PCP concentration is kept within a narrow range and requires small sampling steps to maintain accuracy,

- Lotrario's model can be applied to situations where the first-order substrate degradation assumption does not apply, and Stuart's model fails.

Appendix B: Experimental Protocol

Experimental Protocol for Chlorophenol Degradation Experiments

Date:

Phase I – Transfer

- ___ Calibrate pumps.
- ___ Rinse, dry, and tare membrane (Millipore) filters for solids analyses.
- ___ Turn on gas flow controller and allow it to warm up for thirty minutes.
- ___ Prepare acetate and sulfate primary standard by adding 3.47g NaAc (actual =), 4.39g NaCl (actual =), and 3.70g NaSO₄ (actual =) to 250ml of de-ionized water in a volumetric flask. (Anion concentrations: 10g/L) This solution may be kept up to one month if refrigerated, but bacterial growth may occur. Remove from the refrigerator and allow it to come to room temperature.
- ___ Allow GC/TCD to warm up for 10 minutes, and run blank.
- ___ Mix 2L of IC eluant and regenerant. Replace IC solutions, and purge for 15 minutes.
- ___ Replace reference electrode's internal (saturated Ag/AgCl) and external (10% KNO₃) solutions.
- ___ Insert Teflon rods in electrode holders and connect reactor to gas line.
- ___ Set gas flow controllers to attain the desired headspace concentration.
- ___ N₂
- ___ CO₂
- ___ H₂
- ___ Prepare anion standard curves by adding 0.1, 0.2, 0.3, 0.4, and 0.5 milliliters of primary standard to 100ml volumetric flasks.
- ___ Run anion standard curve on the IC.
- ___ Add 2.0L of reactor media and continue purging.
- ___ Calibrate pH electrodes.
- ___ Prepare 1:10 dilution of glacial acetic acid and 0.3 M acetate solution. Add 25mL of glacial acetic acid and 6.15g anhydrous sodium acetate to de-ionized water in a 250mL volumetric flask, and flush dispenser. ([Ac-] = 2.04 M) Glacial acetic acid is always prepared at the same concentration, but different concentrations of sodium acetate can be used.
- ___ When O₂ is no longer measurable, exchange rods with electrodes. Purge 30-60 minutes.
- ___ Check reactor atmosphere with GC/TCD.
- ___ Change reactor septum.
- ___ Transfer supernatant from culture flask to the reactor. Siphon through the reactor feed tube (suspended mid depth).
- ___ Connect electrodes and begin the program to monitor electrodes.

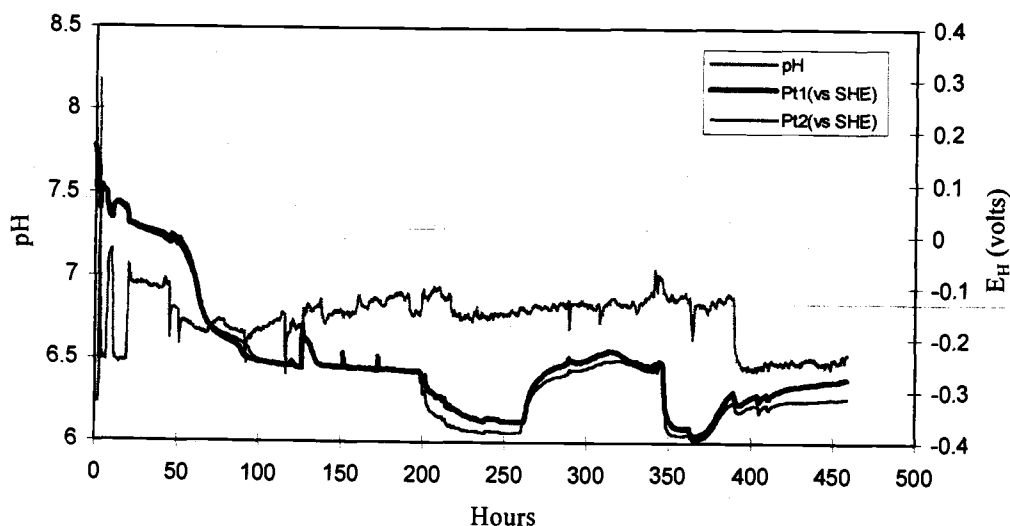
Phase II

- ___ Establish pH set point.
- ___ Wait for apparent E_H to stabilize.
- ___ Measure acetate and hydrogen gas periodically.
- ___ Take protein sample.

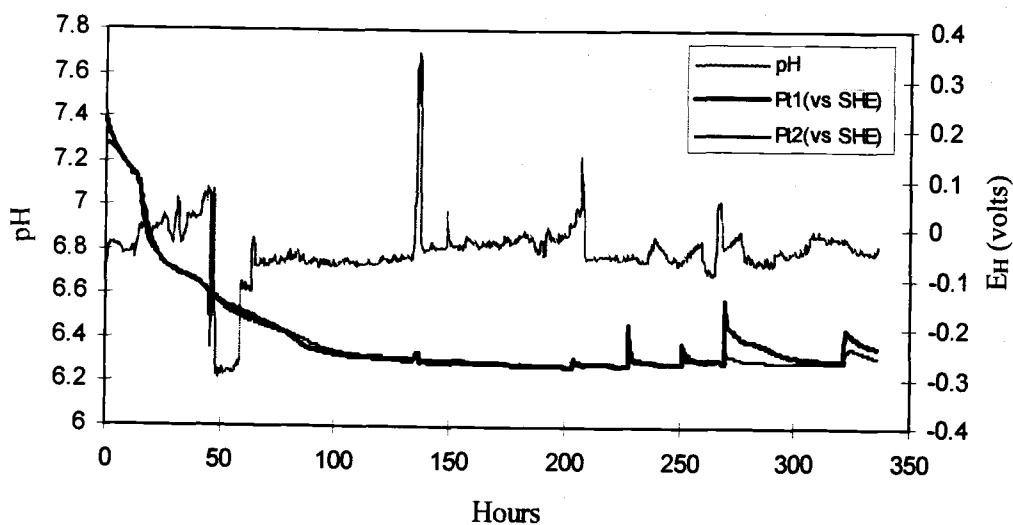
Phase III

- ___ Place 250 ml of 12.8 mg/L PCP solution in an Erlenmeyer flask capped with a septum. Purge with nitrogen.
- ___ Sample PCP concentration periodically.
- ___ Repeat PCP addition and sampling as desired.

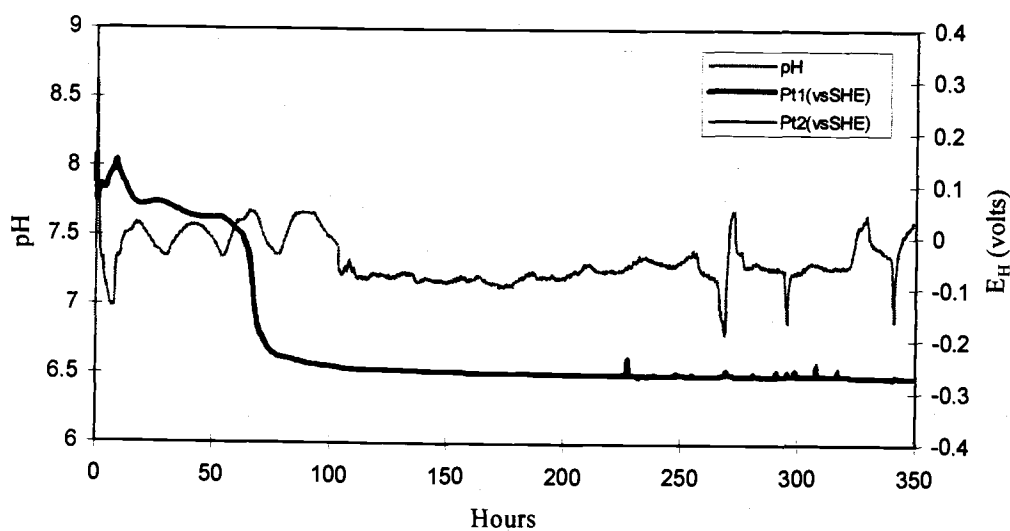
Appendix C: E_H and pH Time Course Studies



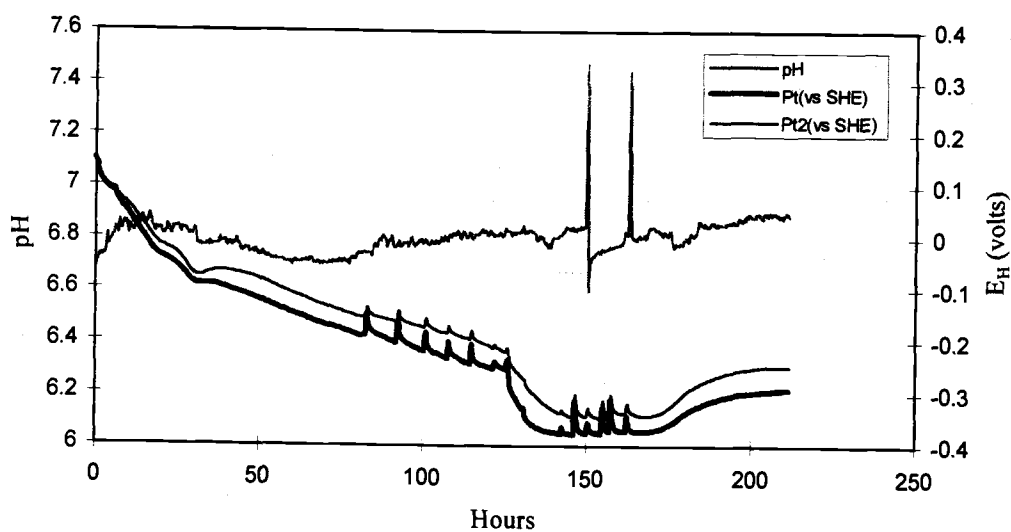
Appendix Figure C.1: Time course of pH and E_H data measured during PCP reductive dechlorination at 9.4×10^{-5} atm of hydrogen



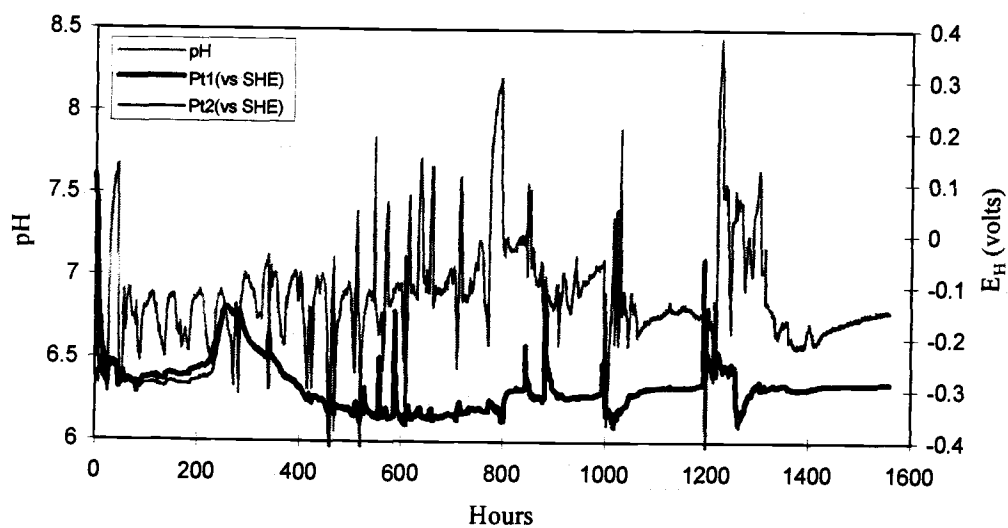
Appendix Figure C.2: Time course of pH and E_H data measured during PCP reductive dechlorination at 2.2×10^{-4} atm of hydrogen



Appendix Figure C.3: Time course of pH and E_H data measured during PCP reductive dechlorination at 2.9×10^{-4} atm of hydrogen



Appendix Figure C.4: Time course of pH and E_H data measured during PCP reductive dechlorination at 5.7×10^{-4} and 3.9×10^{-2} atm of hydrogen



Appendix Figure C.5: Time course of pH and E_H data measured during PCP reductive dechlorination at 7.8×10^{-3} atm of hydrogen

Appendix D: Chlorophenol, Headspace, and Acetate Concentration Data

Appendix Table D.1: Chlorophenol concentrations (μM) measured during the reactor experiment incubated at a hydrogen partial pressure of 2.2×10^{-4}

Hours	PCP	2,3,4,5-TeCP	2,3,4,6-TeCP	2,3,5,6-TeCP	3,4,5-TCP	2,3,4-TCP	2,3,5-TCP	3,4-DCP	3,5-DCP	3-CP	Balance
0.0	0.66	0.11	0.04	0.00	0.12	0.00	0.00	0.00	0.17	0.00	1.10
19.7	0.72	0.00	0.04	0.00	0.06	0.00	0.12	0.00	0.00	0.00	0.95
25.2	0.68	0.00	0.03	0.00	0.06	0.00	0.19	0.00	0.00	0.00	0.96
44.7	0.66	0.00	0.04	0.08	0.16	0.00	0.02	0.00	0.10	0.00	1.06
65.7	0.67	0.00	0.02	0.00	0.09	0.00	0.12	0.00	0.00	0.00	0.89
70.4	0.63	0.00	0.07	0.00	0.07	0.08	0.00	0.00	0.00	0.00	0.85
89.2	0.58	0.02	0.00	0.00	0.15	0.00	0.00	0.00	0.00	0.00	0.76
95.7	0.62	0.02	0.03	0.00	0.09	0.09	0.00	0.00	0.00	0.00	0.85
114.7	0.62	0.05	0.03	0.00	0.09	0.08	0.00	0.00	0.00	0.00	0.88
118.8	0.65	0.07	0.04	0.00	0.10	0.10	0.00	0.00	0.00	0.00	0.95
139.2	0.51	0.14	0.03	0.00	0.11	0.08	0.00	0.00	0.00	0.00	0.87
144.2	0.00	0.00	0.00	0.00	0.00	0.00	0.00	0.00	0.00	0.00	
147.7	0.44	0.21	0.03	0.00	0.21	0.00	0.00	0.00	0.00	0.00	0.90
149.4	0.42	0.16	0.00	0.00	0.22	0.00	0.00	0.00	0.00	0.00	0.80
152.4	0.36	0.17	0.00	0.00	0.23	0.00	0.00	0.00	0.00	0.00	0.76
155.7	0.35	0.29	0.04	0.00	0.27	0.00	0.00	0.00	0.00	0.00	0.94
163.7	0.21	0.29	0.03	0.00	0.36	0.00	0.00	0.00	0.00	0.00	0.88
166.2	0.17	0.30	0.03	0.00	0.40	0.00	0.00	0.00	0.00	0.00	0.90
169.2	0.13	0.32	0.05	0.00	0.47	0.00	0.00	0.00	0.00	0.00	0.97
173.4	0.08	0.20	0.05	0.00	0.54	0.00	0.00	0.00	0.00	0.00	0.88
176.7	0.05	0.11	0.03	0.00	0.61	0.00	0.00	0.00	0.00	0.00	0.80
178.7	0.04	0.18	0.00	0.00	0.56	0.00	0.00	0.00	0.00	0.00	0.78
185.7	0.02	0.13	0.49	0.00	0.73	0.00	0.00	0.00	0.00	0.00	1.37
187.6	0.02	0.12	0.03	0.00	0.79	0.00	0.00	0.00	0.00	0.00	0.96
187.7	0.53	0.10	0.00	0.00	0.72	0.00	0.00	0.00	0.00	0.00	1.34
188.2	0.52	0.12	0.03	0.00	0.74	0.00	0.00	0.00	0.00	0.00	1.41
189.3	0.51	0.18	0.03	0.00	0.79	0.00	0.00	0.00	0.00	0.00	1.51
191.7	0.40	0.20	0.03	0.00	0.72	0.00	0.00	0.00	0.00	0.00	1.35
193.9	0.33	0.26	0.03	0.00	0.78	0.00	0.00	0.00	0.00	0.00	1.40
196.2	0.27	0.28	0.02	0.00	0.83	0.00	0.00	0.00	0.00	0.00	1.41
200.6	0.22	0.34	0.04	0.05	1.01	0.00	0.00	0.00	0.00	0.00	1.64
202.9	0.11	0.32	0.05	0.00	1.08	0.00	0.00	0.00	0.00	0.00	1.56
207.3	0.05	0.00	0.00	0.00	1.08	0.00	0.00	0.00	0.00	0.00	1.13
210.8	0.03	0.20	0.05	0.00	1.31	0.00	0.00	0.00	0.00	0.00	1.60
210.8	0.44	0.28	0.00	0.00	1.12	0.00	0.00	0.00	0.00	0.00	1.84

Hours	PCP	2,3,4,5 -TeCP	2,3,4,6 -TeCP	2,3,5,6 -TeCP	3,4,5- TCP	2,3,4- TCP	2,3,5- TCP	3,4- DCP	3,5- DCP	3-CP	Balance
211.4	0.51	0.23	0.03	0.00	1.34	0.00	0.00	0.00	0.00	0.00	2.11
212.7	0.44	0.26	0.03	0.31	1.28	0.00	0.00	0.00	0.00	0.00	2.31
214.3	0.38	0.31	0.04	0.02	1.40	0.00	0.00	0.00	0.00	0.00	2.14
216.3	0.30	0.34	0.03	0.00	1.41	0.00	0.00	0.00	0.00	0.00	2.08
217.7	0.26	0.36	0.03	0.00	1.44	0.00	0.00	0.00	0.00	0.00	2.10
219.7	0.19	0.33	0.03	0.00	1.52	0.00	0.00	0.00	0.00	0.00	2.08
221.7	0.14	0.27	0.02	0.00	1.56	0.00	0.00	0.00	0.00	0.00	2.00
224.2	0.10	0.19	0.04	0.00	1.59	0.00	0.00	0.00	0.00	0.00	1.92
227.7	0.05	0.18	0.00	0.00	1.61	0.00	0.00	0.00	0.00	0.00	1.85
233.0	0.02	0.16	0.02	0.00	1.89	0.00	0.00	0.00	0.00	0.00	2.09
235.2	0.02	0.13	0.03	0.00	1.82	0.00	0.00	0.00	0.00	0.00	2.01
235.2	0.51	0.13	0.04	0.00	1.92	0.00	0.00	0.00	0.00	0.00	2.59
235.8	0.49	0.15	0.04	0.00	1.82	0.00	0.00	0.00	0.00	0.00	2.49
236.7	0.45	0.18	0.04	0.00	1.83	0.00	0.00	0.00	0.00	0.00	2.50
238.7	0.37	0.22	0.42	0.02	1.90	0.00	0.00	0.00	0.00	0.00	2.93
240.9	0.28	0.26	0.03	0.00	1.89	0.00	0.00	0.00	0.00	0.00	2.47
242.7	0.22	0.12	0.03	0.00	1.91	0.00	0.00	0.00	0.00	0.00	2.28
245.7	0.15	0.24	0.00	0.00	1.97	0.00	0.00	0.00	0.00	0.00	2.37
247.6	0.12	0.29	0.06	0.00	2.15	0.00	0.00	0.00	0.00	0.00	2.63
250.6	0.08	0.27	0.03	0.00	2.23	0.00	0.00	0.00	0.00	0.00	2.61
257.2	0.04	0.17	0.05	0.00	2.47	0.00	0.00	0.00	0.00	0.00	2.73
258.2	0.03	0.14	0.05	0.00	2.37	0.00	0.00	0.00	0.00	0.00	2.59
258.2	0.49	0.15	0.04	0.00	2.45	0.00	0.00	0.00	0.00	0.00	3.12
259.3	0.44	0.19	0.04	0.00	2.37	0.00	0.00	0.00	0.00	0.00	3.03
261.2	0.34	0.22	0.03	0.00	2.36	0.00	0.00	0.00	0.00	0.00	2.95
263.9	0.25	0.30	0.33	0.00	2.46	0.00	0.00	0.00	0.00	0.00	3.34
266.0	0.18	0.23	0.00	0.00	2.51	0.00	0.00	0.00	0.00	0.00	2.92
268.7	0.12	0.28	0.03	0.00	2.63	0.00	0.00	0.00	0.00	0.00	3.06
271.9	0.07	0.18	0.00	0.00	2.59	0.00	0.00	0.00	0.00	0.00	2.84
274.9	0.04	0.17	0.00	0.00	2.62	0.00	0.00	0.00	0.00	0.00	2.82
277.2	0.02	0.12	0.00	0.00	2.64	0.00	0.00	0.00	0.00	0.00	2.78
277.2	0.48	0.17	0.03	0.00	2.75	0.00	0.00	0.00	0.00	0.00	3.43
277.7	0.46	0.17	0.03	0.02	2.72	0.00	0.00	0.00	0.00	0.00	3.40
283.8	0.19	0.24	0.00	0.00	2.76	0.00	0.00	0.00	0.00	0.00	3.19
285.7	0.13	0.25	0.00	0.00	2.74	0.00	0.00	0.00	0.00	0.00	3.12
287.7	0.09	0.21	0.00	0.00	2.94	0.00	0.00	0.00	0.00	0.00	3.24
289.7	0.06	0.21	0.00	0.00	2.63	0.00	0.00	0.00	0.00	0.00	2.89
290.9	0.05	0.19	0.03	0.00	3.12	0.00	0.00	0.00	0.00	0.00	3.39
296.3	0.02	0.09	0.00	0.00	2.59	0.00	0.00	0.00	0.00	0.00	2.71
309.8	0.01	0.02	0.00	0.00	3.76	0.19	0.00	0.00	0.00	0.00	3.98
329.2	0.48	0.00	0.02	0.00	3.53	0.27	0.00	0.00	0.00	0.00	4.30
331.2	0.38	0.08	0.00	0.00	3.35	0.18	0.00	0.00	0.00	0.00	3.99
333.7	0.25	0.14	0.00	0.00	3.40	0.19	0.00	0.00	0.00	0.00	3.98
336.0	0.17	0.15	0.00	0.00	0.35	0.20	0.00	0.00	0.00	0.00	0.86
338.2	0.10	0.13	0.00	0.00	2.43	0.00	0.00	0.00	0.00	0.00	2.67

Hours	PCP	2,3,4,5 -TeCP	2,3,4,6 -TeCP	2,3,5,6 -TeCP	3,4,5- TCP	2,3,4- TCP	2,3,5- TCP	3,4- DCP	3,5- DCP	3-CP	Balance
344.3	0.02	0.09	0.00	0.00	2.59	0.11	0.00	0.00	0.00	0.00	2.82

Appendix Table D.2: Headspace (atm) and acetate (μM) concentrations measured during the reactor experiment incubated at a hydrogen partial pressure of 2.2×10^{-4}

Hours	H ₂	N ₂	CO ₂	Acetate
0.0	1.41E-04	0.00E+00	0.00E+00	
19.7	1.87E-04	8.67E-01	0.00E+00	2.42
25.2	2.28E-04	8.51E-01	0.00E+00	1.65
44.7	2.26E-04	8.74E-01	1.03E-02	1.43
65.7	2.26E-04	8.74E-01	1.05E-02	2.09
70.4	2.50E-04	9.11E-01	1.96E-02	2.32
89.2	2.39E-04	9.00E-01	1.39E-02	2.05
114.7	2.37E-04	0.00E+00	0.00E+00	
144.2	1.74E-04	7.11E-01	1.02E-02	3.10
147.7	2.58E-04	8.50E-01	1.29E-02	1.97
149.4	2.17E-04	8.28E-01	1.28E-02	1.78
152.4	2.33E-04	8.92E-01	1.36E-02	2.07
166.2	2.36E-04	8.66E-01	1.34E-02	2.18
169.2	2.36E-04	8.66E-01	1.34E-02	
173.4	2.15E-04	8.80E-01	1.38E-02	2.03
176.7	2.24E-04	8.39E-01	1.31E-02	
187.7	2.20E-04	8.55E-01	1.15E-02	2.53
191.7	2.31E-04	8.85E-01	1.24E-02	
193.9	2.33E-04	8.77E-01	1.39E-02	1.99
212.7	2.45E-04	8.78E-01	9.37E-03	1.54
214.3	2.30E-04	8.69E-01	1.09E-02	
224.2	2.26E-04	8.60E-01	1.55E-02	1.34
235.2	2.28E-04	8.67E-01	1.65E-02	
250.6	2.31E-04	8.64E-01	1.46E-02	
268.7	2.20E-04	8.55E-01	2.01E-02	2.17

Appendix Table D.3: Chlorophenol concentrations (μM) measured during the reactor experiment incubated at a hydrogen partial pressure of 9.8×10^{-4}

Hours	PCP	2,3,4,5 -TeCP	2,3,4,6 -TeCP	2,3,5,6 -TeCP	3,4,5- TCP	2,3,4- TCP	2,3,5- TCP	3,4- DCP	3,5- DCP	3-CP	Balance
0.0	0.66	0.11	0.04	0.00	0.12	0.00	0.00	0.00	0.17	0.00	1.10
22.7	0.48	0.00	0.00	0.00	0.13	0.00	0.00	0.00	0.00	0.00	0.61
30.0	0.56	0.00	0.00	0.00	0.09	0.00	0.00	0.00	0.00	0.00	0.65
34.7	0.54	0.00	0.00	0.00	0.08	0.00	0.00	0.00	0.00	0.00	0.63
58.7	0.52	0.00	0.00	0.00	0.13	0.00	0.00	0.00	0.00	0.00	0.65
75.0	0.55	0.00	0.00	0.00	0.17	0.00	0.00	0.00	0.00	0.00	0.72
96.0	0.29	0.28	0.00	0.00	0.34	0.00	0.00	0.00	0.00	0.00	0.90
101.7	0.16	0.22	0.00	0.00	0.51	0.00	0.00	0.00	0.00	0.00	0.89

Hours	PCP	2,3,4,5 -TeCP	2,3,4,6 -TeCP	2,3,5,6 -TeCP	3,4,5- TCP	2,3,4- TCP	2,3,5- TCP	3,4- DCP	3,5- DCP	3-CP	Balance
105.5	0.11	0.30	0.00	0.00	0.58	0.00	0.00	0.00	0.00	0.00	0.99
118.8	0.14	0.14	0.00	0.00	0.13	0.00	0.00	0.00	0.00	0.00	0.41
121.0	0.14	0.16	0.00	0.00	1.09	0.00	0.00	0.00	0.00	0.00	1.40
123.0	0.11	0.14	0.00	0.00	1.00	0.00	0.00	0.00	0.00	0.00	1.24
125.8	0.05	0.10	0.00	0.00	1.12	0.00	0.00	0.00	0.00	0.00	1.27
130.0	0.07	0.12	0.00	0.00	1.21	0.00	0.00	0.00	0.00	0.00	1.40
130.2	0.32	0.50	0.00	0.00	1.18	0.00	0.00	0.00	0.00	0.00	1.99
140.3	0.10	0.64	0.00	0.00	1.18	0.00	0.00	0.00	0.00	0.00	1.91
191.0	0.00	0.00	0.00	0.00	0.90	0.00	0.00	0.00	0.24	0.00	1.15
195.2	0.40	0.00	0.00	0.00	2.13	0.00	0.00	0.00	0.30	0.00	2.83
196.2	0.32	0.14	0.00	0.00	2.44	0.00	0.00	0.00	0.35	0.00	3.24
198.7	0.18	0.19	0.10	0.00	2.24	0.00	0.00	0.00	0.36	0.00	3.07
203.0	0.06	0.07	0.00	0.00	2.28	0.00	0.00	0.00	0.50	0.00	2.90
214.5	0.04	0.03	0.00	0.00	1.72	0.00	0.00	0.00	0.95	0.00	2.74
216.2	0.41	0.06	0.00	0.00	1.82	0.00	0.00	0.00	1.11	0.00	3.40
217.2	0.27	0.17	0.00	0.00	1.78	0.00	0.00	0.00	1.05	0.00	3.27
218.3	0.16	0.18	0.00	0.00	1.78	0.00	0.06	0.00	1.03	0.00	3.22
219.8	0.07	0.12	0.00	0.00	1.91	0.00	0.09	0.00	1.15	0.00	3.34
221.7	0.14	0.07	0.04	0.00	1.64	0.00	0.08	0.20	1.20	0.00	3.38
223.5	0.21	0.07	0.06	0.00	1.44	0.00	0.07	0.22	1.25	0.00	3.31
225.0	0.12	0.04	0.09	0.00	1.19	0.00	0.05	0.24	1.17	0.00	2.90
229.5	0.14	0.05	0.00	0.00	0.82	0.00	0.00	0.31	1.08	0.00	2.41
239.8	0.22	0.08	0.06	0.00	0.29	0.00	0.05	0.35	0.43	0.00	1.48
241.7	0.47	0.08	0.00	0.03	0.27	0.00	0.00	0.43	0.37	0.00	1.66
242.7	0.24	0.14	0.04	0.04	0.37	0.00	0.08	0.42	0.34	4.10	5.77
244.9	0.09	0.04	0.05	0.00	0.33	0.00	0.08	0.44	0.40	0.00	1.44
246.2	0.15	0.05	0.05	0.00	0.29	0.00	0.07	0.47	0.38	3.34	4.79
246.5	0.39	0.07	0.04	0.00	0.29	0.00	0.06	0.46	0.37	0.00	1.69
252.5	0.13	0.00	0.00	0.00	0.22	0.00	0.07	0.54	0.39	3.72	5.07
253.0	0.13	0.05	0.00	0.00	0.25	0.00	0.07	0.54	0.39	0.00	1.43
253.5	0.20	0.00	0.00	0.00	0.26	0.00	0.07	0.59	0.41	5.10	6.62
255.0	0.07	0.00	0.00	0.00	0.24	0.00	0.09	0.55	0.36	4.61	5.93
263.4	0.34	0.00	0.00	0.00	0.24	0.00	0.09	0.55	0.36	4.61	6.20
264.5	0.07	0.00	0.05	0.02	0.14	0.00	0.05	0.50	0.23	5.34	6.40
267.0	0.07	0.02	0.00	0.00	0.16	0.00	0.08	0.58	0.24	3.07	4.22
288.0	0.05	0.00	0.00	0.00	0.00	0.00	0.00	0.66	0.00	4.54	5.24
335.4	0.00	0.00	0.00	0.00	0.00	0.00	0.00	0.59	0.00		
335.5	0.00	0.00	0.00	0.00	0.83	0.00	0.00	0.59	0.29	0.00	1.71
339.0	0.00	0.00	0.00	0.00	0.77	0.00	0.00	0.62	0.38	0.00	1.77
341.3	0.00	0.00	0.00	0.00	0.63	0.00	0.00	0.00	0.32	0.00	0.94
359.3	0.00	0.00	0.00	0.00	0.65	0.00	0.00	0.55	0.30	4.48	5.99
383.0	0.00	0.00	0.00	0.00	0.61	0.00	0.00	0.00	0.35	0.00	0.96

Appendix Table D.4: Measured headspace (atm) concentrations measured during the reactor experiment incubated at a hydrogen partial pressure of 9.8×10^{-4}

Hours	H ₂	N ₂	CO ₂
0.0	1.05E-03	8.24E-01	1.85E-01
118.8	9.43E-04	8.26E-01	2.63E-02
123.0	9.48E-04	8.25E-01	2.86E-02
125.8	6.89E-04	8.62E-01	2.52E-02
130.0	7.02E-04	8.18E-01	2.45E-02
195.2	1.08E-03	8.76E-01	2.97E-02
218.3	1.47E-03	8.76E-01	2.90E-02
219.8	9.84E-04		
241.7	1.59E-03	8.58E-01	2.91E-02
267.0	1.56E-03	8.62E-01	2.89E-02

Appendix Table D.5: Chlorophenol concentrations (μM) measured during the reactor experiment incubated at a hydrogen partial pressure of 5.7×10^{-4}

Hours	PCP	2,3,4,5- TeCP	2,3,4,6- TeCP	2,3,5,6- TeCP	3,4,5- TCP	2,3,4- TCP	2,3,5- TCP	3,4- DCP	3,5- DCP	2,4- DCP	3-CP	Balance
0.0	0.60	0.00	0.02	0.00	0.06	0.00	0.00	0.00	0.00	0.00	0.00	0.68
20.0	0.54	0.00	0.02	0.00	0.07	0.00	0.00	0.00	0.00	0.00	0.00	0.62
44.0	0.53	0.00	0.00	0.00	0.10	0.00	0.00	0.00	0.00	0.00	0.00	0.63
56.5	0.50	0.04	0.00	0.00	0.15	0.00	0.00	0.00	0.00	0.00	0.00	0.69
67.5	0.30	0.11	0.00	0.00	0.27	0.00	0.00	0.00	0.00	0.00	0.00	0.67
72.0	0.22	0.22	0.00	0.00	0.44	0.00	0.00	0.00	0.00	0.00	0.00	0.87
75.2	0.12	0.20	0.00	0.00	0.62	0.00	0.00	0.00	0.00	0.00	0.00	0.94
82.2	0.04	0.08	0.00	0.00	0.74	0.00	0.00	0.00	0.00	0.30	0.00	1.16
83.7	0.00	0.00	0.00	0.00	0.00	0.00	0.00	0.00	0.00	0.00	0.00	0.00
83.7	0.34	0.06	0.00	0.00	0.76	0.00	0.00	0.00	0.00	0.23	0.00	1.39
89.3	0.08	0.13	0.00	0.00	0.83	0.00	0.04	0.00	0.00	0.00	0.00	1.07
91.5	0.05	0.10	0.00	0.00	1.06	0.00	0.05	0.00	0.00	0.00	0.00	1.27
92.7	0.04	0.07	0.00	0.00	1.01	0.00	0.05	0.00	0.00	0.00	0.00	1.16
93.2	0.03	0.07	0.00	0.00	1.05	0.00	0.05	0.00	0.00	0.00	0.00	1.20
93.2	0.37	0.08	0.00	0.00	1.09	0.00	0.05	0.00	0.00	0.00	0.00	1.58
94.5	0.28	0.15	0.00	0.00	1.11	0.00	0.05	0.00	0.00	0.00	0.00	1.58
95.5	0.21	0.17	0.00	0.00	1.14	0.00	0.05	0.00	0.00	0.00	0.00	1.56
96.5	0.15	0.16	0.00	0.00	1.15	0.00	0.05	0.00	0.00	0.00	0.00	1.51
96.7	0.11	0.15	0.00	0.04	1.24	0.00	0.03	0.00	0.16	0.00	0.00	1.73
99.2	0.07	0.13	0.00	0.00	1.33	0.07	0.07	0.00	0.20	0.00	0.00	1.87
100.0	0.05	0.09	0.00	0.00	1.41	0.09	0.00	0.00	0.21	0.00	0.00	1.84
101.7	0.03	0.07	0.00	0.00	1.27	0.08	0.00	0.00	0.22	0.00	0.00	1.66
101.7	0.35	0.08	0.00	0.00	1.28	0.08	0.00	0.00	0.25	0.00	0.00	2.03
103.4	0.24	0.17	0.00	0.00	1.36	0.08	0.00	0.00	0.23	0.00	0.00	2.07
104.1	0.20	0.19	0.00	0.00	1.51	0.10	0.00	0.00	0.23	0.00	0.00	2.23
106.7	0.08	0.14	0.00	0.00	1.46	0.08	0.00	0.00	0.23	0.30	0.00	2.30
107.7	0.06	0.13	0.00	0.00	1.53	0.07	0.00	0.00	0.27	0.27	0.00	2.31

Hours	PCP	2,3,4,5 -TeCP	2,3,4,6 -TeCP	2,3,5,6 -TeCP	3,4,5- TCP	2,3,4- TCP	2,3,5- TCP	3,4- DCP	3,5- DCP	2,4- DCP	3-CP	Balance
108.5	0.05	0.09	0.00	0.00	1.49	0.00	0.05	0.00	0.29	0.00	0.00	1.97
108.6	0.38	0.09	0.00	0.00	1.52	0.00	0.05	0.00	0.29	0.28	0.00	2.62
109.0	0.36	0.12	0.00	0.00	1.66	0.00	0.06	0.00	0.30	0.23	0.00	2.72
113.9	0.06	0.13	0.00	0.00	1.79	0.00	0.07	0.00	0.43	0.00	0.00	2.48
114.8	0.05	0.11	0.00	0.00	1.81	0.00	0.08	0.00	0.50	0.20	0.00	2.75
115.7	0.03	0.07	0.00	0.00	1.69	0.00	0.08	0.00	0.57	0.00	0.00	2.44
115.7	0.36	0.06	0.00	0.00	1.70	0.00	0.07	0.00	0.56	0.00	0.00	2.75
115.7	0.36	0.06	0.00	0.00	1.70	0.00	0.07	0.00	0.56	0.00	0.00	2.75
116.5	0.26	0.14	0.00	0.00	1.65	0.00	0.08	0.00	0.56	0.00	0.00	2.70
117.2	0.20	0.17	0.00	0.00	1.80	0.00	0.08	0.00	0.58	0.00	0.00	2.84
119.1	0.08	0.13	0.00	0.00	1.79	0.00	0.00	0.00	0.67	0.22	0.00	2.89
119.7	0.04	0.09	0.00	0.00	1.68	0.11	0.10	0.00	0.74	0.00	0.00	2.76
121.6	0.04	0.06	0.00	0.03	1.77	0.11	0.10	0.14	0.90	0.24	0.00	3.37
122.3	0.02	0.03	0.00	0.00	1.56	0.00	0.09	0.00	0.94	0.18	0.00	2.82
122.4	0.32	0.03	0.00	0.00	1.55	0.00	0.10	0.00	0.97	0.00	0.00	2.97
122.4	0.32	0.03	0.00	0.00	1.55	0.00	0.10	0.00	0.97	0.00	0.00	2.97
123.6	0.19	0.14	0.00	0.00	1.66	0.00	0.09	0.00	0.98	0.21	0.00	3.28
124.7	0.10	0.14	0.00	0.00	1.70	0.00	0.10	0.15	0.98	0.22	0.00	3.38
125.8	0.05	0.10	0.00	0.00	1.66	0.00	0.11	0.00	1.05	0.00	0.00	2.97
126.5	0.04	0.08	0.00	0.00	1.69	0.00	0.10	0.16	1.08	0.27	0.00	3.42
126.7	0.35	0.07	0.00	0.00	1.65	0.00	0.10	0.16	1.10	0.25	0.00	3.69
130.3	0.04	0.06	0.00	0.00	1.60	0.00	0.13	0.19	1.26	0.37	0.00	3.64
131.7	0.37	0.04	0.00	0.03	1.71	0.00	0.11	0.22	1.37	0.33	0.00	4.18
131.7	0.37	0.04	0.00	0.03	1.71	0.00	0.11	0.22	1.37	0.33	0.00	4.18
132.2	0.23	0.09	0.00	0.00	1.42	0.00	0.09	0.19	1.27	0.32	0.00	3.62
139.7	0.07	0.00	0.00	0.02	1.08	0.00	0.03	0.30	1.12	0.41	0.00	3.03
141.5	0.05	0.00	0.00	0.57	1.02	0.00	0.06	0.28	1.08	0.41	0.00	3.45
143.3	0.37	0.00	0.00	0.00	0.71	0.00	0.00	0.33	0.57	0.43	0.00	2.42
143.3	0.37	0.00	0.00	0.00	0.71	0.00	0.00	0.33	0.57	0.43	0.00	2.42
144.8	0.07	0.05	0.00	0.02	0.78	0.00	0.03	0.38	0.43	0.46	0.00	2.22
146.0	0.03	0.04	0.00	0.00	0.77	0.00	0.04	0.40	0.34	0.46	0.00	2.09
147.3	0.38	0.00	0.00	0.00	0.67	0.00	0.00	0.35	0.23	0.48	0.00	2.12
147.3	0.38	0.00	0.00	0.00	0.67	0.00	0.00	0.35	0.23	0.48	0.00	2.12
147.8	0.20	0.12	0.00	0.00	0.65	0.00	0.05	0.43	0.26	0.49	0.00	2.20
148.5	0.08	0.10	0.00	0.00	0.71	0.00	0.08	0.40	0.25	0.55	0.00	2.17
150.2	0.02	0.03	0.00	0.00	0.68	0.00	0.06	0.51	0.25	0.56	0.00	2.10
150.8	0.00	0.00	0.00	0.00	0.00	0.00	0.00	0.00	0.00	0.00	0.00	0.00
150.8	0.39	0.04	0.00	0.03	0.66	0.00	0.04	0.54	0.22	0.62	0.00	2.54
151.2	0.28	0.09	0.00	0.00	0.68	0.00	0.06	0.53	0.23	0.57	0.00	2.46
151.8	0.11	0.09	0.00	0.00	0.71	0.00	0.04	0.55	0.23	0.65	0.00	2.38
154.5	0.05	0.00	0.00	0.00	0.67	0.00	0.00	0.67	0.22	0.66	0.00	2.27
155.7	0.00	0.00	0.00	0.00	0.00	0.00	0.00	0.00	0.00	0.00	0.00	0.00
155.7	0.39	0.00	0.00	0.00	0.50	0.00	0.00	0.56	0.17	0.65	0.00	2.27
155.9	0.36	0.04	0.00	0.00	0.52	0.00	0.00	0.61	0.20	0.65	0.00	2.39
156.2	0.33	0.15	0.00	0.19	0.66	0.00	0.05	0.66	0.42	0.69	0.00	3.15

Hours	PCP	2,3,4,5 -TeCP	2,3,4,6 -TeCP	2,3,5,6 -TeCP	3,4,5- TCP	2,3,4- TCP	2,3,5- TCP	3,4- DCP	3,5- DCP	2,4- DCP	3-CP	Balance
156.5	0.17	0.13	0.00	0.06	0.65	0.00	0.04	0.67	0.17	0.65	0.00	2.55
157.0	0.10	0.09	0.00	0.00	0.61	0.00	0.00	0.62	0.17	0.64	0.00	2.23
157.5	0.05	0.06	0.00	0.00	0.63	0.00	0.00	0.67	0.17	0.72	0.00	2.30
158.2	0.04	0.05	0.00	0.00	0.68	0.00	0.04	0.75	0.19	0.69	0.00	2.43
158.3	0.38	0.03	0.00	0.00	0.61	0.00	0.00	0.67	0.20	0.70	0.00	2.58
158.3	0.38	0.03	0.00	0.00	0.61	0.00	0.00	0.67	0.20	0.70	0.00	2.58
163.3	0.07	0.00	0.00	0.00	0.62	0.00	0.00	0.84	0.20	0.77	0.00	2.50
163.3	0.39	0.00	0.00	0.00	0.64	0.00	0.00	0.87	0.20	0.77	0.00	2.88
163.5	0.32	0.06	0.00	0.00	0.61	0.00	0.00	0.88	0.20	0.75	0.00	2.82
163.8	0.23	0.12	0.00	0.03	0.69	0.00	0.00	0.90	0.18	0.81	0.00	2.96
164.4	0.12	0.10	0.00	0.00	0.67	0.00	0.04	0.85	0.20	0.83	0.00	2.81
165.5	0.06	0.06	0.00	0.00	0.69	0.00	0.04	0.93	0.21	0.82	0.00	2.80
166.0	0.03	0.03	0.00	0.00	0.63	0.00	0.04	0.88	0.23	0.83	0.00	2.67

Appendix Table D.6: Headspace (atm) and acetate (μM) concentrations measured during the reactor experiment incubated at a hydrogen partial pressure of 5.7×10^{-4}

Hours	H2	N2	CO2	Acetate
20.0	6.13E-04	8.62E-01	2.75E-02	7.70E-01
44.0	5.84E-04	8.43E-01	2.72E-02	9.56E-01
67.5	5.43E-04	8.21E-01	2.78E-02	8.61E-01
83.7	5.50E-04	8.24E-01	1.48E-02	0.00E+00
89.3	6.19E-04	8.30E-01	1.61E-02	9.27E-01
115.7	5.52E-04	8.53E-01	0.00E+00	0.00E+00
124.7	5.49E-04	8.17E-01	2.89E-02	0.00E+00
125.8	5.73E-04			
126.7	1.27E-02	8.10E-02	2.88E-02	0.00E+00
130.3	2.26E-02	8.10E-01	2.89E-02	0.00E+00
139.7	3.88E-02	8.18E-01	2.87E-02	0.00E+00
166.0	3.88E-02			

Appendix Table D.7: Chlorophenol concentrations (μM) measured during the reactor experiment incubated at a hydrogen partial pressure of 9.4×10^{-5}

[illegible]

Hours	PCP	2,3,4,5 -TeCP	2,3,4,6 -TeCP	2,3,5,6 -TeCP	3,4,5- TCP	2,3,4- TCP	2,3,5- TCP	3,4- DCP	3,5- DCP	2,4- DCP	3-CP	Balance
91.3	0.4	0.09	0.00	0.00	0.17	0.00	0.00	0.00	0.00	0.00	0.00	0.68
102.3	0.3	0.13	0.00	0.00	0.25	0.00	0.00	0.00	0.00	0.00	0.00	0.68
115.7	0.1	0.14	0.00	0.00	0.39	0.00	0.00	0.00	0.00	0.00	0.00	0.63
118.2	0.1	0.10	0.00	0.00	0.40	0.00	0.00	0.00	0.00	0.00	0.00	0.63
118.2	0.1	0.10	0.00	0.00	0.40	0.00	0.00	0.00	0.00	0.00	0.00	0.63
121.9	0.1	0.16	0.00	0.00	0.56	0.00	0.03	0.00	0.00	0.00	0.00	0.83
126.7	0.1	0.08	0.00	0.00	0.52	0.00	0.00	0.00	0.00	0.00	0.00	0.66
126.8	0.4	0.09	0.00	0.00	0.54	0.00	0.05	0.00	0.00	0.00	0.00	1.04
127.5	0.3	0.08	0.00	0.00	0.55	0.00	0.05	0.00	0.00	0.00	0.00	1.03
130.4	0.3	0.13	0.00	0.00	0.53	0.00	0.06	0.00	0.00	0.00	0.00	1.01
132.4	0.3	0.16	0.00	0.00	0.65	0.00	0.07	0.00	0.00	0.00	0.00	1.18
135.8	0.2	0.14	0.00	0.00	0.57	0.00	0.06	0.00	0.00	0.00	0.00	0.98
137.6	0.2	0.17	0.00	0.00	0.60	0.00	0.08	0.00	0.00	0.00	0.00	1.01
140.1	0.1	0.19	0.00	0.00	0.73	0.00	0.08	0.00	0.00	0.00	0.00	1.14
142.3	0.1	0.27	0.00	0.00	0.85	0.08	0.11	0.00	0.00	0.00	0.00	1.44
145.0	0.1	0.20	0.00	0.00	0.78	0.00	0.08	0.00	0.00	0.00	0.00	1.19
147.6	0.1	0.18	0.00	0.00	0.81	0.09	0.11	0.00	0.00	0.00	0.00	1.29
151.5	0.1	0.14	0.00	0.00	0.78	0.00	0.08	0.00	0.00	0.00	0.00	1.07
151.6	0.4	0.15	0.00	0.00	0.85	0.00	0.08	0.00	0.00	0.00	0.00	1.48
152.8	0.4	0.17	0.00	0.00	0.86	0.00	0.10	0.00	0.00	0.00	0.00	1.50
154.6	0.3	0.20	0.00	0.00	0.85	0.00	0.09	0.00	0.00	0.00	0.00	1.47
157.6	0.3	0.25	0.00	0.00	0.89	0.00	0.09	0.00	0.00	0.00	0.00	1.54
160.1	0.2	0.25	0.00	0.00	0.87	0.00	0.10	0.00	0.00	0.00	0.00	1.44
163.2	0.2	0.25	0.00	0.00	0.92	0.00	0.08	0.00	0.20	0.40	0.00	2.01
165.1	0.2	0.25	0.00	0.00	0.95	0.00	0.13	0.00	0.21	0.75	0.00	2.44
167.8	0.1	0.22	0.00	0.00	0.92	0.00	0.12	0.00	0.00	0.00	0.00	1.37
170.4	0.1	0.20	0.00	0.00	0.99	0.00	0.12	0.00	0.19	0.00	0.00	1.59
173.0	0.1	0.20	0.00	0.07	1.18	0.00	0.16	0.00	0.20	0.00	0.00	1.89
173.0	0.4	0.20	0.00	0.00	1.10	0.00	0.13	0.00	0.22	0.00	0.00	2.08
175.8	0.3	0.16	0.00	0.00	1.01	0.00	0.13	0.00	0.23	0.00	0.00	1.86
177.3	0.4	0.26	0.00	0.00	1.20	0.00	0.14	0.00	0.23	0.00	0.00	2.18
180.3	0.3	0.20	0.00	0.00	1.11	0.00	0.14	0.00	0.23	0.24	0.00	2.20
182.3	0.2	0.18	0.00	0.00	0.99	0.00	0.13	0.00	0.24	0.00	0.00	1.76
189.3	0.1	0.20	0.00	0.00	0.68	0.00	0.00	0.00	0.26	0.00	0.00	1.28
191.7	0.1	0.20	0.00	0.00	0.84	0.00	0.14	0.00	0.27	0.00	0.00	1.57
194.1	0.1	0.15	0.00	0.00	0.79	0.00	0.14	0.00	0.28	0.00	0.00	1.43
197.5	0.1	0.14	0.00	0.00	0.82	0.00	0.13	0.00	0.28	0.00	0.00	1.45
217.3	0.1	0.20	0.00	0.00	1.22	0.00	0.15	0.00	0.35	0.40	0.00	2.38
218.0	0.4	0.19	0.03	0.00	1.27	0.00	0.15	0.00	0.35	0.40	0.00	2.80
218.6	0.4	0.20	0.00	0.00	1.28	0.00	0.17	0.00	0.34	0.35	0.00	2.77
219.4	0.4	0.21	0.04	0.00	1.29	0.00	0.15	0.00	0.34	0.53	0.00	2.99
221.5	0.4	0.21	0.03	0.00	1.31	0.00	0.10	0.00	0.66	0.00	0.00	2.72
236.2	0.4	0.22	0.00	0.00	1.29	0.00	0.15	0.00	0.38	0.24	0.00	2.67
237.6	0.4	0.21	0.00	0.00	1.26	0.00	0.15	0.00	0.65	0.00	0.00	2.66

Hours	PCP	2,3,4,5 -TeCP	2,3,4,6 -TeCP	2,3,5,6 -TeCP	3,4,5- TCP	2,3,4- TCP	2,3,5 - TCP	3,4- DCP	3,5- DCP	2,4- DCP	3-CP	Balance
242.3	0.4	0.21	0.00	0.11	1.31	0.00	0.19	0.00	0.31	0.00	0.00	2.49
244.4	0.3	0.16	0.00	0.00	1.33	0.00	0.14	0.00	0.35	0.28	0.00	2.61
247.3	0.3	0.00	0.00	0.00	1.32	0.00	0.15	0.00	0.34	0.25	0.00	2.40
250.8	0.3	0.16	0.00	0.00	1.24	0.00	0.10	0.00	0.33	0.25	0.00	2.40
261.5	0.2	0.16	0.00	0.00	1.30	0.00	0.17	0.00	0.35	0.19	0.00	2.40
262.8	0.2	0.24	0.00	0.00	1.40	0.00	0.15	0.00	0.37	0.27	0.00	2.67
283.3	0.1	0.10	0.00	0.00	1.52	0.00	0.00	0.00	0.46	0.25	0.00	2.38
288.8	0.4	0.05	0.00	0.00	1.56	0.00	0.13	0.00	0.49	0.25	0.00	2.86
290.0	0.4	0.09	0.00	0.00	1.49	0.00	0.12	0.00	0.51	0.28	0.00	2.85
293.1	0.2	0.07	0.00	0.00	1.43	0.00	0.11	0.00	0.51	0.00	0.00	2.37
296.5	0.2	0.13	0.00	0.00	0.98	0.00	0.04	0.00	0.49	0.25	0.00	2.12
298.3	0.2	0.12	0.00	0.00	1.36	0.00	0.11	0.00	0.49	0.25	0.00	2.53
300.3	0.2	0.14	0.00	0.00	1.50	0.00	0.12	0.00	0.50	0.26	0.00	2.70
302.5	0.2	0.25	0.00	0.00	1.53	0.00	0.12	0.00	0.51	0.29	0.00	2.85
305.3	0.1	0.11	0.00	0.00	1.43	0.00	0.12	0.00	0.49	0.25	0.00	2.52
307.6	0.1	0.18	0.00	0.00	1.59	0.00	0.12	0.00	0.51	0.25	0.00	2.74
310.6	0.1	0.10	0.00	0.00	1.41	0.00	0.11	0.00	0.51	0.27	0.00	2.46
312.0	0.1	0.07	0.00	0.00	1.54	0.00	0.11	0.00	0.56	0.26	0.00	2.61
312.1	0.4	0.13	0.00	0.00	1.60	0.00	0.11	0.00	0.56	0.27	0.00	3.03
314.1	0.3	0.10	0.00	0.00	1.53	0.00	0.11	0.00	0.54	0.28	0.00	2.87
316.3	0.2	0.12	0.00	0.00	1.53	0.00	0.12	0.00	0.57	0.22	0.00	2.79
319.3	0.2	0.15	0.00	0.00	1.61	0.00	0.11	0.00	0.54	0.26	0.00	2.87
321.0	0.2	0.17	0.00	0.00	1.82	0.00	0.13	0.00	0.62	0.32	0.00	3.26
324.5	0.1	0.23	0.00	0.05	1.92	0.00	0.14	0.00	0.68	0.48	0.00	3.62
328.5	0.1	0.11	0.00	0.00	1.80	0.00	0.14	0.00	0.72	0.41	0.00	3.26
330.1	0.1	0.15	0.00	0.00	1.84	0.00	0.15	0.00	0.77	0.35	0.00	3.32
330.2	0.4	0.19	0.00	0.00	1.83	0.00	0.15	0.00	0.75	0.36	0.00	3.66
331.2	0.4	0.19	0.00	0.05	1.83	0.00	0.15	0.00	0.75	0.36	0.00	3.71
331.3	0.4	0.18	0.00	0.04	1.86	0.00	0.16	0.00	0.78	0.32	0.00	3.69
333.8	0.2	0.10	0.00	0.05	1.81	0.00	0.15	0.00	0.75	0.44	0.00	3.54
336.0	0.2	0.21	0.00	0.05	1.90	0.00	0.17	0.00	0.84	0.43	0.00	3.75
337.3	0.1	0.18	0.00	0.04	1.75	0.00	0.17	0.00	0.84	0.35	0.00	3.45
338.9	0.1	0.13	0.00	0.03	1.78	0.00	0.19	0.00	0.95	0.32	0.00	3.47
341.3	0.1	0.11	0.00	0.04	1.76	0.00	0.19	0.19	1.03	0.40	0.00	3.77
342.1	0.4	0.10	0.00	0.05	1.71	0.00	0.19	0.19	1.04	0.36	0.00	4.07
345.8	0.2	0.21	0.00	0.06	1.75	0.00	0.00	0.21	1.16	0.40	0.00	4.02
357.8	0.0	0.00	0.00	0.00	0.87	0.00	0.16	0.23	1.58	0.49	0.00	3.36
360.3	0.4	0.00	0.02	0.04	0.53	0.00	0.07	0.15	1.01	0.65	0.00	2.86
361.8	0.1	0.06	0.00	0.09	0.55	0.00	0.13	0.32	0.80	0.72	0.00	2.81
380.6	0.0	0.00	0.00	0.00	0.11	0.00	0.00	0.25	0.00	0.48	0.00	0.88
382.8	0.4	0.00	0.00	0.00	0.11	0.00	0.00	0.25	0.00	0.48	0.00	1.23
384.8	0.1	0.00	0.00	0.00	0.11	0.00	0.00	0.25	0.00	0.48	0.00	0.93
385.8	0.0	0.00	0.00	0.00	0.11	0.00	0.00	0.25	0.00	0.48	0.00	0.88
452.6	0.0	0.00	0.00	0.00	0.00	0.00	0.00	0.27	0.00	0.00	0.00	0.28

Hours	PCP	2,3,4,5 -TeCP	2,3,4,6 -TeCP	2,3,5,6 -TeCP	3,4,5- TCP	2,3,4- TCP	2,3,5 - TCP	3,4- DCP	3,5- DCP	2,4- DCP	3-CP	Balance
452.6	0.3	0.00	0.00	0.00	0.13	0.00	0.00	0.43	0.00	0.48	0.00	1.38
455.7	0.0	0.03	0.00	0.04	0.30	0.00	0.09	0.48	0.07	0.00	0.00	1.06

Appendix Table D.8: Headspace (atm) and acetate (μM) concentrations measured during the reactor experiment incubated at a hydrogen partial pressure of 9.4×10^{-5}

Hours	H2	N2	CO2	Acetate
0.0	9.67E-05	8.31E-01	2.24E-02	2.67E+00
20.8	7.20E-05	8.48E-01	2.76E-02	8.80E-01
24.3	8.34E-05	8.42E-01	8.32E-03	9.34E-01
43.8	8.06E-05	7.96E-01	9.70E-03	6.53E-01
48.3	8.85E-05	8.37E-01	1.13E-02	8.42E-01
51.1				9.83E-01
68.1	9.42E-05	8.88E-01	1.39E-02	1.18E+00
91.3	8.40E-05	7.95E-01	1.02E-02	7.18E-01
102.3	9.39E-05	8.63E-01	1.23E-02	1.06E+00
115.7	9.26E-05	9.21E-01	1.12E-02	1.05E+00
118.2	1.01E-04	8.63E-01	1.21E-02	1.56E+00
118.2	1.01E-04	8.63E-01	1.21E-02	1.56E+00
121.9				0.00E+00
126.8				2.02E+00
132.4	1.24E-04	9.57E-01	1.76E-02	1.09E+00
135.8				1.21E+00
140.1	7.90E-05	8.51E-01	1.23E-02	1.20E+00
142.3	8.47E-05	8.62E-01	1.17E-02	1.10E+00
147.6				4.49E-01
151.6	8.50E-05	8.69E-01	1.19E-02	1.09E+00
160.1	9.36E-05	8.75E-01	1.07E-02	9.43E-01
167.8	9.90E-05	8.30E-01	1.13E-02	1.06E+00
170.4	9.13E-05			
182.3	9.13E-05	8.59E-01	1.21E-02	8.74E-01
189.3	8.63E-05	8.67E-01	1.31E-02	9.70E-01
197.5	5.60E-04	4.32E+00	9.01E-02	7.55E-01
218.0	7.99E-02	8.30E-01	0.00E+00	
218.6	1.08E-01	0.00E+00	0.00E+00	8.26E-01
221.5	1.63E-01	9.12E-01	0.00E+00	7.26E-01
237.6	1.23E-01	0.00E+00	0.00E+00	
242.3	5.50E-02	8.00E-01	2.06E-02	
244.4	4.97E-02	7.48E-01	1.92E-02	
261.5	5.59E-02	7.63E-01	2.38E-02	
283.3	3.41E-04	0.00E+00	0.00E+00	
298.3	6.38E-05	0.00E+00	0.00E+00	
300.3	1.04E-04	0.00E+00	0.00E+00	7.62E-01

Hours	H2	N2	CO2	Acetate
305.3	6.98E-05	7.44E-01	2.11E-02	
307.6	6.98E-05	7.18E-01	8.73E-03	
314.1	3.73E-04	7.57E-01	2.01E-02	9.82E-01
319.3				9.33E-01
321.0	1.10E-04	7.69E-01	2.22E-02	
328.5	2.37E-04	2.14E+00	5.92E-02	
336.0	1.16E-04	6.92E-01	9.22E-04	
337.3				7.33E-01
338.9	8.15E-05	8.41E-01	2.22E-02	
341.3	7.71E-05	8.56E-01	2.30E-02	8.68E-01
345.8	2.73E-03	4.25E+00	1.18E-01	
357.8	6.33E-02	7.21E-01	2.23E-02	
452.6	2.49E-01	5.57E-01	6.01E-02	
455.7	2.38E-01	5.95E-01	6.20E-02	

Appendix Table D.9: Chlorophenol concentrations (μM) measured during the reactor experiment incubated at a hydrogen partial pressure of 7.8×10^{-3}

[illegible]

Hours	PCP	2,3,4,5 -TeCP	2,3,4,6 -TeCP	2,3,5,6 -TeCP	3,4,5- TCP	2,3,4- TCP	2,3,5- TCP	3,4- DCP	3,5- DCP	2,4- DCP	3-CP	Balance
226.7	0.2	0.1	0.04	0.00	0.17	0.00	0.00	0.00	0.00	0.00	0.00	0.56
229.9	0.2	0.1	0.19	0.00	0.25	0.00	0.06	0.00	0.00	0.00	0.00	0.82
240.1	0.1	0.1	0.19	0.00	0.39	0.00	0.07	0.00	0.18	0.00	0.00	1.03
244.4	0.1	0.1	0.14	0.00	0.40	0.00	0.11	0.00	0.18	0.00	0.00	1.02
251.7	0.0	0.0	0.07	0.00	0.38	0.00	0.07	0.00	0.21	0.00	0.00	0.81
262.2	0.0	0.0	0.05	0.00	0.34	0.00	0.05	0.00	0.14	0.00	0.00	0.60
262.3	0.3	0.0	0.07	0.00	0.36	0.00	0.05	0.00	0.14	0.00	0.00	0.91
264.1	0.2	0.1	0.05	0.00	0.35	0.00	0.06	0.00	0.15	0.00	0.00	0.89
267.1	0.2	0.1	0.05	0.00	0.37	0.00	0.06	0.00	0.22	0.00	0.00	0.95
269.7	0.1	0.1	0.07	0.00	0.40	0.00	0.07	0.00	0.14	0.00	0.00	0.91
271.2	0.1	0.1	0.05	0.00	0.40	0.00	0.07	0.00	0.14	0.00	0.00	0.85
274.0	0.1	0.1	0.05	0.00	0.41	0.00	0.08	0.00	0.14	0.00	0.00	0.83
275.6	0.1	0.1	0.08	0.00	0.41	0.00	0.12	0.00	0.23	0.00	0.00	1.03
275.7	0.4	0.1	0.06	0.00	0.43	0.00	0.08	0.00	0.14	0.00	0.00	1.15
277.2	0.4	0.1	0.14	0.00	0.44	0.00	0.06	0.00	0.30	0.00	0.00	1.44
279.9	0.2	0.2	0.09	0.00	0.50	0.06	0.08	0.00	0.25	0.00	0.00	1.36
283.0	0.2	0.2	0.18	0.00	0.54	0.06	0.10	0.00	0.15	0.00	0.00	1.37
286.2	0.1	0.1	0.13	0.00	0.51	0.00	0.06	0.00	0.15	0.00	0.00	1.08
288.5	0.1	0.1	0.24	0.00	0.50	0.00	0.05	0.00	0.28	0.00	0.00	1.26
290.1	0.1	0.1	0.24	0.00	0.50	0.00	0.05	0.00	0.28	0.00	0.00	1.26
290.2	0.5	0.2	0.12	0.00	0.58	0.00	0.06	0.00	0.30	0.00	0.00	1.73
291.9	0.4	0.2	0.07	0.00	0.57	0.00	0.08	0.00	0.14	0.00	0.00	1.44
294.2	0.2	0.2	0.00	0.04	0.61	0.00	0.08	0.00	0.22	0.00	0.00	1.39
296.3	0.4	0.3	0.08	0.00	0.65	0.00	0.08	0.00	0.25	0.00	0.00	1.71
298.8	0.2	0.2	0.05	0.00	0.68	0.00	0.07	0.00	0.12	0.00	0.00	1.33
300.3	0.1	0.2	0.12	0.00	0.70	0.00	0.07	0.00	0.29	0.00	0.00	1.54
302.8	0.1	0.2	0.09	0.00	0.77	0.00	0.08	0.00	0.29	0.00	0.00	1.54
306.7	0.1	0.2	0.16	0.00	0.73	0.00	0.07	0.00	0.28	0.00	0.00	1.46
309.2	0.1	0.1	0.09	0.00	0.86	0.00	0.11	0.00	0.31	0.00	0.00	1.57
309.3	0.3	0.2	0.09	0.00	0.91	0.00	0.09	0.00	0.29	0.00	0.00	1.86
313.2	0.2	0.2	0.37	0.00	0.86	0.00	0.08	0.00	0.28	0.00	0.00	2.05
315.8	0.3	0.3	0.12	0.00	0.95	0.04	0.09	0.00	0.30	0.00	0.00	2.08
318.2	0.3	0.3	0.11	0.00	1.06	0.05	0.12	0.00	0.29	0.00	0.00	2.15
320.3	0.2	0.3	0.13	0.00	1.10	0.00	0.12	0.00	0.30	0.00	0.00	2.14
324.4	0.1	0.2	0.14	0.00	1.12	0.07	0.08	0.00	0.36	0.00	0.00	1.98
326.0	0.0	0.1	0.19	0.00	1.22	0.08	0.09	0.00	0.28	0.00	0.00	2.02
326.1	0.3	0.1	0.16	0.00	1.19	0.06	0.09	0.00	0.31	0.00	0.00	2.26
332.6	0.1	0.2	0.31	0.00	1.30	0.09	0.13	0.00	0.32	0.00	0.00	2.39
333.8	0.0	0.1	0.20	0.00	1.37	0.05	0.11	0.00	0.32	0.00	0.00	2.24
334.7	0.0	0.1	0.13	0.00	1.44	0.06	0.09	0.00	0.30	0.00	0.00	2.19
334.7	0.3	0.1	0.12	0.00	1.38	0.00	0.08	0.00	0.32	0.00	0.00	2.34
336.7	0.3	0.3	0.10	0.00	1.46	0.06	0.10	0.00	0.34	0.00	0.00	2.60
338.7	0.3	0.3	0.19	0.00	1.47	0.04	0.10	0.00	0.33	0.00	0.00	2.66
340.7	0.2	0.2	0.14	0.00	1.48	0.06	0.10	0.00	0.32	0.00	0.00	2.52
341.8	0.1	0.2	0.09	0.00	1.65	0.05	0.09	0.00	0.32	0.00	0.00	2.53

Hours	PCP	2,3,4,5 -TeCP	2,3,4,6 -TeCP	2,3,5,6 -TeCP	3,4,5- TCP	2,3,4- TCP	2,3,5- TCP	3,4- DCP	3,5- DCP	2,4- DCP	3-CP	Balance
346.8	0.1	0.1	0.10	0.00	1.62	0.00	0.10	0.00	0.35	0.00	0.00	2.30
346.9	0.3	0.1	0.09	0.00	1.61	0.00	0.07	0.00	0.35	0.00	0.00	2.49
349.4	0.1	0.2	0.08	0.00	1.71	0.00	0.09	0.00	0.35	0.00	0.00	2.57
353.0	0.0	0.1	0.28	0.00	1.85	0.04	0.11	0.00	0.43	0.00	0.00	2.90
357.0	0.0	0.1	0.21	0.00	1.83	0.00	0.08	0.00	0.40	0.00	0.00	2.59
357.1	0.3	0.1	0.00	0.00	1.88	0.00	0.09	0.00	0.40	0.00	0.00	2.70
358.3	0.2	0.2	0.16	0.00	1.84	0.04	0.08	0.00	0.38	0.00	0.00	2.82
362.4	0.2	0.1	0.16	0.00	1.96	0.09	0.09	0.00	0.37	0.00	0.00	2.95
363.4	0.1	0.1	0.10	0.00	1.83	0.06	0.08	0.00	0.35	0.00	0.00	2.63
367.5	0.1	0.1	0.07	0.00	1.81	0.06	0.05	0.14	0.40	0.00	0.00	2.70
371.0	0.0	0.0	0.00	0.00	1.83	0.05	0.05	0.00	0.36	0.00	0.00	2.30
647.8	0.0	0.0	0.00	0.00	1.64	0.11	0.00	0.51	0.00	0.59	0.00	2.85
676.2	0.0	0.0	0.07	0.00	1.52	0.00	0.00	0.43	0.00	0.34	0.00	2.38
676.2	0.3	0.0	0.10	0.00	1.54	0.16	0.00	0.53	0.00	0.39	0.00	2.96
678.8	0.3	0.0	0.08	0.00	1.55	0.16	0.00	0.53	0.00	0.36	0.00	2.99
681.8	0.3	0.1	0.22	0.00	1.50	0.13	0.00	0.50	0.00	0.30	0.00	3.04
693.8	0.2	0.0	0.00	0.44	1.02	0.07	0.00	0.78	0.30	0.35	0.00	3.17
695.8	0.2	0.0	0.00	0.00	1.25	0.13	0.00	0.48	0.00	0.41	0.00	2.49
699.3	0.3	0.0	0.00	0.18	1.28	0.07	0.00	0.90	0.43	0.49	0.00	3.63
705.6	0.3	0.0	0.24	0.00	1.34	0.09	0.00	0.75	0.49	0.86	0.00	4.05
716.3	0.2	0.3	0.18	0.00	1.28	0.13	0.00	0.44	0.33	0.59	0.00	3.36
720.2	0.2	0.1	0.19	0.00	1.35	0.17	0.04	0.47	0.33	0.48	0.00	3.32
726.0	0.1	0.1	0.21	0.00	1.31	0.00	0.00	0.48	0.45	0.62	0.00	3.27
729.6	0.1	0.1	0.00	0.30	1.21	0.04	0.11	0.48	0.53	0.48	0.00	3.37
776.3	0.0	0.0	0.00	0.24	0.23	0.08	0.00	0.55	0.27	0.63	0.00	2.02
777.8	0.3	0.0	0.12	0.00	0.18	0.00	0.00	0.60	0.00	0.67	0.00	1.88
779.8	0.2	0.1	0.17	0.00	0.16	0.00	0.00	0.56	0.00	1.02	0.00	2.23
781.3	0.1	0.1	0.00	0.11	0.15	0.00	0.04	0.59	0.00	0.54	0.00	1.65
782.3	0.1	0.1	0.00	0.13	0.16	0.00	0.06	0.55	0.00	0.81	0.00	1.90
782.8	0.1	0.0	0.00	0.00	0.15	0.08	0.07	0.51	0.09	0.46	0.00	1.42
790.6	0.0	0.0	0.08	0.00	0.15	0.00	0.00	0.59	0.00	0.64	0.00	1.48
793.1	0.3	0.0	0.08	0.00	0.13	0.00	0.00	0.58	0.00	0.57	0.00	1.62
794.6	0.1	0.1	0.16	0.00	0.18	0.00	0.06	0.61	0.00	0.74	0.00	1.97
795.7	0.1	0.1	0.13	0.00	0.18	0.00	0.07	0.59	0.00	0.55	0.00	1.70
796.3	0.1	0.1	0.38	0.00	0.19	0.00	0.10	0.61	0.19	0.74	0.00	2.36
798.1	0.0	0.1	0.17	0.00	0.21	0.00	0.11	0.61	0.00	0.77	0.00	1.97
799.7	0.0	0.0	0.12	0.00	0.21	0.00	0.07	0.62	0.00	0.59	0.00	1.67
799.8	0.3	0.0	0.19	0.00	0.20	0.00	0.07	0.63	0.00	0.56	0.00	2.00
800.9	0.2	0.1	0.00	0.13	0.23	0.00	0.09	0.62	0.00	0.57	0.00	1.93
801.8	0.1	0.1	0.16	0.00	0.26	0.00	0.11	0.65	0.00	0.85	0.00	2.26
802.6	0.1	0.1	0.14	0.00	0.27	0.00	0.13	0.65	0.00	0.99	0.00	2.37
803.1	0.1	0.1	0.16	0.00	0.29	0.00	0.12	0.70	0.00	0.95	0.00	2.39
804.1	0.0	0.1	0.11	0.00	0.26	0.00	0.11	0.64	0.00	0.90	0.00	2.13
804.2	0.3	0.1	0.14	0.00	0.27	0.00	0.11	0.66	0.22	1.06	0.00	2.87
804.8	0.3	0.1	0.00	0.09	0.30	0.00	0.12	0.69	0.00	0.95	0.00	2.55

Hours	PCP	2,3,4,5 -TeCP	2,3,4,6 -TeCP	2,3,5,6 -TeCP	3,4,5- TCP	2,3,4- TCP	2,3,5- TCP	3,4- DCP	3,5- DCP	2,4- DCP	3-CP	Balance
805.6	0.1	0.1	0.00	0.06	0.31	0.00	0.17	0.68	0.22	1.55	0.00	3.20
807.2	0.1	0.1	0.15	0.00	0.39	0.00	0.14	0.72	0.32	1.08	0.00	2.95
807.7	0.0	0.1	0.00	0.10	0.37	0.00	0.14	0.73	0.31	1.04	0.00	2.79
826.7	0.0	0.0	0.09	0.00	0.07	0.05	0.00	0.71	0.00	0.64	0.00	1.55
832.8	0.0	0.0	0.12	0.00	0.32	0.00	0.00	0.70	0.32	1.08	0.00	2.59
959.1	0.1	0.0	0.09	0.00	0.12	0.00	0.00	0.36	0.00	8.11	0.00	8.75
960.6	0.3	0.1	0.07	0.00	0.00	0.00	0.00	0.41	0.00	0.00	0.00	0.83
961.4	0.2	0.1	0.09	0.00	0.00	0.00	0.00	0.44	0.00	0.00	0.00	0.82
962.8	0.1	0.1	0.11	0.00	0.25	0.00	0.00	0.40	0.00	0.93	0.00	1.84
963.3	0.1	0.1	0.00	0.07	0.26	0.00	0.00	0.41	0.00	0.00	0.00	0.90
964.4	0.0	0.1	0.08	0.00	0.26	0.00	0.00	0.45	0.00	0.00	0.00	0.90
965.6	0.0	0.1	0.08	0.00	0.53	0.00	0.00	0.42	0.00	0.00	0.00	1.10
968.0	0.0	0.0	0.09	0.00	0.39	0.00	0.00	0.44	0.00	0.00	0.00	0.96
971.3	0.0	0.1	0.09	0.00	0.31	0.12	0.00	0.46	0.00	0.00	0.00	1.04
973.5	0.0	0.1	0.06	0.00	0.25	0.12	0.00	0.48	0.00	0.00	0.00	0.97
982.5	0.0	0.0	0.07	0.00	0.23	0.00	0.00	0.51	0.00	0.00	0.00	0.81
986.1	0.0	0.0	0.08	0.00	0.23	0.00	0.00	0.53	0.00	0.00	0.00	0.84
994.7	0.0	0.0	0.07	0.00	0.17	0.13	0.00	0.51	0.00	0.00	0.00	0.88
1008.1	0.0	0.0	0.06	0.00	0.15	0.00	0.00	0.44	0.00	0.00	0.00	0.65
1009.1	0.0	0.0	0.06	0.00	0.11	0.00	0.00	0.49	0.00	0.00	0.00	0.67
1010.3	0.0	0.0	0.00	0.00	0.07	0.00	0.00	0.47	0.00	0.00	0.00	0.54
1010.4	0.0	0.0	0.00	0.00	0.87	0.00	0.00	0.48	0.00	0.00	0.00	1.35
1011.8	0.0	0.0	0.00	0.08	0.81	0.00	0.00	0.48	0.00	0.00	0.00	1.37
1013.2	0.0	0.0	0.00	0.00	0.82	0.00	0.00	0.48	0.00	0.00	0.00	1.30
1019.8	0.0	0.0	0.09	0.00	0.58	0.00	0.00	0.44	0.31	0.00	0.00	1.42
1030.8	0.0	0.0	0.00	0.00	0.43	0.00	0.00	0.52	0.33	0.00	0.00	1.28
1035.2	0.0	0.0	0.08	0.00	0.37	0.00	0.00	0.49	0.43	0.50	0.00	1.92
1036.8	0.0	0.0	0.00	0.00	0.34	0.00	0.00	0.49	0.41	0.00	0.00	1.24
1041.4	0.0	0.0	0.08	0.00	0.33	0.00	0.00	0.49	0.36	0.00	0.00	1.26
1046.4	0.0	0.0	0.09	0.00	0.27	0.00	0.00	0.50	0.41	0.70	0.00	1.97
1056.4	0.0	0.0	0.06	0.00	0.16	0.00	0.00	0.53	0.20	0.00	0.00	0.95
1060.8	0.0	0.0	0.00	0.00	0.15	0.00	0.00	0.50	0.00	0.00	0.00	0.65
1064.7	0.0	0.0	0.00	0.00	0.12	0.00	0.00	0.51	0.00	0.00	0.00	0.63
1074.3	0.0	0.0	0.00	0.00	0.05	0.00	0.00	0.38	0.00	0.00	0.00	0.43

Appendix Table D.10: Headspace (atm) and acetate (μM) concentrations measured during the reactor experiment incubated at a hydrogen partial pressure of 7.8×10^{-3}

Hours	H ₂	N ₂	CO ₂	Acetate
0.0	8.06E-03	9.05E-01	3.25E-03	
4.3	8.31E-03	8.87E-01	2.80E-03	5.23E+00
10.5				4.17E+00
20.7	8.48E-03	8.78E-01	5.49E-04	5.91E+00
26.0	6.12E-03	8.41E-01	1.16E-03	4.21E+00

Hours	H2	N2	CO2	Acetate
45.6	8.28E-03	9.54E-01	1.17E-03	
53.3	7.12E-03	8.32E-01	8.38E-04	6.13E+00
66.1	7.29E-03	8.75E-01	3.00E-03	4.84E+00
95.3	7.17E-03	8.95E-01	4.47E-04	4.68E+00
106.8	7.45E-03	8.94E-01	2.71E-03	5.12E+00
118.5	7.56E-03	9.91E-01	7.62E-04	5.06E+00
121.3	7.39E-03	8.74E-01	8.36E-04	4.31E+00
143.1	7.37E-03	8.88E-01	1.16E-03	3.86E+00
151.8	7.36E-03	8.41E-01	1.48E-03	3.55E+00
166.7	7.39E-03	8.84E-01	1.33E-03	3.52E+00
199.1	7.49E-03	8.82E-01	1.16E-03	3.93E+00
214.7	7.63E-03	9.67E-01	2.28E-03	
218.0	8.40E-03	1.08E+00	1.46E-03	
226.7	6.96E-03	9.59E-01	3.62E-03	
229.9	9.47E-03	1.14E+00	2.17E-03	
240.1	8.73E-03	1.01E+00	1.51E-03	
251.7	8.43E-03	1.00E+00	2.03E-03	2.06E+00
267.1	8.51E-03	1.02E+00	1.51E-03	
269.7				3.28E+00
286.2	9.06E-03	1.10E+00	1.60E-03	
294.2	8.81E-03	1.15E+00	1.40E-03	3.40E+00
309.2	7.81E-03	9.11E-01	1.78E-03	2.46E+00
326.1	8.41E-03			
332.6	7.26E-03			2.56E+00
336.7	7.39E-03			
346.9				
353.0	7.73E-03	2.17E-01	1.62E-03	
371.0	6.89E-03	1.92E-01	1.04E-03	
647.8	7.81E-03			
776.3	8.30E-03	1.22E+00	5.14E-03	
777.8	7.93E-03	9.86E-01	4.75E-03	
782.3	1.34E-01	7.70E-01	3.91E-02	
782.8	1.55E-01	7.80E-01	2.42E-02	
961.4				1.90E+00
963.3				2.24E+00
968.0	9.76E-02	8.36E-01	4.96E-03	
973.5	5.79E-03	9.58E-01	5.49E-03	
986.1	4.26E-03	8.78E-01	1.01E-03	
1008.1				1.36E+00
1009.1	1.60E-01	7.99E-01	1.96E-03	
1019.8	8.98E-03	1.26E+00	2.42E-03	
1046.4	9.11E-03	1.02E+00	1.43E-01	
1056.4	9.80E-03	8.69E-01	8.69E-03	
1074.3	2.45E-02	8.37E-01	1.25E-02	

Hours	PCP	2,3,4,5 -TeCP	2,3,4,6 -TeCP	2,3,5,6 -TeCP	3,4,5- TCP	2,3,4- TCP	2,3,5- TCP	3,4- DCP	3,5- DC P	2,4- DCP	3-CP	Balan- ce
247.8	0.3	0.1	0.0	0.00	0.52	0.00	0.00	0.00	0.00	0.00	0.00	0.91
247.8	0.3	0.1	0.0	0.00	0.48	0.00	0.00	0.00	0.00	0.00	0.00	0.87
248.8	0.3	0.1	0.0	0.00	0.44	0.00	0.00	0.00	0.00	0.00	0.00	0.84
248.8	0.3	0.1	0.0	0.00	0.46	0.00	0.00	0.00	0.00	0.00	0.00	0.85
251.8	0.3	0.1	0.0	0.00	0.45	0.00	0.00	0.00	0.00	0.00	0.00	0.85
251.8	0.3	0.1	0.0	0.00	0.46	0.00	0.00	0.00	0.00	0.00	0.00	0.86
255.8	0.2	0.2	0.0	0.00	0.53	0.00	0.00	0.00	0.00	0.00	0.00	0.92
255.8	0.2	0.2	0.0	0.00	0.54	0.00	0.00	0.00	0.00	0.00	0.00	0.95
258.8	0.2	0.2	0.0	0.04	0.54	0.00	0.00	0.00	0.00	0.00	0.00	0.97
258.8	0.2	0.2	0.0	0.00	0.53	0.00	0.00	0.00	0.00	0.00	0.00	0.93
262.8	0.2	0.2	0.0	0.04	0.59	0.00	0.00	0.00	0.00	0.00	0.00	1.00
262.8	0.1	0.2	0.0	0.03	0.61	0.00	0.00	0.00	0.00	0.00	0.00	1.01
268.8	0.1	0.2	0.0	0.04	0.67	0.00	0.00	0.00	0.00	0.00	0.00	1.06
268.8	0.1	0.2	0.0	0.03	0.70	0.00	0.00	0.00	0.00	0.00	0.00	1.05
269.5	0.0	0.0	0.0	0.00	0.00	0.00	0.00	0.00	0.00	0.00	0.00	0.00
269.5	0.3	0.2	0.0	0.00	0.72	0.00	0.00	0.00	0.00	0.00	0.00	1.21
269.5	0.3	0.2	0.0	0.00	0.67	0.00	0.00	0.00	0.00	0.00	0.00	1.16
272.8	0.3	0.2	0.0	0.04	0.67	0.00	0.00	0.00	0.00	0.00	0.00	1.25
272.8	0.2	0.2	0.0	0.04	0.69	0.00	0.00	0.00	0.00	0.00	0.00	1.21
275.8	0.2	0.3	0.0	0.05	0.72	0.00	0.00	0.00	0.22	0.00	0.00	1.45
275.8	0.2	0.3	0.0	0.03	0.73	0.00	0.00	0.00	0.00	0.00	0.00	1.22
277.8	0.2	0.2	0.0	0.00	0.58	0.00	0.00	0.00	0.00	0.00	0.00	0.97
277.8	0.1	0.2	0.0	0.00	0.62	0.00	0.00	0.00	0.00	0.00	0.00	0.99
279.3	0.1	0.2	0.0	0.00	0.65	0.00	0.00	0.00	0.00	0.00	0.00	0.99
280.8	0.1	0.2	0.0	0.00	0.65		0.00	0.00	0.00	0.00	0.00	0.99
280.8	0.1	0.2	0.1	0.00	0.66		0.00	0.00	0.00	0.00	0.00	1.09
281.0	0.3	0.2	0.0	0.00	0.67		0.00	0.00	0.00	0.00	0.00	1.16
281.0	0.3	0.2	0.0	0.00	0.67		0.00	0.00	0.00	0.00	0.00	1.19
284.0	0.2	0.2	0.0	0.00	0.73	0.00	0.00	0.00	0.00	0.00	0.00	1.19
284.0	0.2	0.2	0.0	0.00	0.69	0.00	0.00	0.00	0.00	0.00	0.00	1.13
285.8	0.2	0.2	0.0	0.00	0.71		0.00	0.00	0.00	0.00	0.00	1.12
285.8	0.2	0.3	0.0	0.00	0.74		0.00	0.00	0.00	0.00	0.00	1.18
289.0	0.1	0.2	0.0	0.00	0.76	0.00	0.00	0.00	0.00	0.00	0.00	1.13
289.0	0.1	0.2	0.0	0.00	0.82	0.00	0.00	0.00	0.00	0.00	0.00	1.20
291.0	0.1	0.2	0.0	0.00	0.85		0.00	0.00	0.00		0.00	1.18
291.0	0.1	0.2	0.0	0.00	0.81		0.00	0.00	0.00	0.00	0.00	1.12
291.1	0.3	0.2	0.1	0.00	0.91		0.00	0.00	0.77		0.00	2.26
291.1	0.3	0.2	0.0	0.00	0.84		0.00	0.00	0.00	0.00	0.00	1.35
294.1	0.2	0.2	0.0	0.00	0.88	0.00	0.00	0.00	0.00	0.00	0.00	1.30
294.1	0.2	0.2	0.0	0.00	0.91	0.00	0.00	0.00	0.00	0.00	0.00	1.35
295.5	0.2	0.2	0.0	0.00	0.94	0.00	0.00	0.00	0.00	0.00	0.00	1.32
295.5	0.2	0.2	0.0	0.00	0.92	0.00	0.00	0.00	0.00	0.00	0.00	1.31
296.5	0.1	0.2	0.0	0.00	0.94	0.00	0.00	0.00	0.00	0.00	0.00	1.28
296.5	0.1	0.2	0.0	0.00	0.93	0.00	0.00	0.00	0.00	0.00	0.00	1.28

Appendix Table D.13: Headspace (atm) and acetate (μM) concentrations measured during the reactor experiment incubated at a hydrogen partial pressure of 2.9×10^{-4}

Hours	H ₂	N ₂	CO ₂	Acetate
0.0	1.27E-03	8.89E-01	2.08E-03	2.85E+00
0.0	7.25E-04	8.45E-01	3.78E-04	
7.5	2.21E-05			
86.5	0.00E+00	5.94E-01	6.55E-04	
104.0	3.96E-05	8.90E-01	1.20E-03	2.35E+00
104.0	3.49E-05	9.00E-01	1.14E-03	2.08E+00
110.5	1.04E-04	8.64E-01	2.43E-03	
117.5	1.85E-04	8.70E-01	2.86E-03	
128.8	9.43E-05	8.31E-01	2.81E-03	
132.0	6.90E-05	6.08E-01	1.98E-03	2.97E+00
132.0	1.95E-04	8.36E-01	2.13E-03	2.65E+00
133.0	1.26E-04	8.19E-01	2.72E-03	
134.5	1.33E-04	8.36E-01	2.71E-03	
136.7	2.63E-04	8.53E-01	3.29E-03	
151.8	2.83E-04	8.76E-01	3.28E-03	
151.8	2.51E-04	8.13E-01	3.08E-03	
159.0	2.47E-04	7.55E-01	2.75E-03	
177.8	2.60E-04	7.50E-01	3.10E-03	
203.0	2.62E-04	8.49E-01	3.42E-03	
221.9	2.37E-04	8.09E-01	2.94E-02	
221.9	2.50E-04	7.83E-01	3.32E-03	
247.8	2.35E-04	8.01E-01	2.30E-03	
268.8	2.46E-04	8.20E-01	4.16E-03	
272.8	2.44E-04	7.86E-01	2.07E-03	
294.1	1.91E-04	6.51E-01	3.91E-03	
294.1	5.50E-04	8.27E-01	5.72E-03	
295.5	1.12E-03	8.58E-01	6.02E-02	
295.5	2.61E-04	8.48E-01	3.14E-03	
296.5	2.35E-04	7.89E-01	3.59E-03	
297.5	2.35E-04	7.89E-01	3.59E-03	

Appendix E: Rates of Reductive Dechlorination

Appendix Table E: Calculated Reductive Dechlorination Rates

Reactor Study	Addition Time hour	PCP hour ⁻¹	95% Confidence Interval		2,3,4,5-TeCP hour ⁻¹	95% Confidence Interval	
			+	-		+	-
4	187.7	0.092	0.107	0.080	0.059	0.075	0.042
	210.8	0.111	0.132	0.092	0.104	0.117	0.085
	235.2	0.108	0.129	0.092	0.089	0.097	0.070
	258.2	0.137	0.160	0.114	0.112	0.135	0.092
	277.2	0.154	0.231	0.111	0.129	0.156	0.086
6	83.7	0.255	0.288	0.215	0.270	0.291	0.232
	93.2	0.299	0.314	0.268	0.326	0.344	0.283
	101.7	0.307	0.345	0.339	0.312	0.344	0.267
	108.6	0.339	0.406	0.301	0.366	0.399	0.322
	115.8	0.482	0.544	0.428	0.536	0.594	0.470
	122.4	0.536	0.594	0.467	0.531	0.550	0.462
6b	143.3	0.951	1.127	0.808	1.594	2.227	1.223
	147.3	1.292	1.531	1.145	1.652	1.958	1.168
	150.8	1.097	1.145	1.079	2.175	2.795	1.574
	155.7	1.051	1.170	0.936	1.727	1.892	1.416
7	130.5	0.064	0.068	0.058	0.049	0.056	0.044
	155.3	0.079	0.085	0.072	0.062	0.069	0.057
	176.8	0.067	0.073	0.061	0.081	0.088	0.072
8	262.3	0.123	0.166	0.092	0.127	0.138	0.052
	275.7	0.135	0.170	0.109	0.131	0.146	0.101
	290.2	0.111	0.128	0.095	0.119	0.141	0.130
	309.3	0.076	0.047	0.012	0.080	0.099	0.031
	326.1	0.283	0.466	0.207	0.561	0.696	0.458
	334.7	0.139	0.179	0.107	0.154	0.160	0.110
	346.9	0.346	0.478	0.263	0.221	0.262	0.181
	357.1	0.063	0.085	0.051	0.107	0.085	0.081
	269.5	0.070	0.096	0.044	0.060	0.073	0.017
	281.0	0.094	0.127	0.060	0.071	0.085	0.034
	291.1	0.133	0.179	0.082	0.126	0.150	0.062
9	299.1	0.167	0.232	0.109	0.153	0.181	0.068
	308.1	0.194	0.270	0.135	0.383	0.438	0.292
	317.0	0.409	0.552	0.334	0.534	0.681	0.405

Appendix F: Computer Simulation

Appendix Figure F.1: Sample input of multiple addition reactor simulation

	Constants to be entered	Units
Initial Values	Initial cells, X0	0.001 mg Cells
	Initial substrate, S0	0.09 mg
	Duration of experiment	320 hours
Monod Constants	Half velocity coefficient, Ks	0.12 mg
	Yield, Y	0.023 mg cells/mg acceptor
	Degradation rate, km	3 mg sub/mgCellshour
	Death rate	0.002 1/hours
Spike Values	At what S concentration re-spike	0.013 mg
	Spike stock concentration, Ssp	0.077 mg
Hydrogen Constants	Hydrogen	0.0001 atm
	Hydrogen Half Velocity coefficient, KH	0.0001 atm
Model variables	Delta time	5 hour

Program Text for Multiple Addition Reactor Simulation

'Establish constants

Global Sinitial, Xinitial, Tinitial, km, Yield, Ks, Sspike, Ssyringe, kpump, Tend,
Slow, deltat, death, H, KH As Single

'Variables

Global S, X, T, deltaS, deltaX, cumSub As Single

Global counter As Integer

' Blastoff_Click Macro

Sub Blastoff_Click()

 'Set variables to 0

 S = 0

 X = 0

 T = 0

 counter = 0

 cumSub = 0

 'Get the constants from the spreadsheet

 Worksheets("Initial Values").Select

 Tend = [c5]

 Sspike = [c12]

 Ks = [c7]

 H = [c13]

 KH = [c14]

 Yield = [c8]

 km = [c9]

 Xinitial = [c3]

 Sinitial = [c4]

 deltat = [c16]

 Slow = [c11]

 death = [c10]

 'Set initial values

 X = Xinitial

 S = Sinitial

 T = 0

 'Enter values into the spreadsheet

 [i1] = "Time"

 [j1] = "Substrate"

 [l1] = "Cells"

 [k1] = "dS/dT"

 [i2] = T

 [j2] = S

 [l2] = X

 '[k2] = cumSub

```

'Loop to operate with the change in time
10 If T >= Tend Then GoTo 20
    counter = counter + 1
    calc_dcells
    calc_dsubstrate
    X = X + deltaX
    S = S + deltaS
    If S < 0 Then S = 0
    T = T + deltat
    cumulative_sub
    write_it
    If S <= Slow Then spike_it
    GoTo 10
'use chart subroutine
20 cheesiechart
End Sub
'subroutine to puts the values into the spreadsheet
Sub write_it()
    'Cells(counter + 2, 8) = counter
    Cells(counter + 2, 9) = T
    Cells(counter + 2, 10) = S
    Cells(counter + 2, 12) = X
    Cells(counter + 2, 11) = -deltaS / deltat
    Cells(counter + 2, 13) = cumSub
End Sub
'Subroutine to add spike of penta
Sub spike_it()
    counter = counter + 1
    S = S + Sspike
    write_it
End Sub
'Subroutine to calculate the change in Substrate based on Monod Kinetics
Sub calc_dsubstrate()
    deltaS = -(km * X * S * H * deltat) / ((Ks + S) * (KH + H)) 'Based on Monod
    quation for cell ballance
    'Debug.Print deltaS
End Sub
'Subroutine to calculate change in Cells based on Menod Kinetics
Sub calc_dcells()
    'deltaX = km * Yield * X * S / (Ks + S) * H / (KH + H) * deltat
    deltaX = (km * Yield * X * S / (Ks + S) * H / (KH + H) - death * X) * deltat
    'Based on Monod equation for substrate ballance
    'Debug.Print deltaX

```

```

End Sub
Sub cumulative_sub()
    cumSub = cumSub - deltaS
End Sub
Global Sinitial, Xinitial, Tinitial, km, Yield, Ks, _
    Sspike, Ssyringe, kpump, Tend, Slow, deltat, death, H, KH As Single
'Establish constants
Global S, X, T, deltaS, deltaX, cumSub As Single           'Variables
Global counter As Integer
' Blastoff_Click Macro
Sub Blastoff_Click()
    'Set variables to 0
    S = 0
    X = 0
    T = 0
    counter = 0
    cumSub = 0
    'Get the constants from the spreadsheet
    Worksheets("Initial Values").Select
    Tend = [c5]
    Sspike = [c12]
    Ks = [c7]
    H = [c13]
    KH = [c14]
    Yield = [c8]
    km = [c9]
    Xinitial = [c3]
    Sinitial = [c4]
    deltat = [c16]
    Slow = [c11]
    death = [c10]
    'Set initial values
    X = Xinitial
    S = Sinitial
    T = 0
    Debug.Print X, S, T, H
    'Enter values into the spreadsheet
    [i1] = "Time"
    [j1] = "Substrate"
    [l1] = "Cells"
    [k1] = "dS/dT"
    [i2] = T
    [j2] = S
    [l2] = X

```



```

'[k2] = cumSub
'Loop to operate with the change in time
10 If T >= Tend Then GoTo 20
    counter = counter + 1
    calc_dcells
    calc_dsubstrate
    X = X + deltaX
    S = S + deltaS
    If S < 0 Then S = 0
    T = T + deltat
    cumulative_sub
    write_it
    If S <= Slow Then spike_it
GoTo 10
'Use chart subroutine
20 cheesiechart
'
End Sub
'Subroutine to puts the values into the spreadsheet
Sub write_it()
    'Cells(counter + 2, 8) = counter
    Cells(counter + 2, 9) = T
    Cells(counter + 2, 10) = S
    Cells(counter + 2, 12) = X
    Cells(counter + 2, 11) = -deltaS / deltat
    Cells(counter + 2, 13) = cumSub
End Sub
'Subroutine to add spike of penta
Sub spike_it()
    counter = counter + 1
    S = S + Sspike
    write_it
End Sub
'Subroutine to calculate the change in Substrate based on Monod Kinetics
Sub calc_dsubstrate()
    deltaS = -(km * X * S * H * deltat) / ((Ks + S) * (KH + H)) 'Based on Monod
    quation for cell ballance
    'Debug.Print deltaS
End Sub
'Subroutine to calculate change in Cells based on Monod Kinetics
Sub calc_dcells()
    'deltaX = km * Yield * X * S / (Ks + S) * H / (KH + H) * deltat

```

```

    deltaX = (km * Yield * X * S / (Ks + S) * H / (KH + H) - death * X) * deltat
'Based on Monod equation for substrate balance
'Debug.Print deltaX
End Sub
Sub cumulative_sub()
    cumSub = cumSub - deltaS
End Sub
'
'Subroutine to create chart using a format saved in excel by user
Sub cheesiechart()
    Sheets("Initial Values").Select
    ActiveSheet.ChartObjects.Add(10, 10, 380, 200).Select
    Application.CutCopyMode = False
    ActiveChart.Type = xlXYScatter
    ActiveChart.SeriesCollection.Add Source:=Columns("i:l"), _
        rowcol:=xlColumns, seriesLabels:=True, categoryLabels:=True, _
        Replace:=True
    ActiveSheet.ChartObjects(1).Activate
    ActiveChart.AutoFormat Gallery:=xlCustom, Format:="Reactor Model"

    Windows("Dual Monod Model.xls").Activate
End Sub
"
Subroutine to clear chart and data from spreadsheet
Sub clearit_click()
    ActiveSheet.ChartObjects(1).Select
    Selection.Delete
    Columns("I:M").Select
    Selection.ClearContents
    Range("a2").Select
End Sub

```

Appendix G: Apparent Growth Rate Data

Appendix Table G.1: Activity growth rates of PCP reductively dechlorinating bacteria

Experiment		7	4	9	6	8	6b
Hydrogen	atm	9.40E-05	2.20E-04	2.90E-04	5.70E-04	7.80E-03	3.90E-02
Apparent growth rate	Apparent growth rate	0.0011	0.0056	0.0302	0.0216	0.0054	0.0020
	std. error	0.0048	0.0010	0.0012	0.0034	0.0076	0.0173
	t-value	0.22	5.91	26.03	6.30	0.71	0.12
	2-sided p-value	<i>0.8616</i>	<i>0.0097</i>	<i>0.0015</i>	<i>0.0032</i>	<i>0.5068</i>	<i>0.9171</i>
	95%	0.0608	0.0030	0.0050	0.0095	0.0186	0.0744
	k initial	0.0595	0.0317	1.99E-05	0.0374	0.0294	1.4399
	std. error	0.0444	0.0075	6.73E-06	0.0143	0.0725	1.6068
	t-value	1.34	4.24	2.95	2.62	0.41	0.90
	2-sided p-value	0.4082	0.0240	0.0981	0.0588	0.6992	0.4648
	95% I	0.5640	0.0238	0.0000	0.0397	0.1775	6.9137
d.f.		1	3	2	4	6	2

Appendix Table G.2: Activity growth rates of 2,3,4,5-TeCP reductively dechlorinating bacteria

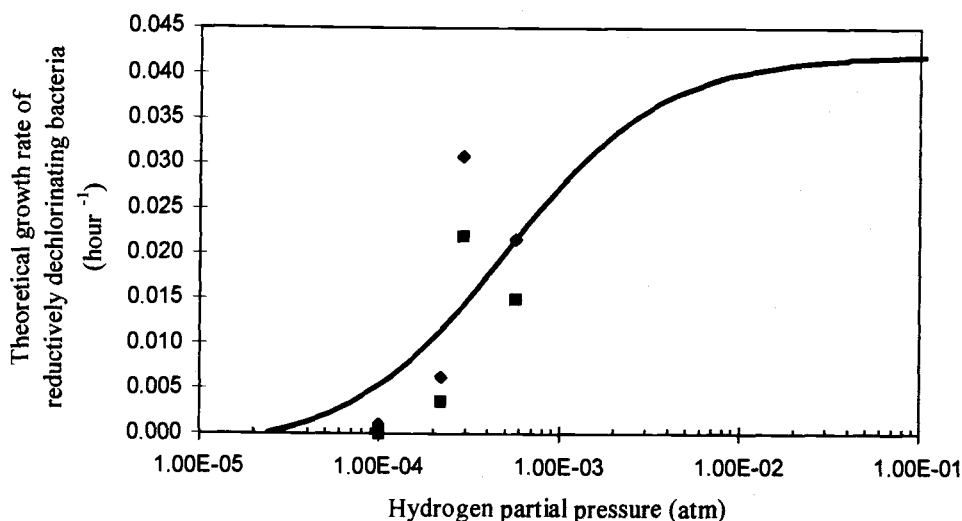
Experiment		7	4	9	6	8	6b
Hydrogen	atm	9.40E-05	2.20E-04	2.90E-04	5.70E-04	7.80E-03	3.90E-02
Apparent growth rate	Apparent growth rate	0.0111	0.0066	0.0352	0.0201	0.0048	0.0102
	std. error	0.0009	0.0022	0.0057	0.0042	0.0102	0.0182
	t-value	12.73	2.95	6.15	4.81	0.47	0.56
	2-s p-value	<i>0.0499</i>	<i>0.0602</i>	<i>0.0254</i>	<i>0.0086</i>	<i>0.6520</i>	<i>0.6327</i>
	95%	0.0111	0.0071	0.0247	0.0116	0.0249	0.0783
	k ₀	0.01135	0.0208	3.2E-06	0.04653	0.04107	0.3918
			4				
	std. error	0.00161	0.0115	4.9E-06	0.02156	0.13518	1.06747
			1				
	t-value	7.07	1.81	0.67	2.16	0.30	0.37
k ₀	2-s p-value	0.0895	0.1680	0.5738	0.0970	0.7715	0.7488
	95%	0.0204	0.0366	0.0000	0.0599	0.3308	4.5930
	df	1	3	2	4	6	2

Appendix H: Monod Kinetic Model Studies

Using Monod kinetics, a correlation between the growth rate of reductively dechlorinating bacteria and hydrogen was calculated. Initial growth constants were based on values listed in the literature (Appendix Table H.1), and then, an optimization program (Microsoft Excel 7.0; Solver) was used to fit the curve to experimental results. Because the experimental data reached a maximum and then declined, only the hydrogen partial pressure experiments between 1×10^{-5} and 1×10^{-3} were used for this analysis (Appendix Figure A.1).

Appendix Table H.1: Monod constants

Symbol	Initial Constant	Solved Constant	Units
k_{\max}	3	3.42	$\text{mg}_{\text{substrate}}\text{mg}_{\text{cells}}^{-1}\text{hour}^{-1}$
K_H	0.0001	0.0005	mgL^{-1}
K_p	0.12	0.12	atm
PCP	0.06	0.06	mgL^{-1}
Y	0.023	0.039	$\text{mg}_{\text{cells}}\text{mg}_{\text{substrate}}^{-1}\text{L}^{-1}$
b	0.002	0.002	hour^{-1}



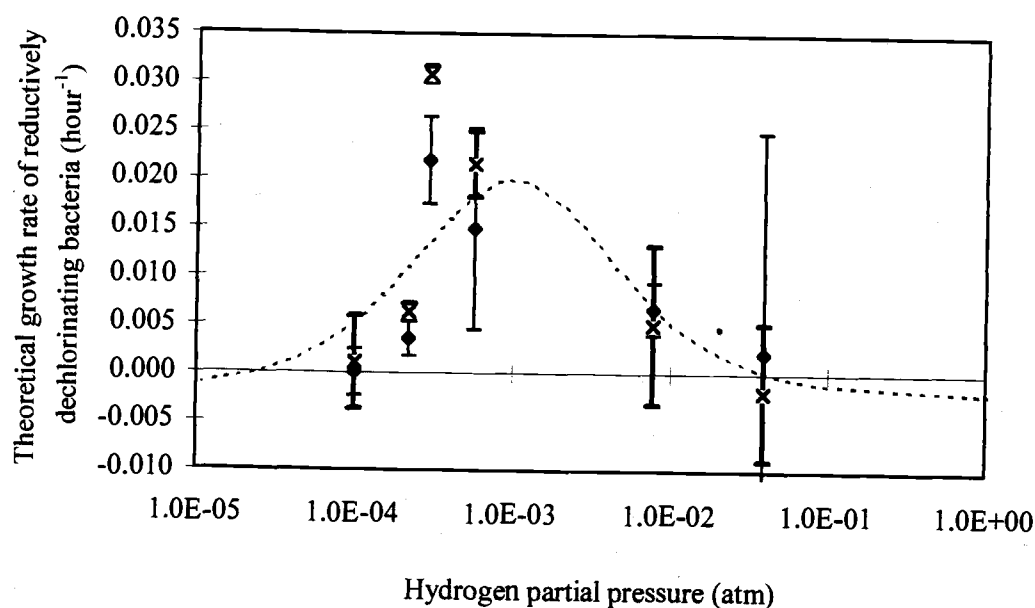
Appendix Figure H.1: Monod kinetics based curve fit of growth rate as a function of hydrogen partial pressure (—) based on Stuart's (◆) and Lotrario's (■) apparent growth rate data

By changing from the standard dual Monod kinetics model to a substrate inhibition model based on Appendix Equation H.1, all of the data can be analyzed. This equation is based on a system in which a portion of the enzyme is misdirected by excess substrate and slows down the desired reaction. As substrate increases the rate initially rises and then declines.

Appendix Equation H.1

$$\frac{dPCP}{dt} = - \frac{Xk_m[PCP]}{K_P + [PCP]} \frac{[H_2]}{K_H + H_2 + \frac{[H_2]^2}{K_i}}$$

A curve based on this model fit well to the apparent growth rate data as shown in Appendix Figure H.2. The constants used for this model are shown in Appendix Table H.2.



Appendix Figure H.2: Apparent growth rates of reductive dechlorination \pm one standard error estimated using Stuart's model ($- \times -$), and Lotrario's model ($- \diamond -$) compared with a substrate inhibition model ($- - -$)

Appendix Table H.2: Constants used in substrate inhibition model

Symbol	Solved Constant	Units
k_{\max}	3.42	$\text{mg}_{\text{substrate}} \text{mg}_{\text{cells}}^{-1} \text{hour}^{-1}$
K_H	0.0005	atm
K_i	0.002	atm
K_P	0.12	mgL^{-1}
PCP	0.06	mgL^{-1}
Y	0.039	$\text{mg}_{\text{cells}} \text{mg}_{\text{substrate}}^{-1} \text{L}^{-1}$
b	0.002	hour^{-1}

Appendix I: S_{\min} calculations

Calculations using the Monod kinetic model help in estimating the growth of bacteria. To ensure that the concentrations of substrates are kept above a theoretical minimum at which point cell growth is zero, S_{\min} is determined. S_{\min} is the theoretical minimum of substrate concentration determined by setting dX/dt equal to zero. Above that substrate concentration growth is theoretically feasible. S_{\min} was determined for PCP within the range of hydrogen concentrations examined. The calculations were performed for both the dual Monod equations using Monod growth coefficients based on literature values (Appendix Table A.2). The values used for the substrate inhibition calculations were determined by a curve fit of the substrate inhibition model to acceleration coefficients (Figure 3.16). Both sets of values are shown in Appendix Table I.1. The subsequent S_{\min} calculations for both scenarios show that the PCP concentrations used during reactor experiments (0.45 - 0.045 μM) were well above theoretical minimums (Appendix Table I.2).

Appendix Table I.1: Monod Coefficients used in S_{\min} Calculations

Term	Dual Monod	Substrate Inhibition	Units
Yield	0.00613	0.103	$\text{mg}_{\text{cells}}/\mu\text{M}_{\text{PCP}} \text{ L}$
k_{\max}	11.3	12.9	$\mu\text{M}_{\text{PCP}} \text{ L}/\text{mg}_{\text{cells}} \text{ hour}$
b	0.002	0.002	hour^{-1}
K_H	0.0001	0.0005	atm
K_{PCP}	0.45	0.45	μM_{PCP}
K_i	NA	0.002	atm

Appendix Table I.2: S_{\min} values for Varying Hydrogen Partial Pressures

Hydrogen (atm)	Dual Monod PCP_{\min} (μM)	Substrate Inhibition PCP_{\min} (μM)
0.00005	0.0427	0.0763
0.00010	0.0276	0.0042
0.00050	0.0161	0.0015
0.00100	0.0148	0.0014
0.00500	0.0137	0.0025
0.01000	0.0135	0.0042